NOTE TO USERS

This reproduction is the best copy available.

UMI®

University of Alberta

Application of the Gravity Assisted Tertiary Gas Injection Processes

Presented By

Weishan Ren ©

A thesis submitted to the Faculty of Graduate Studies and Research in partial fulfillment of the requirements of the degree of

Master of Science

in

Petroleum Engineering

Department of Civil and Environmental Engineering

Edmonton, Alberta, Canada

Spring 2002

National Library of Canada
Acquisitions and Bibliographic Services
395 Wellington Street
Ottawa ON K1A 0N4
Canada

Bibliothèque nationale du Canada
Acquisitions et services bibliographiques
395, rue Wellington
Ottawa ON K1A 0N4
Canada

Your file Votre référence

Our file Notre référence

The author has granted a non-exclusive licence allowing the National Library of Canada to reproduce, loan, distribute or sell copies of this thesis in microform, paper or electronic formats.

L'auteur a accordé une licence non exclusive permettant à la Bibliothèque nationale du Canada de reproduire, prêter, distribuer ou vendre des copies de cette thèse sous la forme de microfiche/film, de reproduction sur papier ou sur format électronique.

The author retains ownership of the copyright in this thesis. Neither the thesis nor substantial extracts from it may be printed or otherwise reproduced without the author's permission.

L'auteur conserve la propriété du droit d'auteur qui protège cette thèse. Ni la thèse ni des extraits substantiels de celle-ci ne doivent être imprimés ou autrement reproduits sans son autorisation.

0-612-69751-7

Canada

University of Alberta

Library Release Form

Name of Author: Weishan Ren

Title of Thesis: Application of the Gravity Assisted Tertiary Gas Injection Processes

Degree: Master of Science

Year this Degree Granted: 2002

Permission is hereby granted to the University of Alberta Library to reproduce single copies of this thesis and to lend or sell such copies for private, scholarly or scientific research purposes only.

The author reserves all other publication and other rights in association with the copyright in the thesis, and except as herein before provided, neither the thesis nor any substantial portion thereof may be printed or otherwise reproduced in any material form whatever without the author's prior written permission.

Weishan Ren

1111 Twin Brooks Point
Edmonton, AB
T6J 7G5 Canada

Dated April 15, 2002

University of Alberta

Faculty of Graduate Studies and Research

The undersigned certify that they have read, and recommended to the Faculty of Graduate Studies and Research for acceptance, a thesis entitled **Application of the Gravity Assisted Tertiary Gas Injection Processes** submitted by **Weishan Ren** in partial fulfillment of the requirements of the degree of **Master of Science in Petroleum Engineering**.

Dr. L. B. Cunha (*Supervisor*)

Dr. R. G. Bentsen (*Co-supervisor*)

Dr. E. Kuru (*Committee Chair and Examiner*)

Dr. R. E. Hayes (*Committee Member*)
Department of Chemical and Materials Engineering

Dated MARCH 25, 2002

ABSTRACT

Gravity assisted tertiary gas injection processes can produce a large amount of incremental tertiary oil from water drive oil reservoirs. These processes include the Double Displacement Process (DDP) and the Second Contact Water Displacement (SCWD) process.

The DDP and the SCWD process were conducted in a transparent sand-pack micromodel, and a pore-level observation was performed to investigate the microscopic mechanisms of the two processes. Observation of the two processes confirmed that the oil films play a very important role in achieving high recovery efficiencies in the DDP. In the SCWD process, trapped gas reduces the possibility of the residual oil being trapped in the center of the pores in the second water flood. Moreover, reservoir simulations at reservoir scale were performed to investigate the macroscopic level mechanisms of the two processes. The results have shown that both processes are efficient methods to recover the residual oil to water.

ACKNOWLEDGMENTS

I would like to express my deep gratitude and appreciation to my former advisor and professor, Dr. Bogdan Lepski, for his guidance and supervision of this research work, for his encouragement and support, and for being a good friend. Although he passed away at the end of this study, many good memories will stay in my heart forever.

I would like to acknowledge the extraordinary help provided by Mr. Sean Watt in building the transparent cell and doing experiments. Without his help, the experiments would not have been finished.

Special thanks and sincere gratitude to Dr. Ramon G. Bentsen for being an excellent advisor and professor, and for his continuous guidance and invaluable help, especially in writing this thesis.

I would like to thank Dr. Luciane B. Cunha for being my advisor, and for her guidance and help in carrying out the reservoir simulations.

Thanks to Dr. Marcel Polikar and Dr. Ergun Kuru for their encouragement and support to complete the work during the hard time after losing my professor.

The financial support from the Natural Sciences and Engineering Research Council of Canada is gratefully acknowledged.

Finally, I would like to extend my thanks and appreciation to my wife, Jiang Bai, and to my dear parents, for their continued support during my studies.

TABLE OF CONTENTS

CHAPTER

1. INTRODUCTION 1

2. LITERATURE REVIEW 3

2.1 Gravity Drainage 4

2.2 Tertiary Gas Injection 7

2.2.1 Introduction of the Processes 8

2.2.2 Principles of the Double Displacement Process 9

2.2.3 Factors Affecting the Double Displacement Process 11

2.2.3.1 Gravity force 11

2.2.3.2 Spreading coefficient 12

2.2.3.3 Rock wettability 13

2.2.3.4 Oil viscosity 14

2.2.3.5 Reservoir heterogeneity 15

2.2.3.6 Three-phase capillary pressure 16

2.2.3.7 Three-phase relative permeability 17

2.2.4 Laboratory Studies 19

2.2.5 Field Studies 20

3. RESERVOIR SIMULATION 31

3.1 Reservoir Model 32

3.2 Reservoir Simulation 33

3.2.1 Injection and Production Rates 34

3.2.2 Production Strategy: Perforation of Production Wells 36

3.2.3 Reservoir Dip Angle 37

3.2.4 Oil Relative Permeability 38

3.2.5 Capillary Pressure 41

3.2.6 Second Contact Water Displacement Process 42

4. TRANSPARENT CELL EXPERIMENTS **79**

4.1 Model Construction 80

4.2 Experimental Setup 81

4.3 Experimental Procedure 82

4.3.1 Preparation for Tertiary Gas Injection 82

4.3.2 Gravity Assisted Tertiary Gas Injection 83

4.3.3 Second Contact Water Displacement Process 84

4.4 Experimental Results and Discussion 85

4.4.1 Properties of Transparent Cells and Production Amounts of the Processes 85

4.4.2 Observation of the Double Displacement Process 87

4.4.3 Observation of the SCWD Process 89

4.5 Interfacial Tension Measurements 91

5. CONCLUSIONS AND RECOMMENDATIONS **101**

5.1 Summary and Conclusions 101

5.2 Recommendations 102

REFERENCES **104**

APPENDIX A: BASIC DDP SIMULATION DATA SET.....111

APPENDIX B: BASIC SCWD SIMULATION DATA SET 117

APPENDIX C: DDP OBSERVATION.....127

APPENDIX D: SCWD OBSERVATION.....133

APPENDIX E: CALCULATIONS OF IFT 136

LIST OF TABLES

Table 2.1: Oil recoveries of tertiary gas injection processes 27

Table 2.2: The reservoir and fluid properties for several field projects 28

Table 3.1: The reservoir and fluid properties from several field projects 44

Table 3.2: The maximum injection and production rate settings 45

Table 3.3: Two end-point saturation settings 45

Table 4.1: Properties of the transparent cell 92

Table 4.2: Data of IFT measurements 92

Table E.1: Oil and water interfacial tension 137

Table E.2: Gas and water interfacial tension 138

Table E.3: Oil and gas interfacial tension 139

LIST OF FIGURES

Figure 2.1: Schematic diagram of the DDP 29

Figure 2.2: Schematic diagram of the SCWD process 29

Figure 2.3: Single pore scale gas displacement of trapped oil 30

Figure 3.1: Reservoir model 46

Figure 3.2: Stabilized pressure distribution 46

Figure 3.3: Oil saturation distribution at the end of waterflood 47

Figure 3.4: Oil distribution after one year of DDP with Setting 1 47

Figure 3.5: Oil distribution after one year of DDP with Setting 2 48

Figure 3.6: Oil distribution after one year of DDP with Setting 3 48

Figure 3.7: Oil distribution after one year of DDP with Setting 4 49

Figure 3.8: Oil distribution after one year of DDP with Setting 5 49

Figure 3.9: Oil distribution after four years of DDP with Setting 1 50

Figure 3.10: Oil distribution after four years of DDP with Setting 2 50

Figure 3.11: Oil distribution after four years of DDP with Setting 3 51

Figure 3.12: Oil distribution after four years of DDP with Setting 4 51

Figure 3.13: Oil distribution after four years of DDP with Setting 5 52

Figure 3.14: Oil distribution after ten years of DDP with Setting 1 52

Figure 3.15: Oil distribution after ten years of DDP with Setting 2 53

Figure 3.16: Oil distribution after ten years of DDP with Setting 3 53

Figure 3.17: Oil distribution after ten years of DDP with Setting 4 54

Figure 3.18: Oil distribution after ten years of DDP with Setting 5 54

Figure 3.19: Cumulative oil production with Setting 1 55

Figure 3.20: Cumulative oil production with Setting 2 55

Figure 3.21: Cumulative oil production with Setting 3 56

Figure 3.22: Cumulative oil production with Setting 4 56

Figure 3.23: Cumulative oil production with Setting 5 57

Figure 3.24: Oil production rate and gas oil ratio curves with Setting 1 57

Figure 3.25: Oil production rate and gas oil ratio curves with Setting 2 58

Figure 3.26: Oil production rate and gas oil ratio curves with Setting 3 58

Figure 3.27: Oil production rate and gas oil ratio curves with Setting 4 59

Figure 3.28: Oil production rate and gas oil ratio curves with Setting 5 59

Figure 3.29: Oil distribution with partially perforated wells (Setting 3) 60

Figure 3.30: Oil distribution with totally perforated wells (Setting 3) 60

Figure 3.31: Oil distribution with totally perforated wells (Setting 4) 61

Figure 3.32: Cumulative oil production curve
with totally perforated wells (Setting 3) 61

Figure 3.33: Oil production rate and GOR curves
with totally perforated wells (Setting 3)) 62

Figure 3.34: Cumulative oil production curve
with totally perforated wells (Setting 4)) 62

Figure 3.35: Oil production rate and gas oil ratio curves
with totally perforated wells (Setting 4) 63

Figure 3.36: Oil distribution after ten years of DDP with reservoir dip of 8° 63

Figure 3.37: Oil distribution after ten years of DDP with reservoir dip of 30° 64

Figure 3.38: Oil distribution with reservoir dip of 30° and higher injection rate 64

Figure 3.39: Oil distribution with reservoir dip of 60° 65

Figure 3.40: Oil distribution with reservoir dip of 60° and higher injection rate 65

Figure 3.41: Oil & Water relative permeability curves (Setting 1) 66
Figure 3.42: Gas & Oil relative permeability curves (Setting 1) 66
Figure 3.43: Oil distribution after ten years of DDP (Stone2) 67
Figure 3.44: Oil distribution after ten years of DDP (Stone1) 67
Figure 3.45: Oil distribution after ten years of DDP (Linear Isoperm) 68
Figure 3.46: Oil distribution after ten years of DDP (Segregated) 68
Figure 3.47: Cumulative oil production curve (Stone2) 69
Figure 3.48: Cumulative oil production curve (Stone1) 69
Figure 3.49: Cumulative oil production curve (Linear Isoperm) 70
Figure 3.50: Cumulative oil production curve (Segregated) 70
Figure 3.51: Oil & Water relative permeability curves (Setting 2) 71
Figure 3.52: Gas & Oil relative permeability curves (Setting 2) 71
Figure 3.53: 2D oil distribution after ten years of DDP (Setting 1) 72
Figure 3.54: 2D oil distribution after ten years of DDP (Setting 2) 72
Figure 3.55: Water-Oil capillary pressure curve 73
Figure 3.56: Gas-Oil capillary pressure curve.....73
Figure 3.57. Oil distribution after ten years of DDP (without capillary pressure).....74
Figure 3.58: Oil distribution after eight years of DDP (with capillary pressure).....74
Figure 3.59: 2D oil distribution after ten years of DDP (without capillary pressure).....75
Figure 3.60: 2D oil distribution after eight years of DDP (with capillary pressure).....75
Figure 3.61: Cumulative oil production curve (SCWD with Sgc of 0.05) 76
Figure 3.62: 2D oil distribution before the SCWD process 76
Figure 3.63: 2D oil distribution after the SCWD process 77
Figure 3.64: Cumulative oil production curve (SCWD with Sgc of 0.15) 77
Figure 3.65: 2D oil distribution before the SCWD process 78

Figure 3.66: 2D oil distribution after the SCWD process 78

Figure 4.1: Transparent cell 93

Figure 4.2: Experimental setup 94

Figure 4.3: Dry sand 95

Figure 4.4: Oil, water, and gas in a spot at the top of the cell 95

Figure 4.5: Oil, water, and gas in a spot at the middle of the cell 96

Figure 4.6: Gas enters the front layer and the middle layer 96

Figure 4.7: Gas front in the DDP 97

Figure 4.8: Oil film between gas and water 97

Figure 4.9: Water front in the SCWD process 98

Figure 4.10: Bypassed area at the end of the SCWD process 98

Figure 4.11: Before the SCWD process 99

Figure 4.12: Water enters from the left 99

Figure 4.13: After the SCWD process 100

Figure C.1: Before the DDP, water (white) and oil (brown) 127

Figure C.2: Gas entered from the left at the bottom 128

Figure C.3: Gas entered the middle layer 128

Figure C.4: Oil moved into the front layer first (the left upper part) 129

Figure C.5: Gas moved into the front layer (center) 129

Figure C.6: Gas entered from the left upper corner 130

Figure C.7: Gas entered from the left lower corner 130

Figure C.8: Gas occupied available space; oil films and oil layers formed 131

Figure C.9: Less oil left in the form of oil films and layers 131

Figure C.10: At a later stage of the DDP 132

Figure D.1: Before the SCWD process, oil in oil films 133

Figure D.2: Water entered from the left 134
Figure D.3: Some gas and oil were displaced 134
Figure D.4: Some gas was trapped 135
Figure D.5: After the SCWD process 135

NOMENCLATURE

A	cross-sectional area of porous medium
BHP	bottom hole pressure
BOPD	barrels of oil per day
BPP	bubble point pressure
DDP	double displacement process
de	equatorial diameter of the unmagnified drop
De	maximum diameter of the unmagnified drop
ds	diameter measured at a distance de up from the bottom of the drop
dt	diameter of the neck of the drop
D_t	outside diameter of the tip
FVF	formation volume factor
g	gravitational constant
GRR	maximum rate of gravity drainage
H	shape factor of the unmagnified drop
IFT	interfacial tension
GOR	gas oil ratio
GOC	gas oil contact
k	absolute permeability of the medium
k_L	effective permeability to liquid
k_{rg}	relative permeability to gas

k_{rog}	relative permeability to oil with gas
k_{row}	relative permeability to oil with connate water and gas
k_{rw}	relative permeability to water
OIP	oil in place
OOIP	original oil in place
OWC	oil water contact
P_c	capillary pressure
P_{co}	threshold capillary pressure
P_{cog}	gas-oil capillary pressure
P_{cow}	water-oil capillary pressure
PV	pore volume
Ri	injection rate
Rp	production rate
SCF	standard cubic foot
SCWD	second contact water displacement
S_g	gas saturation
S_{gc}	critical gas saturation
S_o	oil saturation
S_{oi}	initial oil saturation
$S_{o/w}$	spreading coefficient of oil over water
S_{org}	residual oil saturation in drainage
S_{orw}	residual oil saturation to water
STB	stock tank barrels
S_w	water saturation

S_{wc}	connate water saturation
S_{wir}	irreducible water saturation
$\Delta\rho$	density difference
α	reservoir dip angle
ϕ	porosity of a porous medium
μ_L	viscosity of the liquid
θ	equilibrium contact angle
σ	interfacial tension
σ_{og}	oil/gas interfacial tension
σ_{ow}	oil/water interfacial tension
σ_{wg}	water/gas interfacial tension

CHAPTER 1

INTRODUCTION

In water drive oil reservoirs, a substantial quantity of the oil discovered is left behind in the ground after natural water influx or waterflooding. The oil left in conventional oil reservoirs can range from 40% - 60% of the original oil in place (OOIP). At the beginning of the new millennium, most waterfloods in reservoirs around the world are mature or close to their economic limits. The amount of oil remaining is estimated to be 30 billion barrels in Canada, 350 billion barrels in the USA and 2 trillion barrels in the world (Rao, 2001). As world demand for domestic oil keeps increasing, and as demand greatly exceeds supply, and as conventional oil reserves are quickly declining, the recovery of the oil remaining from previously developed waterflooded reservoirs becomes more and more important. Although several EOR technologies have been developed already, economic feasibility limits their application in the field. Therefore, technological improvements are required. A combined method referred to as *gravity assisted tertiary gas injection* is one of the most promising new technologies used to recover the oil remaining after waterflooding.

The residual oil remaining after a waterflood does not have the ability to flow when it is trapped in the water zone. The trapped oil results from the heterogeneity of the reservoir rock and from the capillary and surface forces acting at the microscopic scale. Gas injection into a watered-out oil column, with gravity assistance, can cause the displacement of excess water and a change in phase distribution within the pore space. As a result of this change, most of the residual oil can be recovered. This process involving the up-dip injection of gas into steeply dipping, high permeability, strongly water-wet, light oil reservoirs to recover the residual oil is called the gravity assisted tertiary gas injection process. It is also known as the *Double Displacement*

Process (DDP) because it involves the use of gas to displace the oil remaining after a waterflood.

In order to improve the economics of the DDP, another oil recovery process called the *Second Contact Water Displacement* (SCWD) process has been suggested. This process, which involves a second waterflood after the tertiary gas injection, is considered an extension of the DDP.

The objective of this study is to get a better understanding of the theory underlying the DDP and the SCWD process. To achieve this objective, two approaches are taken. First, the macroscopic mechanisms of the processes are investigated by undertaking numerical simulations using a 3D reservoir simulator. Second, the microscopic mechanisms of the processes are studied by making pore-level observations of the processes in a transparent sand-pack micro-model.

CHAPTER 2

LITERATURE REVIEW

Field tests and laboratory studies have demonstrated that the gravity assisted tertiary gas injection process is a very efficient method for recovering a larger fraction of the residual oil in waterflooded reservoirs. The mobilization and recovery of the residual oil to water by immiscible gas injection depends on the interactions among the gas, water, oil and surface of the rock, and on the effects of the gravitational force, capillary force, viscous force and structure of the pore space, and so on. In the gravity assisted tertiary gas injection process, the gravity force, spreading coefficient, three phase capillary pressure, three phase relative permeability, reservoir wettability and heterogeneity all play important roles. Understanding the mechanisms of the tertiary gas injection process requires lots of effort, not only in the laboratory, but also in the field. In the earliest studies, emphasis was placed on gravity drainage. According to Hagoort (1980), gravity drainage was defined as a recovery process in which the main driving force is the gravitational force, and in which gas replaces the voidage volume. It can occur in secondary recovery as gas displaces continuous oil, or in tertiary recovery as gas displaces water and residual oil isolated in the water zone. In both cases, the immiscible displacement of oil by gravity stabilized gas injection is characterized by a very high oil recovery efficiency. In the second case, the term "Gravity Assisted" is used to indicate the important role of the gravitational force in the tertiary recovery process, while the term gravity drainage is restricted mainly to secondary recovery.

Because gravity drainage is an essential and dominant mechanism of the gravity assisted tertiary gas injection process, the studies on gravity drainage are reviewed first. Then the studies on tertiary gas injection are reviewed extensively from the theory, the laboratory and the field point of view.

2.1. Gravity Drainage

The earliest studies on gravity drainage were undertaken by Stahl et al. (1943) and by Lewis (1944). Stahl used air to displace liquid from a vertical sand pack composed of Wilcox sand. Liquids used in the displacement were water, Wilcox crude oil, and heptane. Saturations were measured intermittently during the drainage process. They concluded that the liquid saturation was a function of the height of the sand pack for both dynamic and equilibrium conditions. They found also that temperature affected the drainage rate and the ultimate recovery. Lewis discussed various aspects of gravity drainage and reported on three field studies in which gravity drainage dominated.

Cardwell and Parsons (1949) presented a theory for estimating the rate of gravity drainage in a vertical column of a porous medium initially saturated 100% with liquid. Both rates of liquid moving in the upper, unsaturated region and in the lower, completely saturated region were calculated using simple solutions in which the capillary pressure term was omitted. An approximate method, based on the theory, which is valid only for gravity drainage, was used to determine the production rate. They compared their results with the data of Stahl and coworkers for Wilcox crude at 130°F and obtained a good agreement. Later Dykstra (1978) also confirmed Cardwell and Parsons' theory by using seven comparisons of recovery, calculated using their method, with recovery from other people's experiments, and provided three examples of how to apply the method.

Terwilliger et al. (1951) reported on an experimental and theoretical investigation of constant pressure gravity drainage. The experiment involved gas displacing brine in a sand pack, which was 13 ft in length and 2 inches in diameter. Brine was used because its saturation can be measured quickly and accurately by the electrical conductivity method. The production rates were kept constant, as was the case in field operations. The effect of production rate on recovery by gravity drainage was studied extensively. The data from the experiment indicated that the recovery to gas breakthrough by gravity drainage was inversely proportional to production rate, but

that in the immediate vicinity of the "maximum theoretical rate of gravity drainage" the recovery didn't change significantly. The "maximum rate of gravity drainage" was defined as "the rate of production from a 100 percent liquid-saturated system under a flow gradient equal to the gravity gradient or static pressure gradient differential between oil and gas due to density difference." It can be expressed as:

$$GRR = \frac{k_L A}{\mu_L} g \Delta\rho \sin\alpha$$

where k_L is the effective permeability to liquid at 100% liquid saturation, A is the cross-sectional area, μ_L is the viscosity of the liquid, g is the gravitational constant, $\Delta\rho$ is the density difference between the liquid and the gas, and α is the reservoir dip angle. When production rates exceeded the maximum rate of gravity drainage, the oil drained by its own weight will be relatively small and the gas drive will dominate. This equation doesn't account for the effect of capillary pressure, relative permeability and displacing fluid viscosity. Consequently, these three factors should be considered before using the maximum rate of gravity drainage to compare the performance of different systems.

A model based on the Buckley-Leverett equations was also presented. The theoretical predictions from the analytical model were compared to the experimental results, and good agreement was found. This model could be used for accurate prediction of a linear homogeneous gravity drainage system. But as Terwilliger et al. (1951) mentioned in their paper, appropriate adjustments are needed before it can be applied in the field.

Richardson and Blackwell (1970) provided a simple mathematical model for predicting the performance of gravity drainage in steeply dipping reservoirs with high vertical permeabilities. They divided the displacement process of oil by gas invasion into two steps. In the first step the main gas oil contact moves downdip and a thin oil layer forms at the bottom of the formation. In the second step the oil drains vertically through the gas-invaded zone to the thin oil layer and then flows along the bottom of

the formation to the oil zone. Dietz's method (Dietz, 1953) was used to predict the tilt angle of the front between the gas invaded zone and the thin oil layer. Neglecting capillary pressure and the resistance to flow of the gas, the vertical drainage rate depends only on the mobility of the oil in the vertical direction and the gravitational force that arises from the density difference between the oil and the gas. The rate at which a particular oil saturation moves in a reservoir can be determined by taking slopes of the vertical drainage rate versus saturation curve and then dividing the slope by the porosity. This method can be accurate when the displacement rate is less than half of the critical rate. If the rate is greater than half of the critical rate, the oil tends to accumulate rather than flow away at the bottom of the formation. Richardson and Blackwell (1970) also pointed out that the calculated recoveries are very sensitive to the relative permeability to oil at very low oil saturations.

Dumoré and Schols (1974) found that very low residual oil saturations were obtained in the presence of connate water at sufficiently high values of the drainage gas-oil capillary pressure curves. During measurement of the drainage capillary pressure, the core was first saturated with distilled water and then flooded with kerosene to obtain the irreducible water saturation. Then air was used to displace the kerosene. Results from the experiments showed that an oil saturation of some 3 percent PV was obtained with a connate water saturation of about 24% as the capillary pressure reached about 50,000 dyne/cm^2. The effect of oil film flow was investigated by using a non-spreading oil (Ondina 17) instead of a spreading oil (kerosene) to do the same experiments. Low oil saturations were also obtained. Therefore, they concluded that the spreading of the oil phase was not the main reason for the low oil saturation. They also did a drainage experiment on a sand pack 45.5 cm in length and 5 cm in diameter, which had a porosity of 34.5 % and a permeability of 170 Darcies. Low oil saturations were achieved in the gas zone. Based on observation of the experiments, they also concluded that after most of the oil had been produced in a relatively short period of time, film flow of the oil possibly caused the oil to drain at an extremely slow rate. Thus, the oil flow through the oil film was "thought to be generally negligible in the lifetime of the reservoir".

Hagoort (1980) reexamined the gravity drainage process, and described the process mathematically in a way that considered only the stable vertical downward displacement of oil by gas based on the continuity equation and Darcy's law, together with the concepts of relative permeability and capillary pressure. He pointed out that relative permeability is one of the most important factors in gravity drainage, and provided a centrifugal gas/oil displacement method to measure the oil relative permeability quickly and accurately. The results of measurements on several typical rocks confirmed that low residual oil saturations could be obtained in gravity drainage processes in water-wet, connate water bearing reservoirs. But he also pointed out that whether a low residual oil saturation could be reached in the lifetime of a reservoir depended on the ratio of the gravitational forces to the viscous forces, the oil relative permeability curves and the reservoir geometry and heterogeneity.

2.2. Tertiary Gas Injection

In 1988, two field reports by Carlson (1988) and Johnston (1988) and a series of papers describing laboratory studies by Kantzas et al. (1988a, b) and Chatzis et al. (1988) resulted in a new stage in the studies on gravity drainage. The gravity assisted tertiary gas injection process or the double displacement process appears to be a very attractive method to recover the residual oil in water flooded reservoirs. The mobilization of waterflood residual oil by immiscible gas injection and results indicating very low residual oil saturations in the gas zone gained a great deal of attention. Numerous studies investigating various aspects of tertiary gas injection have been published since then. In order to provide clear and sufficient information on the tertiary gas injection process and its extension to the SCWD process, an introduction to both processes is given first, and the principles and important factors are stated after, based on the theoretical studies. Then the laboratory studies and field studies are reviewed.

2.2.1. Introduction of the Processes

The oil remaining after a waterflood consists of two parts. The first part is the bypassed oil, which exists as a continuous oil phase in the regions of the reservoir unswept by water due to reservoir heterogeneity or well placement. This oil can be recovered by improving the sweep efficiency of the driving fluids. The second part is the residual oil existing at the microscopic scale as isolated oil blobs in the water swept regions of the porous medium due to the capillary and surface forces. This trapped oil is referred to as the *residual oil to water* and it can be recovered by restoring the mobility of the oil. Gas injected up-dip, with gravity assistance, into a steeply dipping reservoir can re-establish the hydraulic continuity of the oil and drive the oil down-dip. The residual oil remaining in the gas zone after gas gravity drainage, which is referred to as the *residual oil to gas*, can be much lower than the residual oil to water. The difference between these two leads to the incremental oil recovered by the gravity assisted tertiary gas injection process.

The gravity assisted tertiary gas injection process or the DDP is a tertiary gravity drainage process, which involves up-dip gas injection into a steeply dipping waterflooded reservoir to mobilize and produce incremental oil. Carlson (1988) defined the DDP as "the gas displacement of a previously water displaced oil column". A schematic diagram of the DDP is shown in Figure 2.1.

Imagine a steeply dipping waterflooded reservoir in which gas is being injected into the crestal region of the reservoir. After a short period of gas injection, a gas cap appears and an oil bank is formed ahead of the gas front. The gas front is stable and moves slowly downward to push the oil bank towards the producing wells. In addition to the formation of an oil bank, another important characteristic of the process is that the oil in the gas zone may form a thin oil film connecting all of the residual oil to the oil bank. Oil flowing through the oil film contributes to the development of the oil bank. Therefore, during this process, the residual oil can be recovered by two means at the microscopic level. The first means is the immiscible displacement of oil by gas in

the pore space around the gas front. The second means is the displacement of oil by gravity through the continuous oil films located between the gas and water phases in the region where the gas front has already passed by. Moreover, improvement of the sweep efficiency by the stabilized gas front can result in the recovery of the bypassed oil. When the oil bank reaches the production wells, oil production begins. The production characteristics of the process are that the main oil production takes place in a relatively short period of operating time and that, after gas breakthrough, the oil is produced at a very low rate.

Numerous laboratory studies and some field tests of the gravity-assisted tertiary gas injection process have proven that a very high oil recovery efficiency can be achieved. Recoveries of 85% to 95% of the OOIP have been reported from field tests and higher, even up to 100%, recoveries have been obtained in the laboratory. However, a late oil production response to gas injection and a low oil production rate after gas breakthrough is unfavorable to the economic viability of the process.

To shorten the period of low oil production, the second contact water displacement (SCWD) process can be used, provided the conditions are favorable. The SCWD process was introduced by Lepski (1995) and Lepski et al. (1996) to shorten the operating time of the DDP, and it is referred to as an extension of the DDP. A schematic diagram of the SCWD process is shown in Figure 2.2. During the later production stages of the DDP, stopping gas injection can permit the invasion of water from the bottom part of the reservoir, where most of the remaining oil exists, thus enabling water to push the remaining oil upward through the oil film.

2.2.2. Principles of the Double Displacement Process

The incremental oil of the DDP is a result of the difference between the residual oil saturation to gas and the residual oil saturation to water. The recovery of the waterflood residual oil is by means of the immiscible displacement by gas and by means of oil flow through the spreading films which connect most isolated oil blobs.

Kantzas et al. (1988a) first addressed these mechanisms in detail. The mobilization of the residual oil is shown in Figure 2.3. In a strongly water-wet system, water occupies the pore throats and pore edges, while the trapped oil occupies the center of the pores as isolated oil blobs. When gas goes along a large pore throat and enters the pore, as a non-wetting phase relative to oil, gas also tends to occupy the center of the pore. At this moment, the oil spreads on the water and forms a film between the gas and water if the spreading coefficient is positive. And some of the oil, which is not contained in the spreading film, is pushed out of the pore and into the larger available pore throats. As gas moves on, the mobilized oil accumulates at the head of the gas front and forms an oil bank. Behind the gas front, the continuous oil films connect all the residual oil to the advancing oil bank, providing a way for the oil to flow to the oil bank. Kantzas et al. (1988a) stated that the oil film flow contributed slowly to the growth of the oil bank. Therefore, given sufficient time, the flow of oil through the oil film can result in a very low oil saturation. Based on observations of his experiments, Kantzas et al. (1988a) found that three types of drainage occurred during the process. The first type is gas displacing oil which in turn displaces water. The second type is gas displacing water only, and the third type is gas displacing oil only.

The pore-level visualization study by Oren et al. (1992) confirmed these mechanisms. The important role of oil film flow in obtaining extremely low oil saturations was emphasized. In the detailed discussion of the mechanisms of mobilization of waterflood residual oil, Oren et al. (1992) called the mechanism involving gas displacing oil which in turn displaces water the *double drainage mechanism*, and the other two were called the *direct drainage mechanisms*. They stated that oil was always displaced by the double drainage mechanism in a water-wet system.

Kantzas et al. (1988b) described the four distinct displacement zones observed in two transparent network micromodels. Starting from the bottom, the first zone is the *water zone* in which oil exists as waterflood residual oil and only water can flow. The

second zone is the *oil bank*, where some of the oil is still isolated by water filled pores, but where most of the oil is continuous and mobile. Above the oil bank is the *transition zone*. In this region, all three phases, gas, oil, and water, flow together. Oil left by the advancing gas front flows through oil films towards the oil bank. The last zone is the *gas zone* where oil and water exist primarily as films and where their saturations are very low.

Chatzis et al. (1988), Naylor and Frorup (1989), Oren et al. (1992, 1994), Oren and Pinczewski (1994, 1995), Kalaydjian (1992), Kalaydjian et al. (1993), Catalan et al. (1994), Blunt et al. (1994), Lepski (1995), Pereira et al. (1996), Keller et al. (1997), Fenwick and Blunt (1997) and Lepski et al. (1998) also discussed these mechanisms of the gravity assisted tertiary gas injection process and the effects of several important parameters. It's shown that the gravity force, spreading coefficient, three phase capillary pressure, three phase relative permeability, reservoir wettability and heterogeneity all play important roles in this process. Each of these factors is discussed in the next section.

2.2.3. Factors Affecting the Double Displacement Process

2.2.3.1. Gravity force

Because gravity drainage is essential and dominant in the DDP, some conditions are necessary to ensure that the gravity force is the main driving force. These conditions include a light oil, a high vertical permeability, a strongly water-wet formation and a high angle in a dipping reservoir. The injection and production rates also need to be optimized to achieve a gravity-stable displacement and to obtain a high sweep efficiency.

Gravity acts as an important factor in the process, not only in the creation of a relatively uniform displacement front, but also in the flow of the oil through the continuous spreading films. Hagoort (1980) stated that the rate of oil film flow was

related to the gravitational forces. Kantzas et al. (1988a) and Chatzis et al. (1988) demonstrated the ability of oil films to drain waterflood residual oil efficiently in the presence of the gravitational force.

2.2.3.2. Spreading coefficient

The spreading coefficient is defined in terms of the water/gas, oil/gas, and oil/water interfacial tensions:

$$S_{o/w} = \sigma_{wg} - \sigma_{og} - \sigma_{ow}$$

where $S_{o/w}$ is the final spreading coefficient of oil over water, and σ_{wg}, σ_{og} and σ_{ow} are the water/gas, oil/gas, and oil/water interfacial tensions, respectively. These interfacial tensions should be measured at conditions corresponding to the three phases being in thermodynamic equilibrium. When the spreading coefficient is positive, oil tends to spread on the water. If the spreading coefficient is negative, oil won't spread over water.

Chatzis et al. (1988) were the first to address the effects of reservoir wettability and spreading coefficient on the gravity assisted tertiary gas injection process. They stated that the process efficiency was dependent on the spreading phenomenon. Oren et al. (1992) studied the effect of the spreading coefficient on oil recovery using a network model. Their experimental results showed that oil recovery was significantly higher for positive spreading systems than it was for negative systems. Vizika and Lombard (1996) confirmed these results by conducting gas gravity drainage experiments in a sand pack. These results further indicated the importance of continuous oil films in determining oil recovery. Oren et al. (1994) conducted network modeling to test the validity of the three-phase displacement mechanisms. The simulation results showed that the oil recovery for a positive spreading system is independent of the magnitude of the spreading coefficient and that, for a negative spreading system, the oil recovery decreases dramatically as the spreading coefficient becomes more negative. Mani and Mohanty (1997) also conducted tertiary gas

injection experiments on a network micromodel and the results confirmed the above conclusions drawn by Oren et al. (1992, 1994). However, Blunt et al. (1994) put these conclusions in doubt by showing that both spreading and non-spreading oils could form thin oil films. He stated that the recovery is related to the thickness and stability of the oil film. Although most oils spread over water, the oil films formed were only a few molecules thick and the flow through these films did not contribute significantly to the amount of oil produced. The oil layers, which were of the order of one or more micrometers thick, formed between the water and the gas in the crevices or roughness of the pore space. They contributed significantly to the oil flow. The stability of the oil film depends not only on the spreading coefficient, but also on the capillary and intermolecular forces as well as the geometry of the crevice. Blunt et al. (1994), Dong et al. (1995), and Keller et al. (1997) observed the oil layers for spreading and non-spreading oils in micromodel studies.

2.2.3.3. Rock wettability

In a three-phase system, the distribution and mobilization of the waterflood residual oil are affected not only by interactions among the fluids, which is expressed in terms of the spreading coefficient, but also by interactions between the rock and the fluids, which is expressed in terms of rock wettability.

In an oil-wet system, oil occupies all small pores, pore wedges and pore throats as a continuous wetting film. Water and gas are non-wetting phases. Chatzis et al. (1988) and Oren et al. (1994) observed that water doesn't spread on oil because the spreading coefficient of water over oil in the presence of gas is a large negative number. Oren et al. (1994) considered the water to be an intermediate phase and stated that the intermediate phase is always displaced by a double drainage mechanism. However, the recent study of Hui and Blunt (2000) showed that gas is the intermediate phase in most strongly oil-wet media and water is the intermediate phase in weakly oil-wet media. They indicated that the wettability change would result in more possible ways for the

fluids to be distributed. Ten fluid configurations in a single pore for three-phase flow were found in a mixed-wet system.

For different wetting systems, the mechanisms of tertiary gas injection are different. Comparing the oil recovery from both water-wet and oil-wet systems with a positive spreading coefficient of oil over water, Chatzis et al. (1988) obtained lower oil recoveries in an oil-wet network micromodel and in glass beads. Catalan et al. (1994) obtained lower oil recoveries in oil-wet sandstone cores and glass beads. But Oren et al. (1994) reported a higher oil recovery in an oil-wet network micromodel. Kantzas et al. (1993) tested gravity assisted immiscible gas injection using a 2-D network micromodel, glass beads and sandpacks with different wettability. The results of the micromodel tests indicated that oil recovery in oil-wet micromodels was considerably lower than that in the water-wet micromodel. But the results of the glass beads and sandpacks showed that there was no correlation between wettability and the incremental oil recovery obtained using the tertiary gas injection. However, they stated that, for these tests, the oil recovery obtained using gas injection correlated with the oil recovery obtained from waterflooding. Therefore, in general, the incremental oil recovery by gas injection was lower for the oil-wet system than for the water-wet system. Based on their studies, they demonstrated that gravity assisted tertiary gas injection was feasible not only in a water-wet system, but also in oil-wet and mixed-wet systems. Although the mechanisms of tertiary gas injection in a water-wet system are reasonably well understood, the mechanisms of tertiary gas injection in oil-wet or mixed-wet systems are quite complex and not well understood.

2.2.3.4. Oil viscosity

Oil viscosity is a very important parameter in the DDP. A small increase in oil viscosity increases the mobility ratio of the oil/gas dramatically. Higher mobility ratios make it easier to form viscous fingers or an unstable gas front, resulting in a lower sweep efficiency. Therefore, it is generally preferred to conduct gravity assisted tertiary gas injection process in a light oil reservoir.

Although recoveries are not as high in heavy oil reservoirs as in light oil reservoirs, it has been shown that gravity assisted immiscible gas injection can be used also in a heavy oil reservoir (Kantzas et al. 1991). An extensive literature review in Kantzas et al.'s paper demonstrated that the immiscible CO_2 injection process may be an efficient way to recover moderately viscous oils (less than 1,000 cp). A series of experiments was performed on scaled physical models saturated with dead oils that varied in viscosity from 600 cp to 12,700 cp. Horizontal wells were used for oil production. The experimental results showed that the recoveries of the heavy oils varied from 23 % to 46 % of the OOIP. They pointed out also that changing an oil from 2,000 cp to 3,000 cp increased the recovery time by a factor of twenty. Anyway, they showed that gravity assisted gas injection process was a good alternative to thermal methods in the recovery of heavy oil.

2.2.3.5. Reservoir heterogeneity

The porous media constituting oil reservoirs are normally heterogeneous. The effects of macroscopic and microscopic heterogeneities on the tertiary gravity drainage process were investigated by Catalan et al. (1994). Parallel-type macroscopic heterogeneities in the formation were studied by using a model consisting of three distinct zones of equal volume, which were located one on top of the other. The central zone contained the smaller size of beads and had lower permeability than the zones on either side. Even though capillary retention of fluid in the central zone was higher, less oil remained in the central zone at the end of the experiment. The reason is that the oil in the central zone tended to flow towards the adjacent zones where the capillary pressures were lower. Therefore, the growth rate of the oil bank in the adjacent high permeability zones was enhanced by additional oil from the lower permeability zones. Overall, they concluded that parallel-type macroscopic heterogeneities in the formation might have relatively little effect on oil recovery due to tertiary gravity drainage, but that a non-uniform saturation in the core cross-section

was to be expected. They also indicated that microscopic pore scale heterogeneities decreased the recovery efficiency.

2.2.3.6. Three-phase capillary pressure

Three-phase capillary pressure has been considered usually as a function of the total liquid saturation based on the assumption that the capillary pressures in a three-phase system are similar to their two-phase counterparts. However, Dehghani et al. (1989) showed that, at the same gas saturation, gas-liquid capillary pressure in a three-phase system did not correspond to that obtained in a two-phase system on the basis of two and three phase experiments conducted in Berea core plugs. Kalaydjian (1992) indicated that three-phase capillary pressures differ from two-phase capillary pressures because three-phase flow capillary pressures depend on the spreading coefficient through the contact angle. Capillary pressure is a function of the pore radius, interfacial tension, and the contact angle. The contact angle is defined by the three interfacial tensions involved in the three-phase system. Thus, the contact angle in three-phase flow is strongly associated with the spreading coefficient. According to Kalaydjian (1992), if the spreading coefficient is positive, oil spreading over water in the presence of gas results in a zero degree contact angle. In a negative spreading coefficient system, the equilibrium contact angle θ is related to the spreading coefficient $S_{o/w}$ by the following expression:

$$\cos\theta = 1 + \frac{S_{o/w}}{\sigma_{og}}$$

where σ_{og} is the interfacial tension between the oil and the gas. Therefore, the three-phase capillary pressure is a function of the spreading coefficient for a negative spreading coefficient system.

Kalaydjian (1992) showed that the spreading coefficient not only influenced the contact angle, but also affected the capillary pressure threshold and the residual oil

saturation for both drainage and imbibition processes. Based on the results of both core scale and pore scale experiments, he proposed the following expression for the drainage capillary pressure at the irreducible water saturation:

$$P_c = P_{co}(S_{o/w}) + S'_g \alpha \qquad \text{with} \qquad S'_g = \frac{S_g}{1 - S_{wir} - S_{org}}$$

where P_{co} denotes the threshold capillary pressure above which drainage begins. The threshold capillary pressure is a function of the spreading coefficient. Kalaydjian (1992) observed that as the spreading coefficient became more negative, the threshold capillary pressure decreases in a negative spreading coefficient system. In a positive spreading coefficient system, the threshold capillary pressure is related to the zero degree contact angle. He also observed that once the spreading coefficient became negative, the pressure required to drain an oil pocket was doubled.

Based on these observations, it can be concluded that oil spreads over water in the presence of gas and drains through the spreading films. It enables the possibility of a high recovery efficiency by reestablishing hydraulic conductivity and by decreasing the threshold capillary pressure required to displace the oil through a pore throat.

2.2.3.7. Three-phase relative permeability

Three-phase relative permeabilities are required for predicating the oil recovery of the gravity assisted tertiary gas injection process because it involves three-phase flow. Hagoort (1980) pointed out that the oil relative permeability was a critical factor in gravity drainage. Chalier et al. (1995) showed that the three-phase oil relative permeability was a key factor in the evaluation of a gravity assisted tertiary gas injection project.

Because relative permeability depends on fluid saturation and on saturation history, direct measurements of three-phase relative permeabilities are very difficult, time consuming and often yield unreliable results. Thus, the most common way to obtain three-phase relative permeabilities is the estimation of them from the more reliable and readily available two-phase data by using empirical correlations. These correlations include the models proposed by Corey et al. (1956), Stone (1970), Stone (1973), Alemán and Slattery (1988), Baker (1988) and so on. However, several studies, including Fayers and Matthews (1984), Baker (1988), Delshad and Pope (1989), Oak et al. (1990), Oak (1990), Robinson and Slattery (1994) and Hicks and Grader (1996), have shown that these models can not predict three-phase relative permeabilities accurately. Oak (1990) stated that the experimental data indicated that the displacement of trapped oil by gas was an important factor that should be considered in the empirical models. When initiating three-phase flow from two-phase flow, there is a critical oil saturation, and he thinks it should be considered also. Blunt (1999) pointed out that these models had three major limitations. First, they are missing the wettability effect because they were developed for water-wet media only. Second, they fail to account for the trapping of oil and gas for any displacement sequence. Third, at low oil saturations, they disagree with recent experimental results.

Recently, because the physical understanding of three-phase flow at the pore level has been increasing significantly, three-phase relative permeability models have been developed that are suitable for gas gravity drainage. Bourgoyne (1996) showed that the production behavior of the DDP observed in the laboratory by Lepski (1995) can be predicted accurately using a simple power-law relationship between relative permeability and saturation. Jerauld (1997) presented a three-phase relative permeability model for Prudhoe Bay that accounted for oil and gas trapping. Fenwick and Blunt (1997) derived oil relative permeability models that account for oil film flow and showed that, for low oil and water saturations, $k_{ro} \sim S_o^2$ which was consistent with the results of several experiments. Sahni et al. (1998) measured three-phase relative permeabilities for gravity drainage using CT scanning on vertical cores, and found that, at low oil saturations, $k_{ro} \sim S_o^2$ for hexane and octane as the oil phase with

a positive spreading coefficient. At higher oil saturations, $k_{ro} \sim S_o^4$ for both positive and negative spreading coefficient systems. DiCarlo et al. (1998) measured three-phase relative permeabilities for water-wet, oil-wet, and fractional-wet sandpacks using a CT scanning technique. In a water-wet medium, the oil relative permeabilities were consistent with the results of Sahni et al. (1998). In oil-wet media, the oil relative permeability behaved similarly to the water relative permeability in water-wet systems. On the basis of recent three-phase experiments, Blunt (1999) presented an empirical model for three-phase relative permeability. The model is based on saturation-weighted interpolation between the two-phase relative permeability values, which was suggested by Baker (1988). The effects of wettability, changes in hydrocarbon composition, different saturation paths, and the trapping of oil, water, and gas were all included using a self-consistent treatment. He also showed that oil film flow and oil trapping were necessary in the model to predict three-phase oil relative permeabilities accurately at low oil saturations.

2.2.4. Laboratory Studies

Laboratory studies of the gravity assisted tertiary gas injection process have been conducted in different media for different purposes. Consolidated sandstone cores, unconsolidated sand packs and glass beads were used mainly for investigating the overall production characteristics of the process. Glass network micromodels, capillary tubes and transparent cells were used mainly for investigating the pore-level mechanisms of the mobilization of the residual oil after a waterflood. As important parameters in the process, the effect of wettability, spreading coefficient, three-phase capillary pressure and relative permeability were investigated also in these studies.

Although different methods were used to study the tertiary gas injection process, the results have shown commonly that very low residual oil saturations can be achieved by gravity-stable gas injection (Table 2-1). For sandstone cores, the residual oil saturations after gas injection were in the range of 16 % - 22 %, while for unconsolidated sand packs and glass beads, the residual oil saturation was between

1.5% - 16.5 %. For the higher residual oil saturations to water, high recovery efficiencies were obtained for the process. For sandstone cores, the average recoveries ranged between 33.5 % - 70 %. For sand packs and glass beads, the average recoveries varied between 61 % - 90 % with a positive spreading coefficient and between 17 % - 73.5 % with a negative spreading coefficient. For the network micromodels, the average recoveries were between 35.2 % - 74.4 % with a positive spreading coefficient and between 37.6 % - 84.2 % with a negative spreading coefficient.

Observation of the oil recoveries from these studies reveals that only water was produced at the beginning of the gas injection process; afterwards, oil and water were produced simultaneously. The oil production rate increased rapidly while the water production rate decreased, which indicates that an oil bank was formed and was being produced. Subsequently gas breakthrough occurred and the oil production rate began to drop. The gas production rate increased very quickly, while the oil production rate became very low. Usually about half of the waterflood residual oil was produced at this point. By producing the oil at a low rate, and given sufficient time, almost 100 % of the waterflood residual oil could be produced. Kantzas et al. (1988a) recovered 94.7 % of the residual oil with a final residual oil saturation of 0.6 % in their laboratory studies. Some people's experiments were not conducted for a very long period of time so that oil recoveries varied over a wide range. Typically, for strongly water-wet sandstone cores with a positive spreading coefficient, the recoveries by gravity-stable gas injection were around 60 %, and for strongly water-wet glass beads and sand packs with a positive spreading coefficient, the recoveries were from 70 % - 90 %.

2.2.5. Field Studies

Several operators have field tested the DDP and these tests yielded encouraging results. A brief summary of the results obtained in the Hawkins Field project (Exxon Company), the Weeks Island Field project (Shell Company), the West Hackberry Field project (Amoco Company) and the Handil Field project (Indonesia) is presented below. As can be seen in Table 2-2, high recovery efficiencies by the tertiary gas

injection process were clearly attainable. Recoveries of 85 % - 95 % were reported for the first three field projects and an ongoing project in the Handil field obtained an improved oil recovery of 1.2 % OOIP after 3 years of gas injection. These field tests not only proved the feasibility of the process, but also provided some important information for the further application of the process. Among these field tests, steeply dipping beds and high permeabilities were the critical characteristics for gravity assisted gas injection. The recovery efficiencies and the average reservoir rock and fluid characteristics of these fields are listed in Table 2-2.

Hawkins Field

The Hawkins Field (Carlson, 1988) is located in the central portion of the East Texas Woodbine Basin, about 161 km east of Dallas. It's extensively faulted as the result of a deep-seated salt dome. A large NE-SW fault separated the field into two productive areas, the East Fault Block and the West Fault Block. The Dexter sands of the East Fault Block are braid stream deposits, thick, clean and highly permeable with an average permeability of 3400 md. The quality of the sands increases as one moves downward and the sands extend into the Woodbine aquifer, which surrounds the whole field. Consequently, the East Fault Block has produced under a strong water drive since it started production in the 1940's. After Gamma Ray/Neutron logs showed that the oil column had reached the crest of the gas cap, in March 1975, produced gas was injected into the crest of the East Fault Block at an average rate of 20 MMscf/D. Gas injection almost immediately completely converted the water drive into a gas drive as demonstrated by the average net water influx approaching zero. The Dexter oil column in 1975 was about 280 feet thick. After 12 years of gas injection (1987), the thickness was reduced to 25 feet. Fifty-eight million barrels of stock tank oil were produced. A calculation showed that the recovery was about 85 % of the oil in the gas-invaded zone while the recovery by water drive was about 60 %. Thus, 25 % of the additional oil was recovered by gas displacement. Results from three-phase centrifuge

tests and extensive analyses of the gas drive and water drive recovery efficiencies in the Dexter sands confirmed that gas displacing the water invaded oil column could reduce the residual oil saturation from 35 % to 12 %.

Based on the performance of gas injection in the Dexter sands, Carlson (1988) introduced the concept of the "Double Displacement Process" and proposed a double displacement project on the East Fault Block where the production had approached its economic limit. Injecting gas at 33 MMscf/D would move the 25 ft oil column vertically downward through the water invaded oil zone. The oil bank was expected to reach the original oil-water contact after 8 years. Then the gas injection rate would be reduced to match production rates until all of the oil was recovered. Carlson (1988) mentioned that the distribution of the Dexter sand quality would enhance the project. In a water drive, oil was bypassed at the top portion of the sand body where the sand was of poor quality. When the gas arrives, the residual oil drains down at a relatively high rate behind the gas front due to the large density difference and the high vertical permeability, and accumulates at the bottom of the sand body where the sand has a higher quality.

Langenberg et al. (1994) reported on 6 years of performance for the double displacement project carried out in the East Fault Block of the Hawkins Field Unit. They pointed out that sweep and displacement efficiencies could be improved in the DDP by favorable gravity drainage conditions. In other words, the oil recovered in the DDP might come from both the swept and the bypassed oil zones. According to their paper, the East Fault Block DDP was started in August 1987 and gas was injected into six crestal injectors. Oil production at this time was 3700 barrels of oil per day (BOPD). At the end of 1991 the production declined to 1075 BOPD as expected. During the four years of implementation of the DDP, the water cut was relatively constant at 85% and the GOR increased from 4900 to 5300 scf/bbl. The average gas injection rate was 24.5 MMscf/D which was 25 % lower than the proposed rate of 33MMscf/D because of the transition from inert-gas injection to nitrogen injection.

The average GOC moved 81 ft vertically downward and the average OWC moved 91 ft in 3 years. So the gas was displacing liquid at 27 ft/year. This was very close to the original displacement target of 25 ft/year. During the first 3 years, the oil column grew 10 ft in thickness, which was only 50% of the expected growth. Logs showed that the average residual oil saturation in the gas invaded zone did not change until after 2.5 years of gas exposure. Most of the recovery was actually a result of improved sweep efficiency in the areas of the formation previously bypassed by water. The slower than expected gravity drainage process was attributed to a large change of oil viscosity, which had apparently quadrupled from 4 to 16 cp in just 5 years due to a shallow viscous crude existing near the original OWC, and a lower oil relative permeability than expected in poor quality sand where most of the targeted oil was located. Despite these problems, Langenberg et al. (1994) still thought the East Fault Block DDP was a successful project, and described the adjustments made to optimize the operations as well as the expansion plan for the larger West Fault Block.

Weeks Island Field

The Weeks Island field (Johnston, 1988) is located in New Iberia Parish, Louisiana. The typical structure of the Weeks Island reservoirs is a piercement salt dome. Sand quality and continuity are extremely good. The S sand Reservoir B (S RB), which was selected for the gravity-stable CO_2 pilot, is a relatively small reservoir, which is deep, hot and well confined by faulting. The characteristics of the S RB are steeply dipping (26^o) and highly permeable sands with an average permeability of 1.2 Darcies. The oil column was first produced by the expansion of the original gas cap, then later by water injection. In July 1978, before the pilot was started, the S RB still had a relatively thin oil column of 23 ft remaining, and the average residual oil saturation was evaluated to be 22 %.

According to Johnston (1988), the pilot was started in October 1978 by injecting a mixture of CO_2 and methane. In January 1981, the oil column had grown from 23 ft to

57 ft and soon after that production began. The core analyses of a production well indicated that more than 90 % of the residual oil was recovered in the gas invaded zone and the final oil saturation was on average about 1.9 %. It's shown that dilution of CO_2 had little effect on the oil recovery. In 1983, when the gas production rates increased, the produced gas was re-injected together with CO_2. By 1987, the oil recovery had reached 261.5 thousand barrels or 64.1 % of the OIP at the start of CO_2 injection. The pilot was expected to end in 1988 if the cumulative oil production reached 270 M STB, of which 65 thousand barrels of oil came from the 23 ft oil column and 205 thousand barrels of oil from tertiary gas injection. So gravity assisted tertiary gas injection in Weeks Island recovered 60% of the oil remaining after the waterflood.

West Hackberry Field

The West Hackberry field (Fassihi and Gillham, 1993, Fassihi et al., 1996) is a salt dome located in Cameron Parish, southwestern Louisiana. It was discovered in 1924. The primary recovery was strongly affected by an active aquifer at the bottom of the Camerina sands. The reservoir was watered out in January 1993. Due to the aquifer, the oil pressure was maintained above the bubble point pressure of 3295 psi. In the water zone, the residual oil saturation to water was around 26 %. According to Fassihi and Gillham (1993) and Fassihi et al. (1996), the overall recovery by natural water drive was 50 % - 60 % of the OOIP. Field performance indicated that oil recovery by gravity drainage could reach 90 % of the original oil in place. The high-pressure (2,500 - 3,300 psi) reservoir targeted for the air injection project was the Camerina C-1, 2, 3 sands on the west flank of the field. Similar to Weeks Island, the reservoir is permeable and steeply dipping with a dip angle from 23 to 35 degrees. However, the ongoing West Hackberry project is different from previous tests because it combined the Double Displacement Process with Air Injection. Air as an inexpensive injectant contributed to the economic success of the project, and the flue

gas and heat generation from in-situ combustion also played a role in the tertiary oil recovery process.

Air injection was started in November 1994, and by January 1996, 730 MMscf of air had been injected. A production response was expected during 1997. Combustion was proved, but high corrosion rates on the air injectors had affected the injection of air.

The air injection process was also implemented in some of the low-pressure (300 - 600 psi) reservoirs on the north flank of the West Hackberry field. These reservoirs had large gas caps and thin oil rims with limited water influx. Air was injected to push the oil rims downward to the production wells. Gravity drainage or partial DDP caused very low oil saturations. Gillham et al. (1997, 1998) reported on the performance of air injection in small reservoirs A and B. In reservoir A, air injection began in July 1996 while in reservoir B it began in December 1996. By May of 1997, oil production from the two low-pressure reservoirs had increased 60 % above the normal decline of 300 BOPD to 424 BOPD.

The economic evaluation of these air injection projects by Fassihi et al. (1996) concluded that air could provide considerable enhancement to the economic success of tertiary gas injection.

Handil Field

The Handil field (Gunawan and Caié, 1999) is a simple anticline located in the Mahakam Delta of the island of Borneo, Indonesia. More than 500 hydrocarbon accumulations were discovered. They were divided vertically into a Shallow Zone (300 - 1,500 m), a Main Zone (1,500 - 3,000 m), and a Deep Zone (below 3,000 m). The geology of the field is complex. Rock properties are quite variable. Structural dip ranges from 5 to 12 degrees. Aquifers surrounding the field are very strong in the

Shallow Zone, but relatively weak in the Main and Deep Zones. So water injection was initiated shortly after the natural depletion of these zones.

At the end of 1995, five reservoirs of the Main Zone had reached the end of their waterfloods with an average oil recovery factor of 58 %. They were selected for crestal lean gas injection. These reservoirs represented 20 % of the field's total OOIP, and the original oil columns ranged from 120 m to 185 m, and the permeabilities ranged from 100 md to 2,000 md. Logging data indicated that water had flooded the reservoirs up to the original GOC so that no mobile oil rim existed before gas injection. The residual oil saturation in the water invaded zone was around 28 %. A tertiary gas injection project was started in November 1995. Gunawan and Caié (1999) reported on the project performance of the first 3 years. After 3 years of gas injection, the gas cap had expanded between 35 m and 75 m below the original GOC. The cumulative oil production had reached 3.6 MM STB of oil, which is equivalent to 1.2 % of the OOIP. Gunawan and Caié (1999) showed that the tertiary gas injection project was a success both technically and economically. They also pointed out that control of the areal and vertical sweep by a stable gas front was key to the success of the project. The good production response led to the gas injection project being extended to six more reservoirs in 2000. And 30 MM STB of oil was predicted to be recovered by the tertiary gas injection from the 11 reservoirs in 15 years.

Table 2.1: Oil recoveries of tertiary gas injection process

Study	Media	Wettability	Spreading Coefficient o/w	Average Final Oil Saturation, %	Average Oil Recovery, %
Kantzas et. al. (1988a)	glass beads	Water-wet	*	1.5	90
Kantzas et. al. (1988a)	Berea core	Water-wet	*	*	60
Naylor and Frorup (1989)	sandstone core	Water-wet	*	14	70
Catalan et. al. (1992)	sandstone core	Water-wet	*	16.5	59
Catalan et. al. (1992)	sandstone core	oil-wet	*	20	33.5
Catalan et. al. (1992)	glass beads	Water-wet	+	2.0	87.5
Catalan et. al. (1992)	glass beads	Water-wet	-	16.9	17.3
Catalan et. al. (1992)	glass beads	oil-wet	+	12.7	63.5
Oren et. al. (1994)	network	Water-wet	+17.7	*	35.2
Oren et. al. (1994)	network	Water-wet	-8.1	*	17.6
Oren et. al. (1994)	network	oil-wet	+17.7	*	74.4
Oren et. al. (1994)	network	oil-wet	-8.1	*	84.2
Lepski (1995)	sand pack	Water-wet	*	*	61
Lepski (1995)	Berea core	Water-wet	*	22	38

Note: * means the value was not reported.

Table 2.2: The reservoir and fluid properties for several field projects

Properties	Hawkins Dexter sand	Weeks Island S RB	W. Hackberry Cam C1-C3	Handil Main Zone
Porosity ϕ, %	27	26	27.6~23.9	17~25
Permeability k, md	3400	1200	300~1000	100~2000
Connate water S_{wc}, %	13	10	19~23	15~19
S_{orw}, %	35	22	26	28
S_{org}, %	12	1.9	8	*
Reservoir Temp., °F	168	225	205~195	*
Bed Dip Angle, degrees	8	26	23-35	5~12
Pay Thickness, ft	230	186	31~30	120~185 m
API Gravity, °API	25	32.7	33	31~34
Viscosity, cp	3.7	0.45	0.9	0.6~1.0
Bubble Point Pressure, psi	1985	6013	3295	2800~3200
GOR, SCF/STB	900	1386	500	2000
Oil FVF at BPP	1.225	1.62	1.285	1.1~1.4
Water-drive Recovery, % OOIP	60	60~70	60	58
Gas Injection Recovery, % OIP	85	95	90	59.2 (3 years)

Note: * means the value was not reported

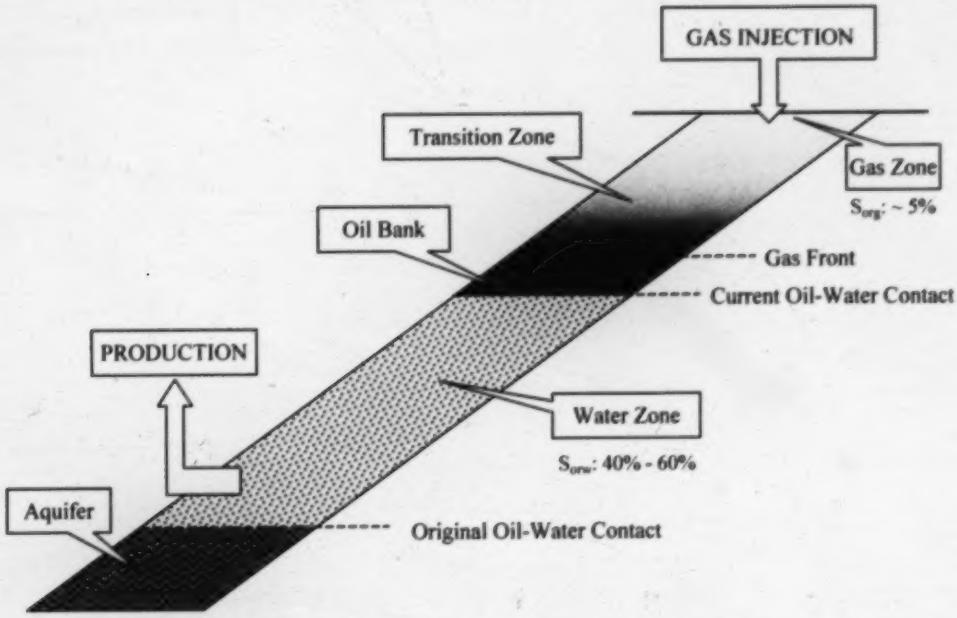

Figure 2.1: Schematic diagram of the DDP

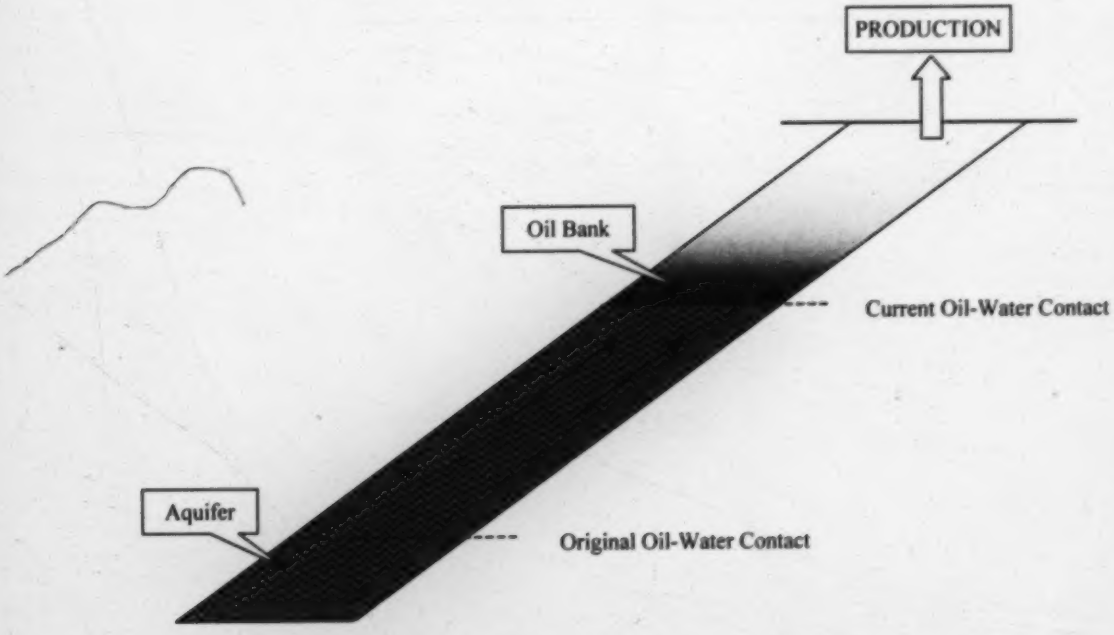

Figure 2.2: Schematic diagram of the SCWD process

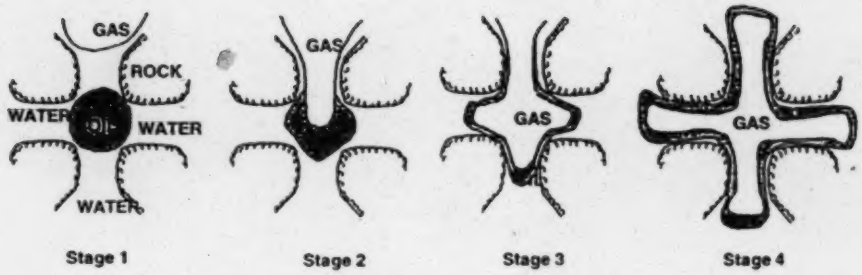

Figure 2.3: Single pore scale gas displacement of trapped oil (after Lepski)

CHAPTER 3

RESERVOIR SIMULATION

Numerical reservoir simulation can help in understanding the mechanisms underlying the double displacement process (DDP) and the second contact water displacement (SCWD) process at the reservoir scale. Numerical simulation can be used to investigate also the effects of various parameters on the performance of the gravity assisted tertiary gas injection process. These parameters may include three-phase relative permeability, absolute permeability, reservoir dip angle, injection and production rates, oil viscosity and API gravity, and rock wettability as well as the oil-gas, oil-water and water-gas interfacial tensions and capillary pressures. Faycel Bensaid (1995) investigated the effects of reservoir dip angle, absolute permeability and relative permeability on oil bank growth rate and oil drainage rate in the DDP by using the IMEX 300 CMG reservoir simulator. The simulation results indicated that the higher the dip angle the higher the maximum drainage rate, and the higher the absolute permeability, the shorter the time it took to recover a given amount of residual oil. The effect of the absolute permeability on the performance of the immiscible DDP was larger than that of the dip angle. A closed, homogeneous and anisotropic, cross-sectional dipping porous model was used in these simulations. The closed system implies that there was neither fluid injection nor fluid withdrawal; that is, fluids in the system were in counter-current flow. In practice, counter-current flow in these processes rarely takes place. Therefore, these parameters need to be revisited, and the effects of some other parameters need to be studied. Injection and production rates affect significantly the oil drainage rate so that they need to be considered as well. The three-phase relative permeability, as an essential parameter in tertiary gas injection, needs to be studied further.

The main objective of this reservoir simulation study is to investigate the effects of injection and production rates, reservoir dip angles, three-phase relative

permeabilities and capillary pressures on the DDP. Another objective is to investigate the feasibility of the SCWD process. A new version of the IMEX CMG black oil numerical simulator (CMG, 2000) is used here to conduct the study. A three-dimensional, homogeneous, anisotropic reservoir model with injection and production wells was constructed. The injection and production wells were perforated according to the production strategy. All the reservoir properties were taken from a summary of several fields in which the DDP was employed. The simulations were started at the end of waterflooding. In other words, the reservoir had been swept completely by water at the beginning of the DDP simulations. An initial oil saturation uniformly distributed over the whole reservoir was used, and an adjustment was applied so that the conditions in the reservoir were the same as those that pertain to a reservoir which had been subjected to a waterflood.

3.1. Reservoir Model

The reservoir model selected for simulation of the DDP and the SCWD process is a homogeneous, anisotropic, three-dimensional system consisting of 9000 grid blocks (Figure 3.1). Each block is 10 ft long, 10 ft wide and 6 ft high, so that the reservoir is 1800 ft in the X-direction, 100 ft in the Y-direction and 30 ft in the Z-direction. With a porosity of 25%, the total pore volume (PV) of the reservoir is 1,350,000 ft^3. The absolute permeability is 1500 md in the X and Y directions and 800 md in the vertical direction. The reservoir dip angles used were 8^o, 30^o and 60^o. All the reservoir and fluid properties are listed in Table 3.1. The values of these properties are based on several fields: the West Hackberry oil field (Louisiana), the Hawkins oil field (Texas), the Weeks Island oil field (Louisiana) and the Handil oil field (Indonesia), in which up-dip gas injection was undertaken. Because the DDP and the SCWD process are conducted in reservoirs after waterflooding, the initial conditions were set to be the same as those existing in the reservoir at the end of the waterflood.

With respect to the initial conditions, it's assumed that the homogeneous reservoir is completely swept by the water and that the initial oil saturation and pressure are

uniformly distributed over the whole reservoir. However, in the DDP, mobile oil comes not only from the gas invaded water zone, but also from areas bypassed by the waterflood. To add this bypassed oil, the initial oil saturation was set slightly higher than the residual oil saturation to water; that is, $S_{oi} = 30\% > S_{orw} = 25\%$. Then, the reservoir simulator was set to run without injection and production for two simulation years so that phase stabilization was reached in the reservoir, and so that the distributions of reservoir pressure, fluid saturations, and other fluid properties were closer to the conditions that would pertain at the end of a waterflood. The reservoir pressure distribution and oil saturation distribution at this point are shown in Figures 3.2 and 3.3. Note that the oil saturations are higher in the upper layer than in the lower layers; consequently, the water saturations are higher in the lower layers. This is the case because the effect of gravity is to displace water more efficiently in the lower part of the reservoir as compared to the upper part of the reservoir. When this stabilization process is completed, the DDP is initiated. To ensure that this is an immiscible displacement, nitrogen is used for gas injection in the DDP.

3.2. Reservoir Simulation

The DDP was simulated primarily to investigate the effects of various parameters on the up-dip gas injection process. Initially, the injection and production rates were studied to determine the maximum drainage rate and the highest oil recovery. The effect of reservoir dip angles was also studied. Placement of the perforations in the production wells was studied to ascertain the impact of perforation strategy on oil recovery. Then the oil relative permeability and capillary pressure were studied to observe their effects on oil recovery efficiency. After carrying out these sensitivity studies on the DDP, the SCWD process was simulated to determine the feasibility of the process. For each process, a basic simulation data set is presented in Appendices A and B.

3.2.1. Injection and Production Rates

The reservoir model with a dip angle of 8 degrees was used for different injection and production rates. The initial average reservoir pressure was 3000 psi. To avoid mass transfer taking place, and to maintain an immiscible displacement, the average reservoir pressure during the process was constrained to change over only a small range. This was achieved by setting the maximum bottom hole pressure (BHP) of the injection wells at 3100 psi, a value that was only slightly higher than the average reservoir pressure. Also the minimum BHP of the production wells was set equal to the initial reservoir pressure.

Five sets of injection and production rates were selected to show their effects on the DDP. Table 3.2 lists the maximum injection and production rates for the reservoir simulations in the order of the slowest rates to the fastest rates. For simplicity, Jan. 1, 1990 was selected as the beginning of the gas injection. The oil distributions after one year (1991), four years (1994) and ten years (2000) of gas injection are presented in Figures 3.4 - 3.15. Note that, in these figures, the oil bank appears to be unconnected because an insufficient number of grid blocks was used in the Z direction. This situation arose because the commercial CMG simulator used permits only a limited number of blocks for simulation. The reservoir dip angle, the maximum injection rate (Ri) and the maximum production rate (Rp) are given in the information box for each figure.

The oil saturation results (Figures 3.4 - 3.8) show that the oil bank starts to form after one year of gas injection (1991). Moreover, the shapes of the oil banks change with different gas injection rates. That is, as the rate decreases, the gas-oil front becomes flatter. After four years of gas injection (1994), the oil banks formed show nearly flat shapes in reservoirs with injection rates less than or equal to 20,000 ft^3/day (Figures 3.9 - 3.12). But for a reservoir with an injection rate of 30,000 ft^3/day (Figure 3.13), gas broke through, resulting in a gas flood, not a DDP, because gravity did not dominate the process. After ten years of gas injection (2000), the oil bank had moved

to the bottom of the reservoir for an injection rate of 15,000 ft^3/day (Figure 3.16). However, for lower injection rates (Figures 3.14 and 3.15), the oil bank had only moved slowly down to the middle of the reservoir. For higher injection rates (Figures 3.17 and 3.18), gas breakthrough had already occurred. The cumulative oil production curve for each setting is given in Figures 3.19 - 3.23. In addition, the oil production rate and gas oil ratio (GOR) curves are given in Figures 3.24 - 3.28. After 26 years of gas injection (2016), for the slowest rate, Setting 1, not much oil was produced because the oil bank didn't reach the production wells. For the rest of the rate settings, the cumulative oil production by year 2016 falls between 30,000 bbl and 40,000 bbl. It can be seen also that the higher the rate setting, the larger the cumulative oil production. However, the gas oil ratio curves show that the higher the rate setting, the earlier the gas breakthrough and the faster the GOR increases. The amount of produced gas is related to the economic success of the process. A fast increase in GOR brings an early end to the gas injection process. If a GOR of 30,000 ft^3/bbl is taken to be an acceptable upper limit, rate Settings 2 and 5 result in unacceptable oil recovery performances. Setting 2 is too slow because the cumulative oil production is low and the oil production rate and GOR curves (Figure 3.25) show that the main oil production period is still not finished by the year 2016. Setting 5 is too fast because the oil production rate and GOR curves (Figure 3.28) show that a GOR of 30,000 ft^3/bbl is exceeded soon after the oil production begins. Both Setting 3 and 4 are acceptable because they both result in about 34,000 bbl of oil being produced by the time the GOR reaches 30,000 ft^3/day (Figures 3.26 and 3.27). Setting 4 requires less time than Setting 3 to recover the same amount of oil. However, the injection and production rates for Setting 4 don't result in the maximum oil drainage rate for the tertiary gas injection process. This is because the oil recovery of the DDP with Setting 4 is enhanced significantly by where the production wells are perforated, an issue which is discussed in the next section.

These results indicate that the injection and production rates play a very important role in controlling the formation of the oil bank, the shape of the oil-gas front and the oil drainage rate in the reservoir. So, once a candidate reservoir for the gravity assisted

tertiary gas injection process has been selected, the injection rate and production rate can be adjusted to achieve the maximum oil drainage rate.

3.2.2. Production Strategy: Perforation of Production Wells

Where the production wells are perforated can make a difference in the amount of oil recovered by the gravity assisted tertiary gas injection process. In the previous simulations, the production wells were perforated only next to the three lower layers so that the upper two layers comprising a total of 12 ft were closed to the production wells. This case is called the *partially perforated well case* in this study. The case in which the production wells were perforated next to all five layers is called the *totally perforated well case*. Settings 3 and 4 were used for simulations with totally perforated wells. The effect of the perforation strategy can be observed easily in Figures 3.29 to 3.35. In the totally perforated well case (Figures 3.30 and 3.31), there is still, in year 2016, a significant amount of oil left in the lower layers because the gas moved directly to the production well through the top layer without displacing any oil. In the partially perforated well case (Figure 3.29), very little oil is left in the two lower layers. This is because, when gas reaches the production well, gas accumulates in the top layers and pushes oil down to the bottom layers because of the density difference. Thus, more oil is recovered from the partially perforated production wells than from the totally perforated production wells. The oil production rate and gas oil ratio curves indicate that the oil production rate is lower, and the time when the GOR surpasses 30,000 ft^3/bbl is earlier, in the totally perforated well case. Comparing the cumulative oil production curves for both cases for Setting 3 (Figures 3.21 and 3.32), the difference in oil recovery at the end of the process is about 5000 bbl. For Setting 4 (Figures 3.22 and 3.34), the difference in oil recovery at the end of the process is about 7000 bbl. Therefore, perforating only the lower part of the production wells can improve the oil recovery of the gravity assisted tertiary gas injection process. This perforation strategy has a more significant effect when higher injection and production rates are used.

For simplicity, totally perforated production wells and the injection and production rates listed for Setting 3 are used for the rest of the reservoir simulation studies.

3.2.3. Reservoir Dip Angle

The reservoir dip angle is studied here to see its effect on the injection rate and the incremental recovery. Three angles were used: 8°, 30° and 60°. In simulations of a steeply dipping reservoir, using the Corner Point grid method can better define contact faces and transmissibility than using the rectangular Cartesian grid method. Thus, the corner point grid method can provide more accurate results for dipping reservoirs, especially with respect to the oil production. The higher the dip angle, the more accurate the results. Therefore, the corner point grid method was used for simulations of three different angles. The results of these simulations (Figures 3.36 to 3.40) show that the injection rate needed to achieve the maximum oil drainage rate increases as the angle of dip increases, and that, consequently, the DDP operating time decreases. In a reservoir with a dip angle of 8° (Figure 3.36), the oil bank reaches the production wells after 10 years of operation. With dip angles of 30° and 60° (Figures 3.37 and 3.39), the oil bank is still in the middle of the reservoir. A higher injection rate of 20,000 ft^3/day is used for a dipping reservoir with an angle of 30° (Figure 3.38). The time required for the oil bank to reach the production wells with a very good shape is only 8 years. Moreover, in a dipping reservoir with an angle of 60° (Figure 3.40), when an injection rate of 25,000 ft^3/day is used, the time for the oil bank to reach the production wells is only 6 years. The flat shape of the oil bank, when a high injection rate is used, indicates that the gravity effect is enhanced by the high angle of the reservoir dip. Therefore, a highly dipping reservoir is a more favorable candidate for the gravity assisted tertiary gas injection process; the higher the angle, the better the performance of the process.

It was found that, for a low dip angle of 8°, a simulation using the Corner Point grid method or using the rectangular Cartesian grid method had identical results with

respect to the oil saturation distribution and the oil production. So, for simplicity, the rectangular Cartesian grid with a dip angle of 8° was used for the rest of the reservoir simulation studies.

3.2.4. Oil Relative Permeability

Oil relative permeability is a key parameter in the gravity assisted gas injection process. Because this process involves gas, oil and water, the three-phase oil relative permeability should be the one that is utilized in the simulation. It has been shown that the three-phase relative permeability is not only a function of the phase saturation, but also a function of the phase saturation history. Due to the complexities of three-phase fluid flow, the measurement of three-phase relative permeabilities is very difficult and the results are often not reliable. Therefore, the most common methods used to obtain three-phase relative permeabilities are correlations based on two-phase relative permeabilities. These methods include Corey's method (Corey et al., 1956), Stone 1 (Stone, 1970) and Stone 2 (Stone, 1973) methods, Baker's method (Baker, 1988) and so on. Although these methods also give unsatisfactory results, they have the advantage that they can be used easily for reservoir simulation. Moreover, the cost of obtaining three-phase relative permeabilities from two-phase data is significantly less than the direct measurement of three-phase relative permeabilities in the laboratory. The empirical model proposed recently by Blunt (1999) is probably the best model to date for obtaining three-phase relative permeabilities for use with the DDP; unfortunately, the CMG reservoir simulator does not provide it.

Only four methods for evaluating the three-phase oil relative permeability are provided by the CMG reservoir simulator. These are the Stone 1 Model and the Stone 2 Model, both of which have been normalized by Aziz and Settari (1979), the Linear Isoperm Model and the Segregated Model, both of which have been proposed by Baker (1988). Typical two-phase relative permeability curves for a water-wet formation are shown in Figures 3.41 and 3.42. Using these two-phase relative permeability curves, the four methods listed above were used in simulations of the

DDP. The simulation results after ten years of gas injection are given in Figures 3.43 to 3.46, and the cumulative oil production curves for year 2016 are given in Figures 3.47 to 3.50. Obviously, the simulations using the Stone 1, Linear Isoperm and Segregated Methods have similar results. When using these methods, the oil bank is very close to the production wells after ten years of gas injection. Moreover, the transition zone between the oil bank and gas zone is very short. In addition, the oil saturation of the gas zone is already close to the residual oil saturation to gas (S_{org} = 0.05) in year 2000. Finally, the cumulative oil production by year 2016 is above 50,000 bbl. The only difference among the three methods is that with the Linear Isoperm method, the oil production by year 2016 is slightly lower and the gas zone in the bottom layer is shorter than the other two methods. However, the results of the simulation using the Stone 2 method are quite different from the other three. When using the Stone 2 method, the oil bank has already reached the production wells after ten years of gas injection. Moreover, the transition zone between the gas zone and oil bank is much longer. Finally, the oil saturation in the gas zone is between 0.12 and 0.13 in year 2000. Therefore, the cumulative oil production by year 2016 is much lower, around 34,000 bbl, than the other three methods. The gradual decreasing of oil saturations in the region above the oil bank and the longer transition zone result in the oil distribution of the simulation using the Stone 2 method being close to the laboratory observation of the DDP described by Kantzas et al. (1988b). Therefore, the Stone 2 method was used for the other simulations in this study. However, it's difficult to determine whether the Stone 2 method can predict reliably the three-phase oil relative permeability for the tertiary gas injection process. This is because oil film flow affects significantly the three-phase oil relative permeability in the low oil saturation region. Therefore, due to oil film flow, a gas zone with an oil saturation lower than 10% should appear at the top of the reservoir. Moreover, oil saturations above the oil bank should differ with time and distance, depending on the drainage rate of the oil film flow.

Although these methods may not provide representative results for three-phase relative permeabilities, the simulation results indicate that different oil relative

permeabilities result in different oil recoveries for the gravity assisted tertiary gas injection process. Moreover, it appears that accurate three-phase oil relative permeabilities in the low oil saturation region are a necessity, if accurate predictions of oil recoveries by reservoir simulation are to be achieved.

End-point saturations can have a significant effect on the relative permeability curves generated by the different methods. Two different sets of end-point saturations (Table 3.3) were used to generate different two-phase relative permeabilities. In Setting 2, the connate water saturation (S_{wc}) was set to be 0.30, two times the value of S_{wc} used in Setting 1, for a strongly water wet formation. The oil saturation after gas flooding (S_{org}) was set to be 0.25, a value much larger than the value of S_{org} used in Setting 1. The two-phase relative permeability curves for Setting 1 are shown in Figures 3.41 and 3.42. The curves for Setting 2 are shown in Figures 3.51 and 3.52. With these curves, the Stone 2 method was used to predict three-phase relative permeabilities.

The 2D results for oil distribution after ten years of gas injection are shown in Figures 3.53 and 3.54. For Setting 1, the oil saturation in the oil bank may be as high as 0.80, while in the gas zone it falls between 0.10 and 0.20, with most values falling between 0.15 and 0.20. For Setting 2, the oil saturation in the oil bank falls between 0.30 and 0.40, with most values falling between 0.30 and 0.35. The shape of the oil bank is undesirable, and in the gas zone, the oil saturation is so high that a significant amount of oil is left in the reservoir after ten years of operation. The oil saturation in the gas zone is related to the value of the residual oil saturation to gas. Therefore, with Setting 2, the high value of S_{org} results in a poor performance of the DDP. From these results, the conclusion can be drawn that the end-point saturation values, especially the value of the residual oil saturation to gas, can influence significantly the simulation results of the DDP. It can be inferred also that relative permeability plays a very important role in the gravity assisted tertiary gas injection process.

3.2.5. Capillary Pressure

Capillary pressure is another important parameter that can affect significantly the oil recovery efficiency of the DDP. Moreover, three-phase capillary pressures should be used because the tertiary gas injection process involves three-phase flow. However, due to knowledge limitations and to the limited settings available in the CMG IMEX reservoir simulator, two-phase capillary pressures were used. Normally, to simplify the multiphase fluid problem, the capillary pressure is neglected. That is, prior simulations have set the capillary pressures to zero. However, it has been shown that capillary pressure is very important in tertiary gravity drainage (Kalaydjian, 1992). Therefore, capillary pressures were studied here to see what kind of impact they have. The water-oil and gas-oil capillary pressures are shown in Figures 3.55 and 3.56. The simulation results are shown in Figures 3.58 and 3.60. These results are compared with the results obtained when the capillary pressure is set equal to zero (Figures 3.57 and 3.59).

Obviously, neglecting the capillary pressure results in a longer process operating time and yields an optimistic oil recovery. Without capillary pressure, the oil bank reaches the production well after ten years of gas injection. The amount of oil left behind the gas-oil front is lower but in the oil bank it is higher, and the shape of the oil bank is too good to be true. With capillary pressure, it only takes eight years for the oil bank to reach the production wells. The 2D simulation results (Figures 3.58 and 3.60) indicate that, with capillary pressure, the transition zone located between the gas zone and the oil bank is much longer than that without capillary pressure. The oil saturation in the transition zone is between 0.20 and 0.25, and in the oil bank it is between 0.50 and 0.60. Without capillary pressure, the oil saturation in the transition zone is between 0.10 and 0.20, and in the oil bank it is between 0.70 and 0.80. Therefore, neglecting capillary pressure results in a higher oil recovery.

The above results and conclusions are based on simulations using two-phase capillary pressures. However, according to Kalaydjian (1992), three-phase capillary

pressures are different from two-phase capillary pressures, and the three-phase capillary pressure thresholds are a function of the spreading coefficient. So, for a positive spreading coefficient system, the possibility of oil being displaced through porous media is much better in the presence of a third phase than when only two phases are flowing. Therefore, the performance of the DDP simulation with three-phase capillary pressures should be better than that with two-phase capillary pressures. Moreover, the true performance of the tertiary gas injection process should fall between the cases with and without two-phase capillary pressure.

3.2.6. Second Contact Water Displacement Process

The SCWD process is an extension of the DDP. It is introduced to shorten the operating time of the DDP by implementing a second waterflood after the main oil production of the DDP. Therefore, the SCWD process was simulated based on the results from the DDP simulations. The second waterflood of the reservoir was implemented by injecting water from the bottom of the reservoir immediately after stopping the gas injection.

The performance of the DDP, with the injection and production rates for Setting 3 and totally perforated wells, has been shown before (Figures 3.32 and 3.33). In this DDP, the main oil production occurred between years 2000 and 2005. After year 2005, the oil production rate became quite low. Based on this, simulations of the SCWD process were started at the beginning of year 2006, when gas injection was stopped and water injection was begun.

The first attempt to test the viability of the SCWD process obtained negative results. The cumulative oil production curve (Figure 3.61) shows there is no oil production after the second waterflood. The oil distributions before and after the SCWD process (Figures 3.62 and 3.63) indicate that the mobile oil was trapped again in the water column when the injected water displaced the oil upward. This may be because the value of the residual oil saturation to water (S_{orw} = 0.25) was higher than

that of the residual oil saturation to gas (S_{org} = 0.05). However, there is an interesting result shown in Figure 3.63. At the bottom of the reservoir where the gas did not invade, the oil saturation was between 0.25 and 0.30. But in the area where the gas invaded, the oil saturation was between 0.2 and 0.25. The difference between the oil saturations in the two regions is close to the value of the irreducible gas saturation (S_{gc} = 0.05). This may suggest that, during the SCWD process, the trapped gas occupies some pore space normally occupied by trapped oil. This can be explained by noting that in the DDP after most of the oil bank has been produced, gas occupies the center of the pore space while oil exists as an oil film. When the second water invasion takes place, the gas is trapped in the center of the pore space and the oil is displaced by the water, causing it to flow through the oil films towards the production wells. Therefore, the residual oil saturation after the SCWD process is less than the residual oil saturation to water. If more gas can be trapped, a smaller amount of oil will be left after the SCWD process. An irreducible gas saturation of 15 percent was then used to run the simulation of the SCWD process again. The results are shown in Figures 3.64 to 3.66. The cumulative oil production curve shows that, under these conditions, the SCWD process was successful. Although the oil recovered by the SCWD process is not as high as the DDP (Figure 3.32), it still recovers a considerable amount of oil. The oil distributions before and after the SCWD process (Figures 3.65 and 3.66) show that the mobile oil wasn't trapped again in the water column, and that the oil saturation in the region where gas had invaded is between 0.1 and 0.15. This confirms that the gas trapped in a reservoir can affect the SCWD process significantly. However, this effect also depends on the type of gas used and the reservoir pressure change. This is because natural gas can dissolve easily into oil with a small increase in pressure, and because the gas volume can be compressed significantly by a large increase in pressure. Therefore, it is important to note that this process is an immiscible process. Overall, for situations where the source of gas is not sufficient, and where the formation has a high irreducible gas saturation, the SCWD process is a good choice.

Table 3.1: The reservoir simulation data selected from several field projects

Properties	Simulation Data	West Hackberry Cam C1-C3	Hawkins Dexter sand	Weeks Island S RB	Handil Main Zone
Porosity ϕ, %	**25**	27.6-23.9	27	26	25
Permeability k, md	**1500**	300-1000	3400	1200	10-2000
Connate water S_{wc}, %	**15**	19-23	13	10	22
S_{orw}, %	**25**	26	35	22	*
S_{org}, %	**5**	8	12	1.9	*
Reservoir Temp., °F	**200**	205-195	168	225	*
Bed Dip Angle, degrees	**8, 30, 60**	23-35	8	26	5-12
Pay Thickness, ft	**100**	31-30	230	186	15-25m
API Gravity, °API	**32**	33	25	32.7	31-34
Viscosity, cp	**0.9**	0.9	3.7	0.45	0.6-1.0
Bubble Point Pressure, psi	**3000**	3295	1985	6013	2800-3200
GOR, SCF/STB	**1000**	500	900	1386	2000
Oil FVF at BPP	**1.25**	1.285	1.225	1.62	1.1-1.4
Water-drive Recovery, % OOIP	**65**	60	60	60-70	58

Note: * means the value was not reported

Table 3.2: The maximum injection and production rate settings

Setting No.	Maximum injection rate Ri (ft^3/day)	maximum production rate Rp (bbl/day)
1	8,000	800
2	10,000	1,000
3	15,000	1,000
4	20,000	1,000
5	30,000	1,500

Table 3.3: Two end-point saturation settings

Setting No.	S_{wc}	S_{gc}	S_{orw}	S_{org}
1	0.15	0.05	0.25	0.05
2	0.30	0.00	0.25	0.25

Figure 3.1: Reservoir model

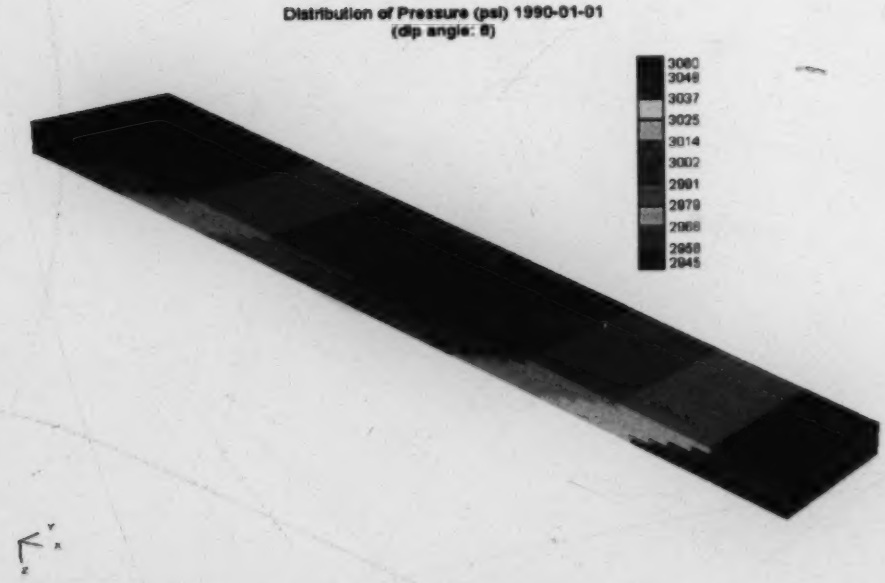

Figure 3.2: Stabilized pressure distribution

Figure 3.3: Oil saturation distribution at the end of waterflood

Figure 3.4: Oil distribution after one year of DDP with Setting 1

Figure 3.5: Oil distribution after one year of DDP with Setting 2

Figure 3.6: Oil distribution after one year of DDP with Setting 3

Figure 3.7: Oil distribution after one year of DDP with Setting 4

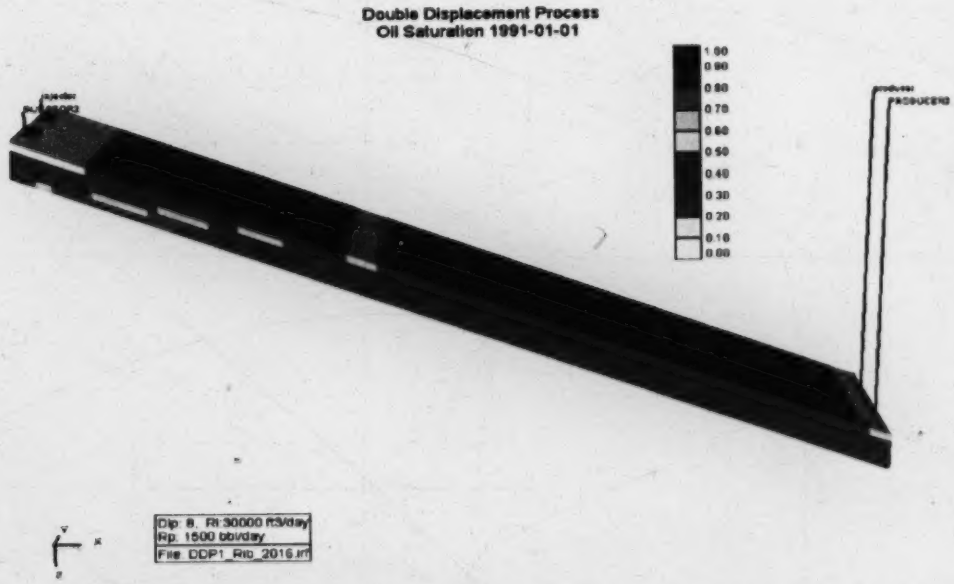

Figure 3.8: Oil distribution after one year of DDP with Setting 5

Figure 3.9: Oil distribution after four years of DDP with Setting 1

Figure 3.10: Oil distribution after four years of DDP with Setting 2

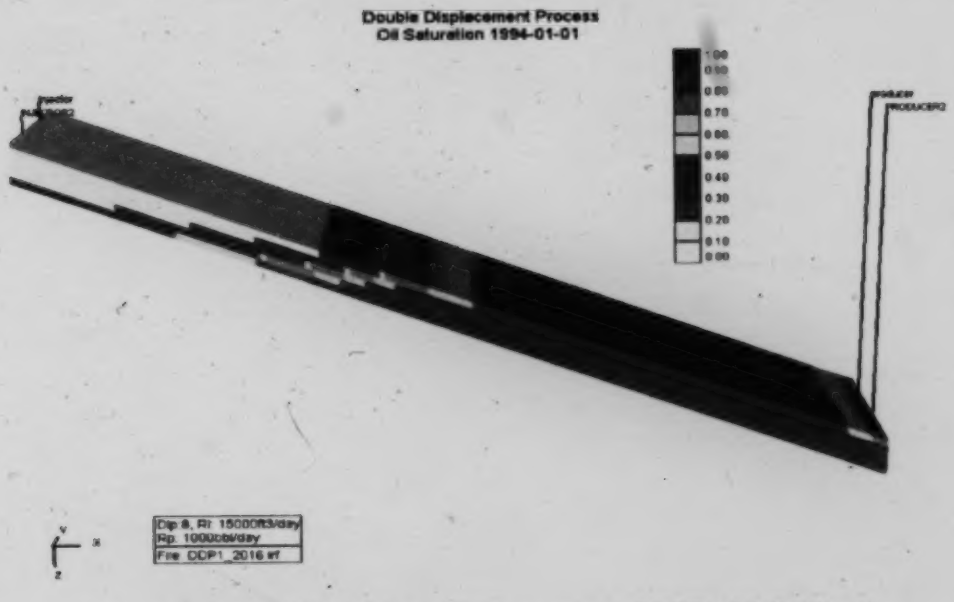

Figure 3.11: Oil distribution after four years of DDP with Setting 3

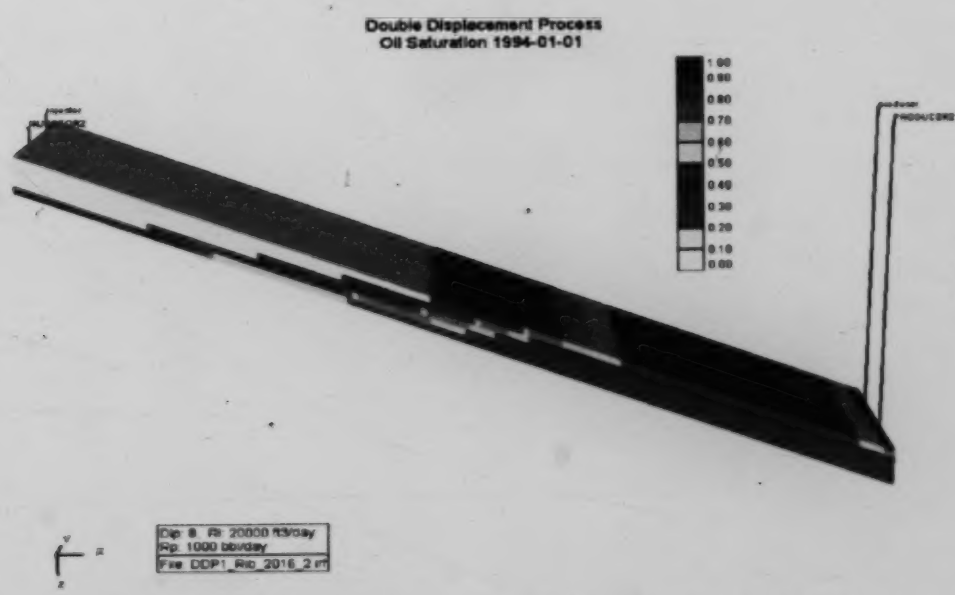

Figure 3.12: Oil distribution after four years of DDP with Setting 4

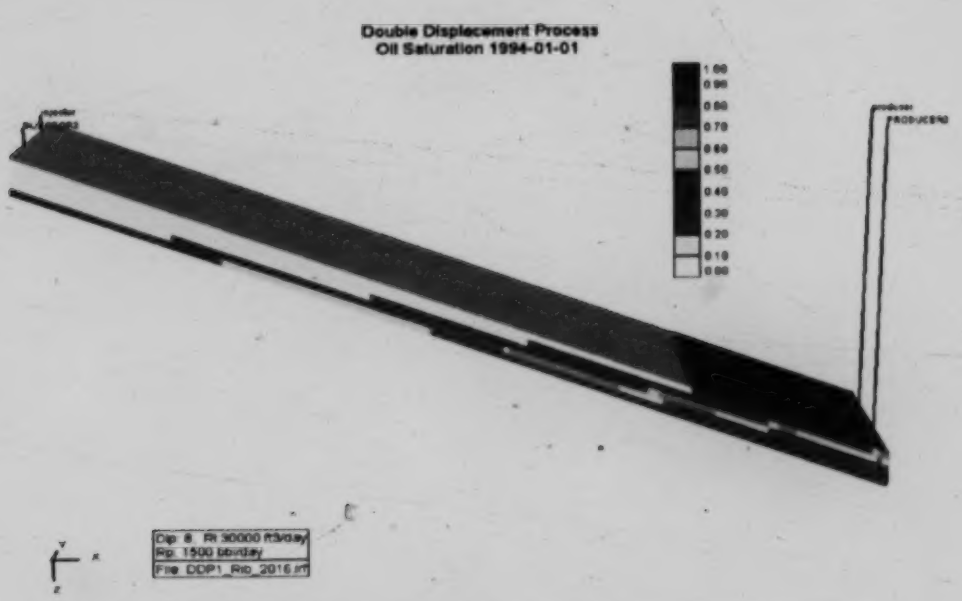

Figure 3.13: Oil distribution after four years of DDP with Setting 5

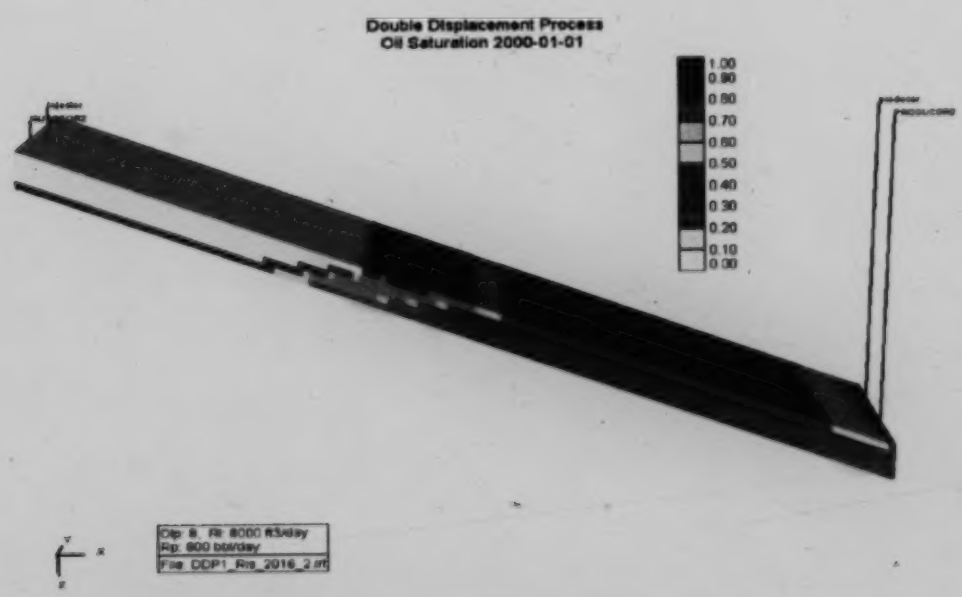

Figure 3.14: Oil distribution after ten years of DDP with Setting 1

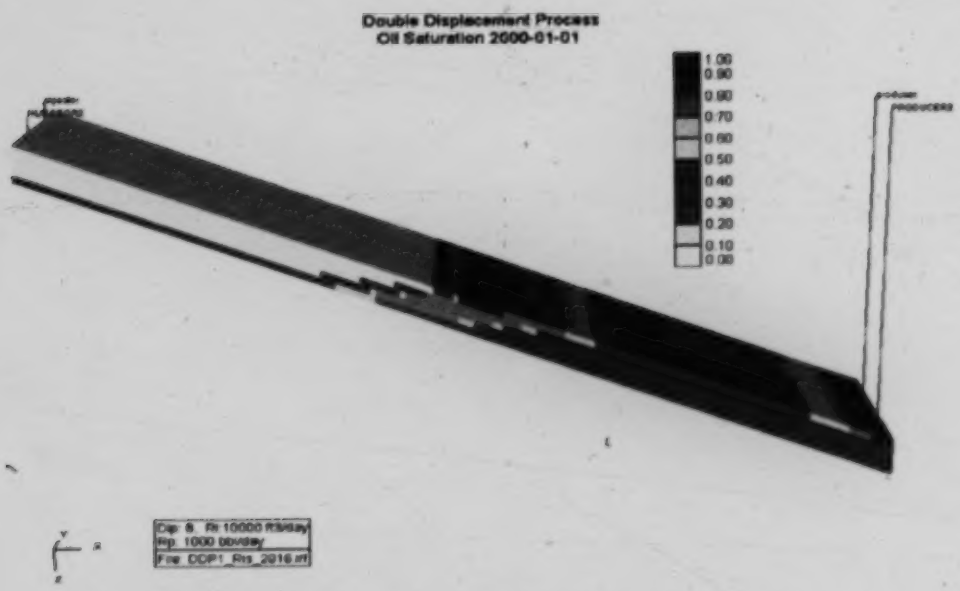

Figure 3.15: Oil distribution after ten years of DDP with Setting 2

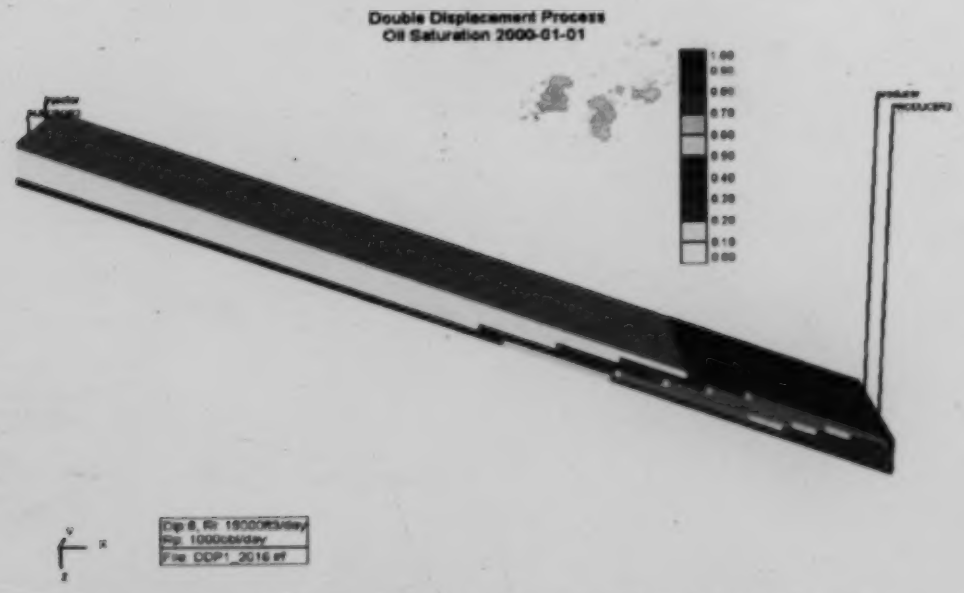

Figure 3.16: Oil distribution after ten years of DDP with Setting 3

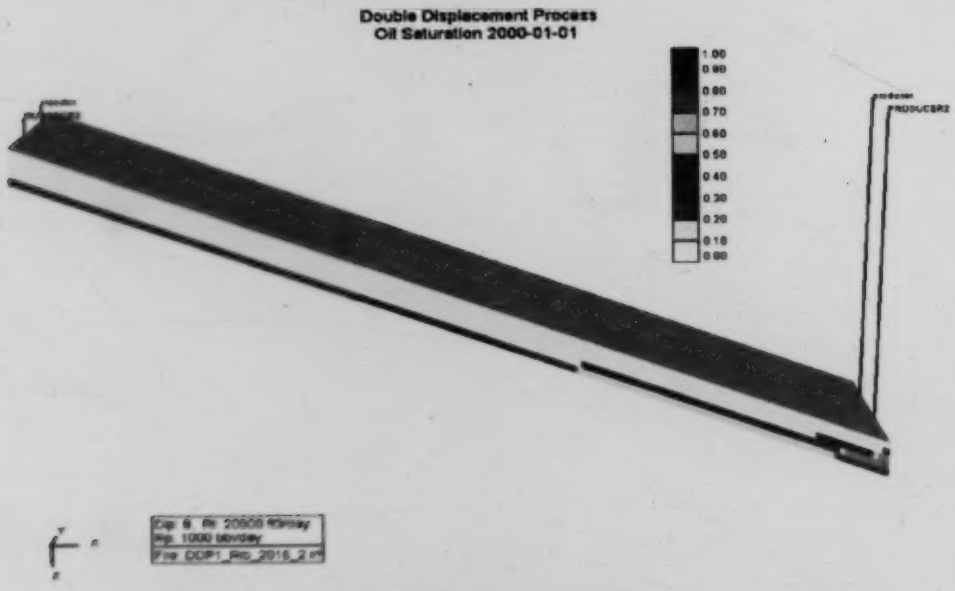

Figure 3.17: Oil distribution after ten years of DDP with Setting 4

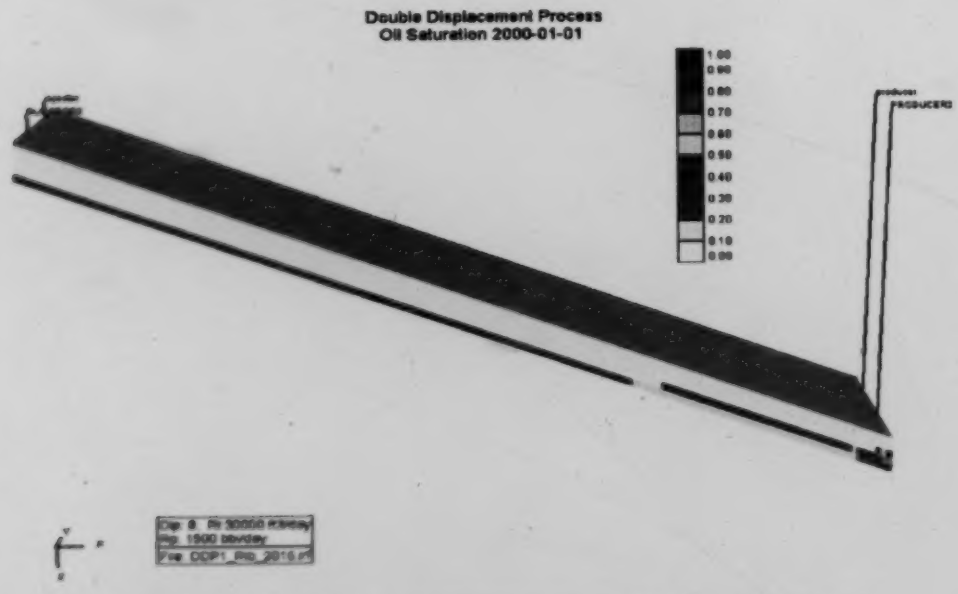

Figure 3.18: Oil distribution after ten years of DDP with Setting 5

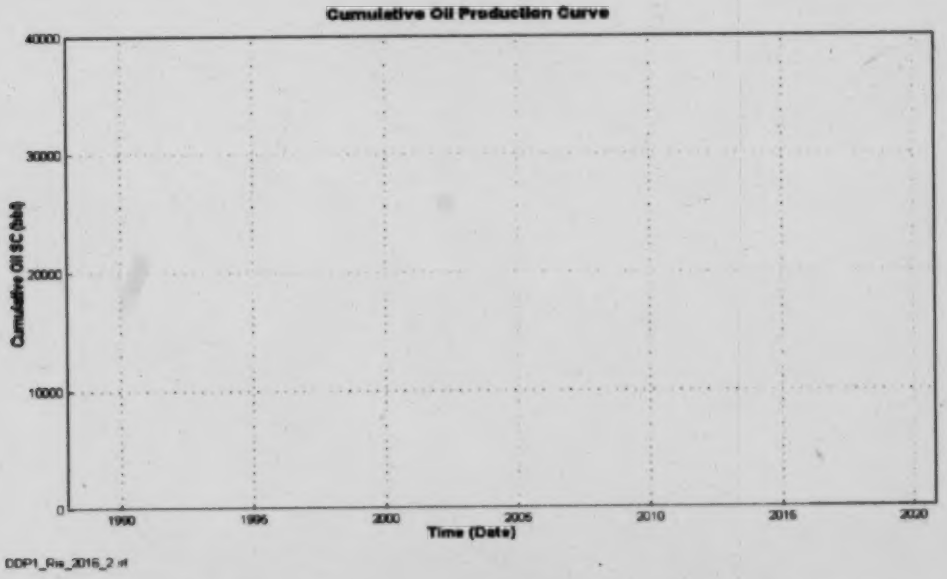

Figure 3.19: Cumulative oil production with Setting 1

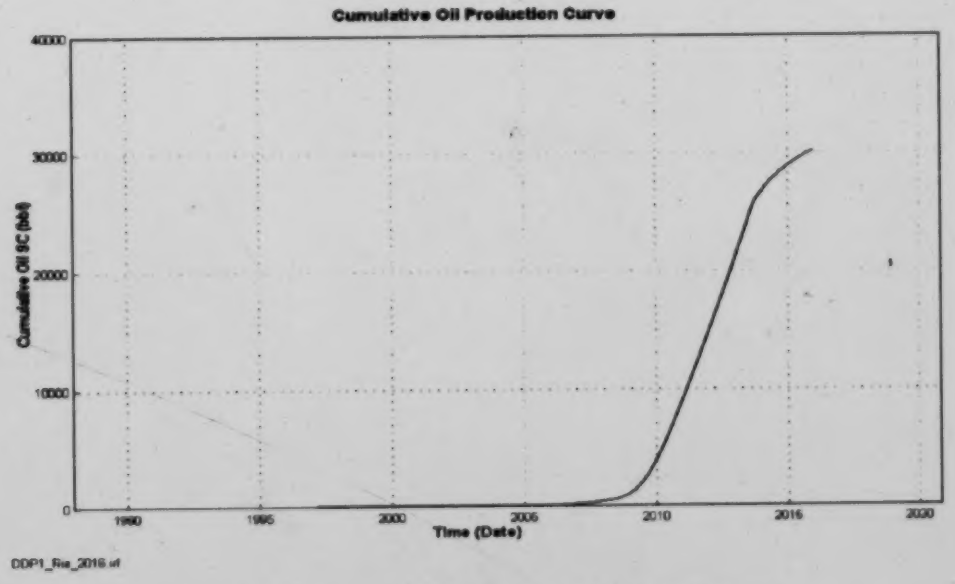

Figure 3.20: Cumulative oil production with Setting 2

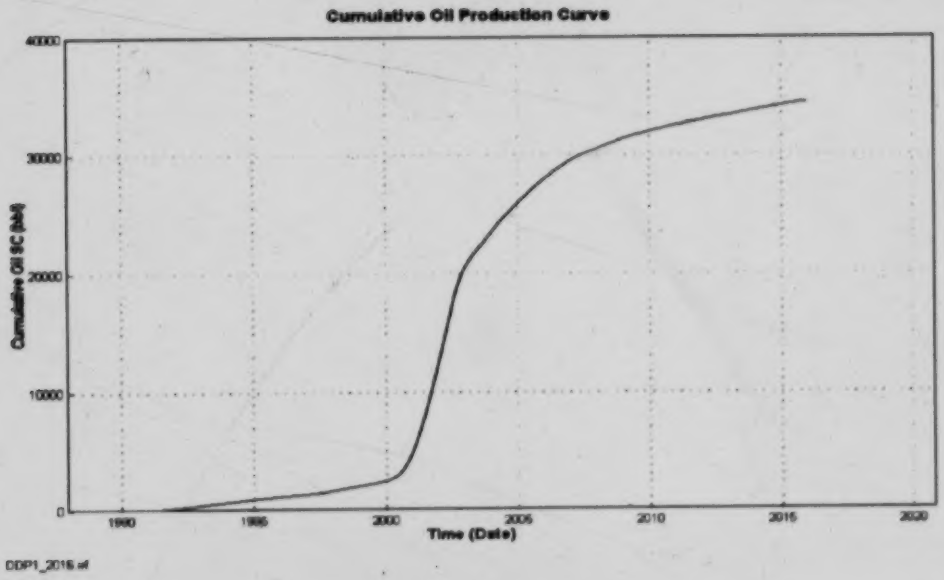

Figure 3.21: Cumulative oil production with Setting 3

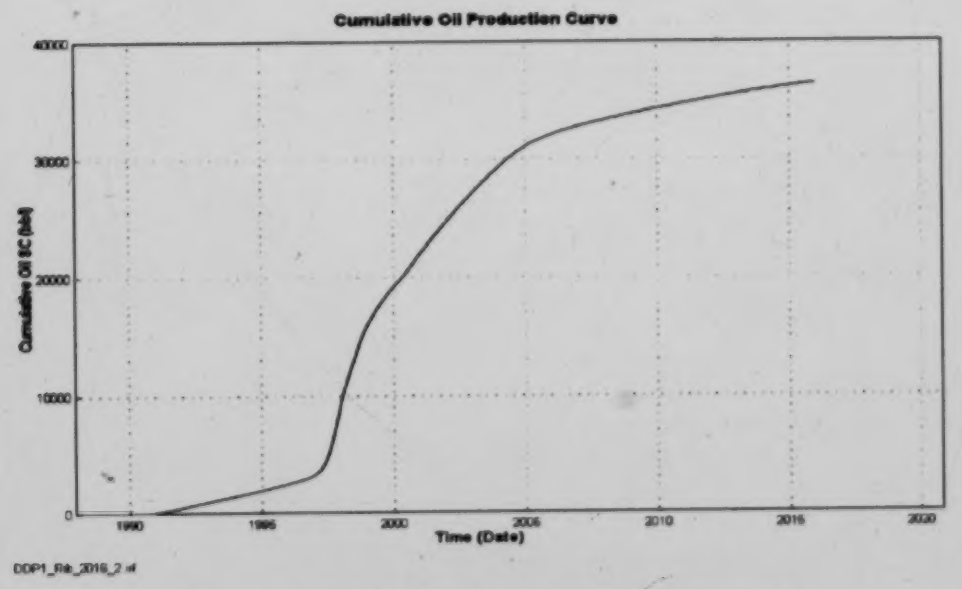

Figure 3.22: Cumulative oil production with Setting 4

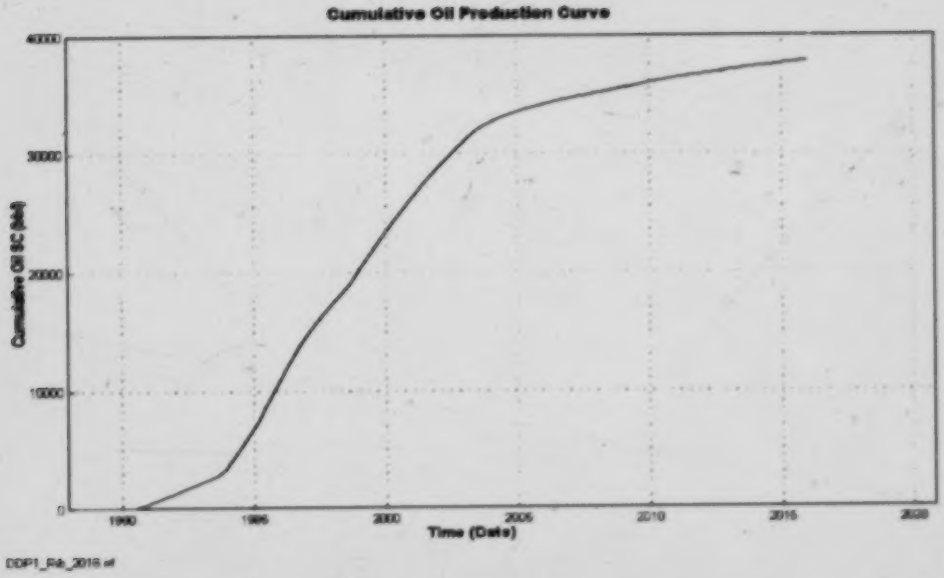

Figure 3.23: Cumulative oil production with Setting 5

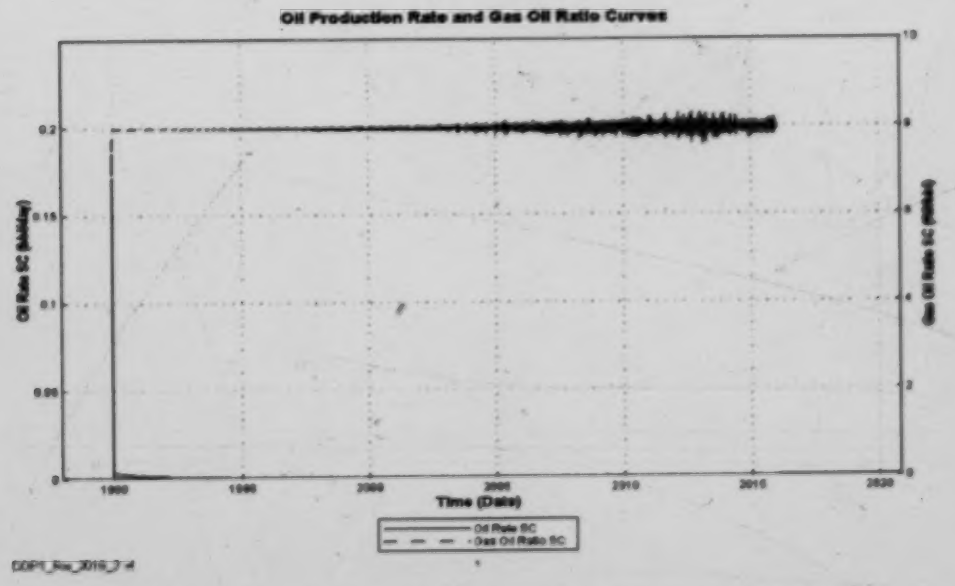

Figure 3.24: Oil production rate and gas oil ratio curves with Setting 1

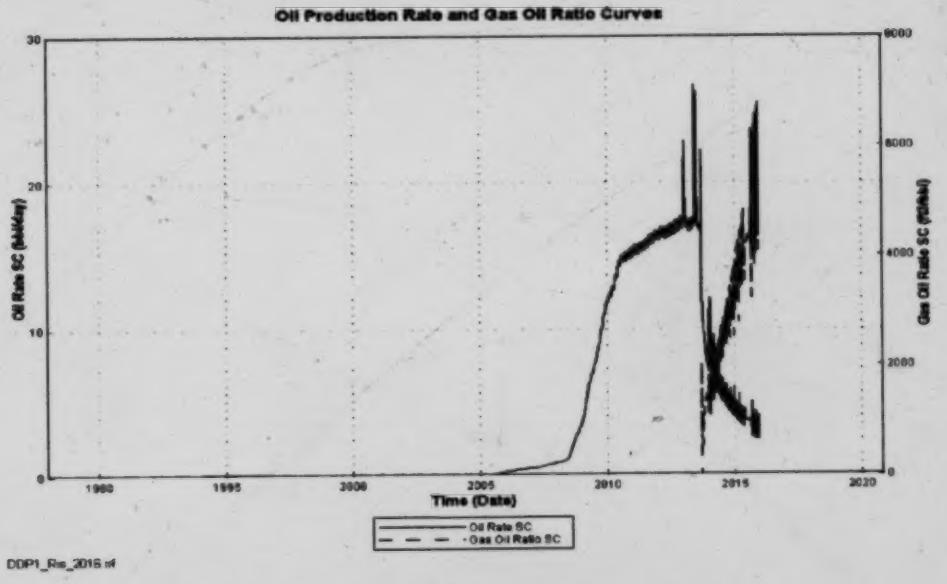

Figure 3.25: Oil production rate and gas oil ratio curves with Setting 2

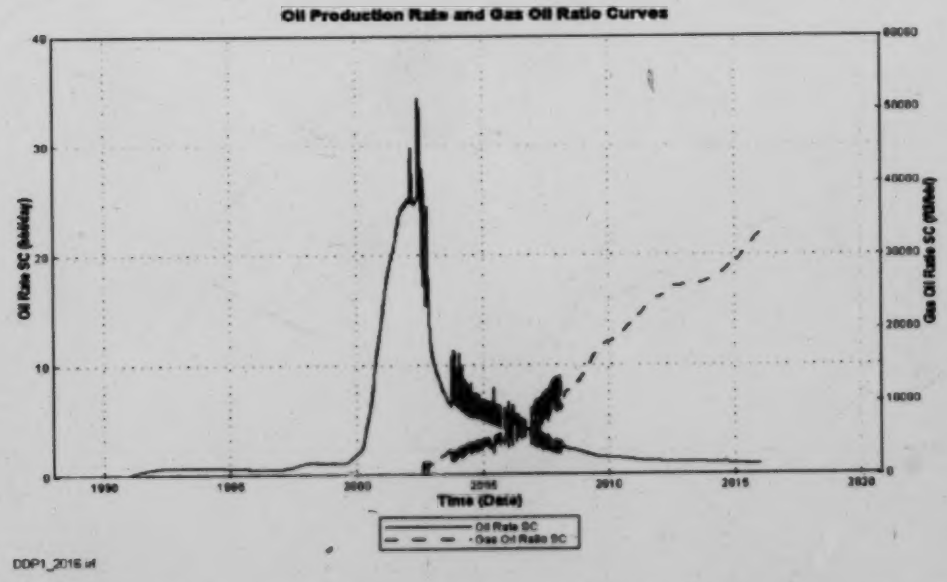

Figure 3.26: Oil production rate and gas oil ratio curves with Setting 3

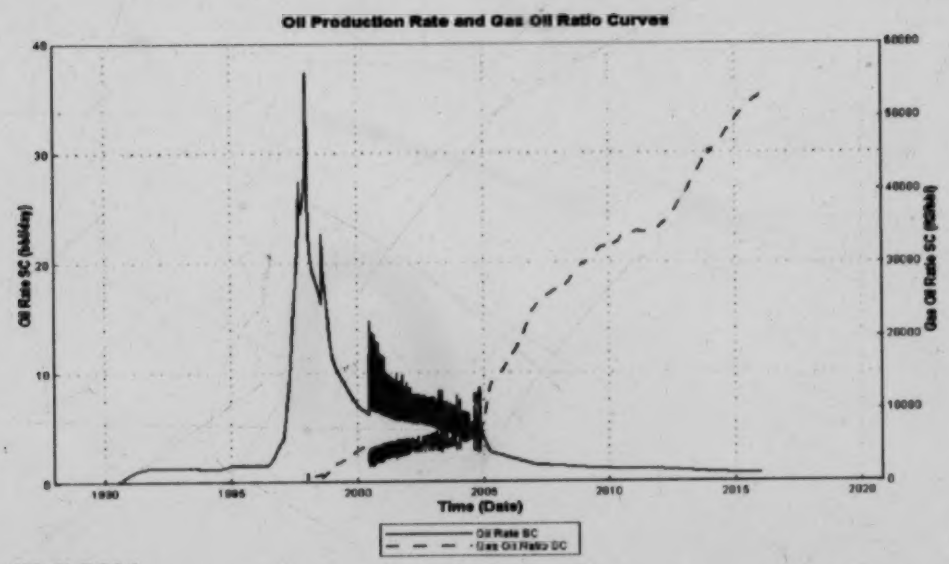

Figure 3.27: Oil production rate and gas oil ratio curves with Setting 4

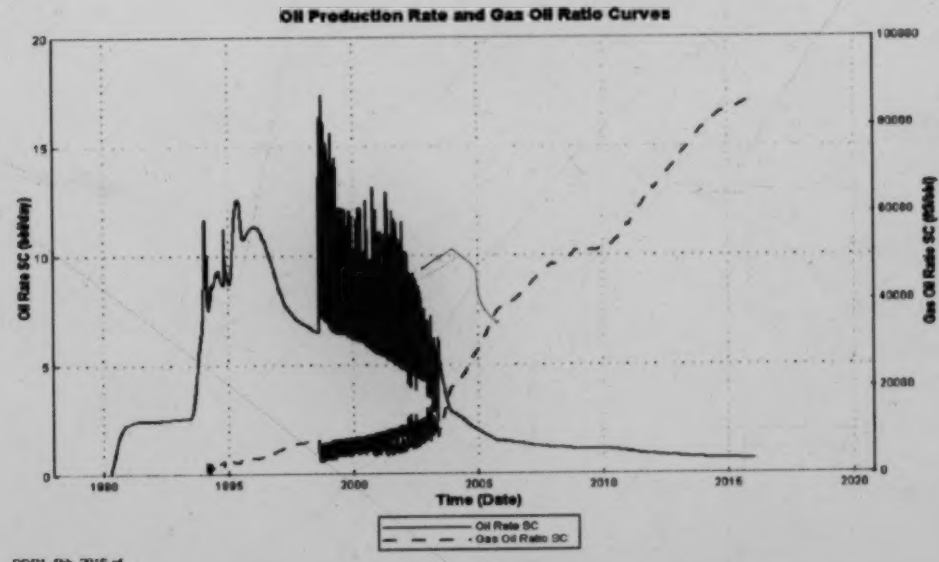

Figure 3.28: Oil production rate and gas oil ratio curves with Setting 5

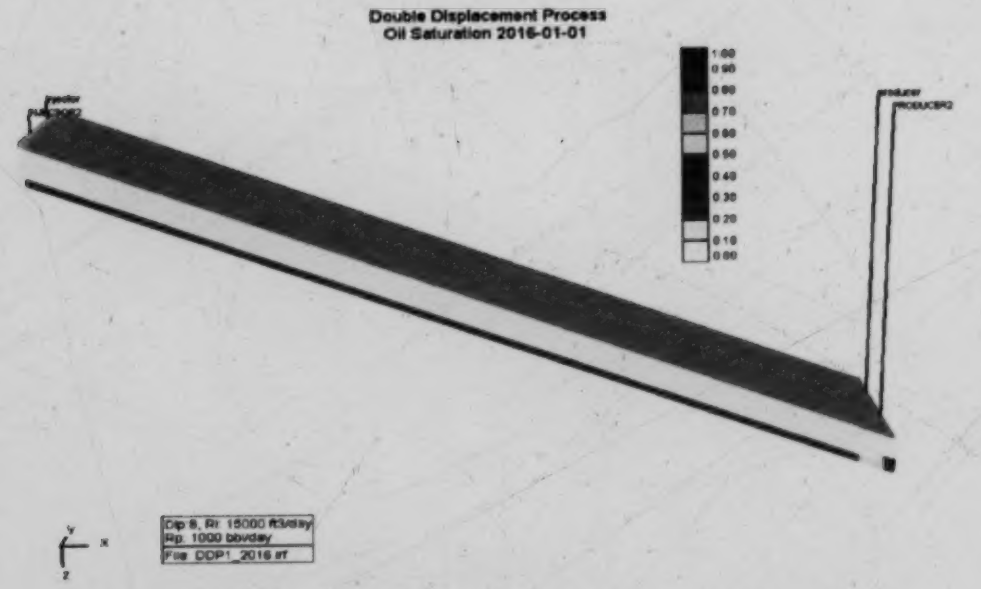

Figure 3.29: Oil distribution with partially perforated wells (Setting 3)

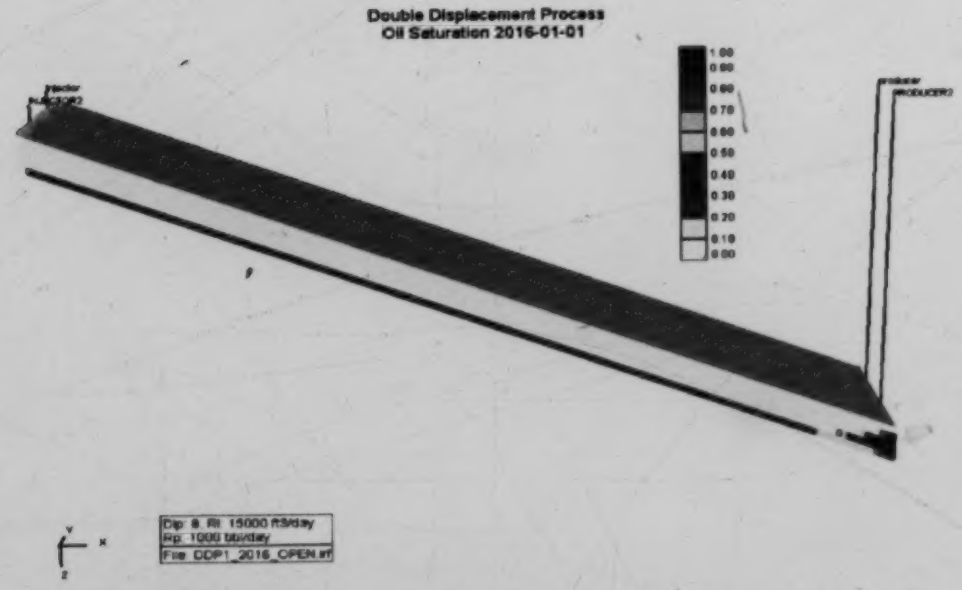

Figure 3.30: Oil distribution with totally perforated wells (Setting 3)

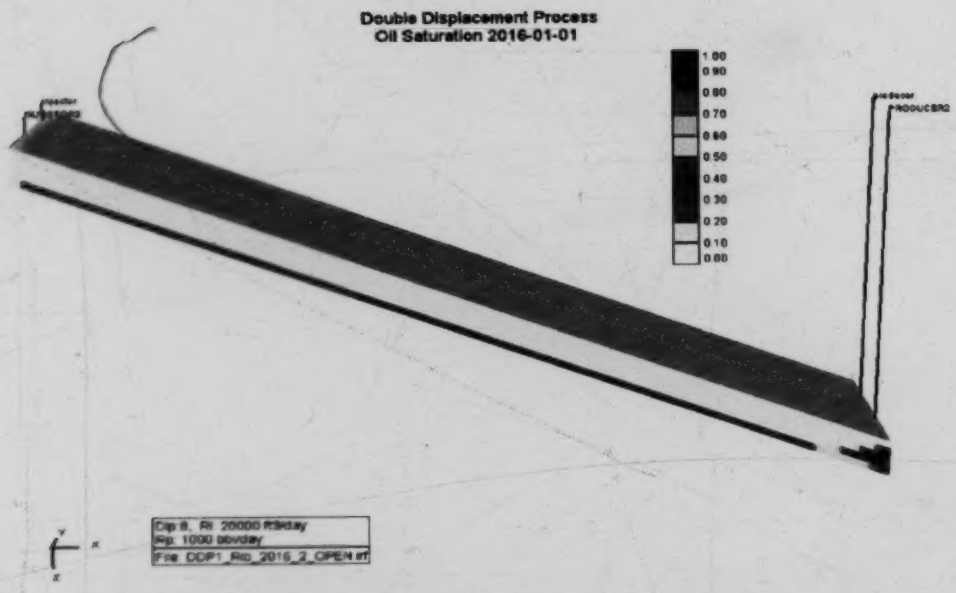

Figure 3.31: Oil distribution with totally perforated wells (Setting 4)

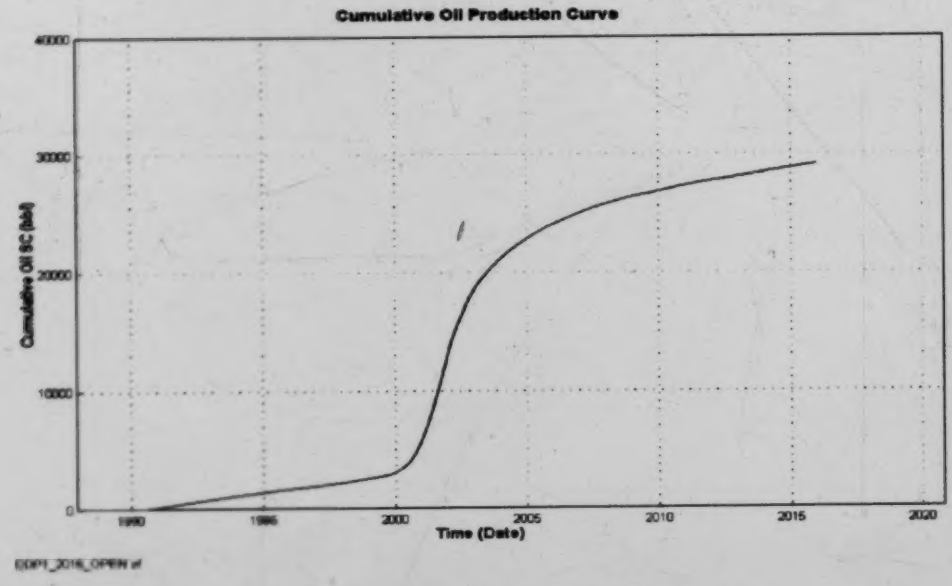

Figure 3.32: Cumulative oil production curve with totally perforated wells (Setting 3)

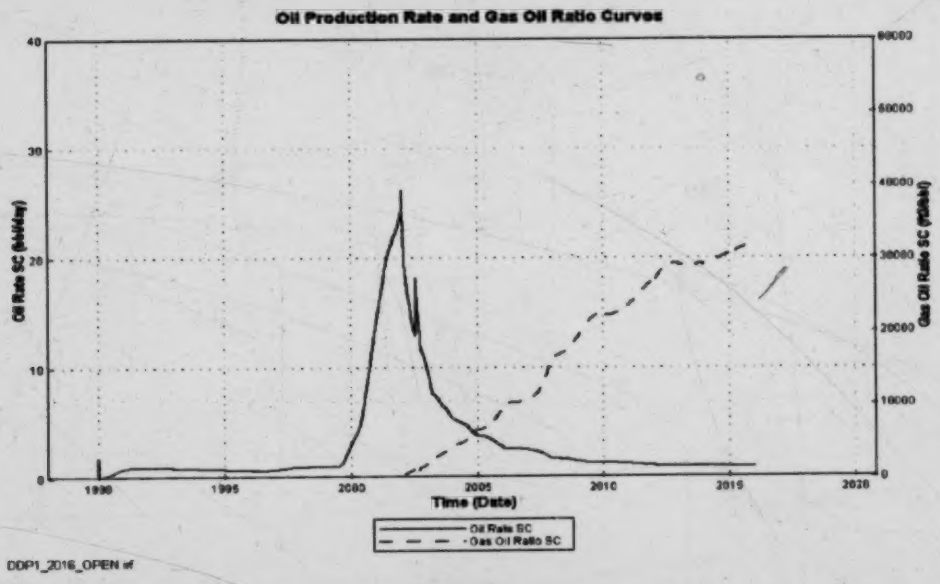

Figure 3.33: Oil production rate and GOR curves with totally perforated wells (Setting 3)

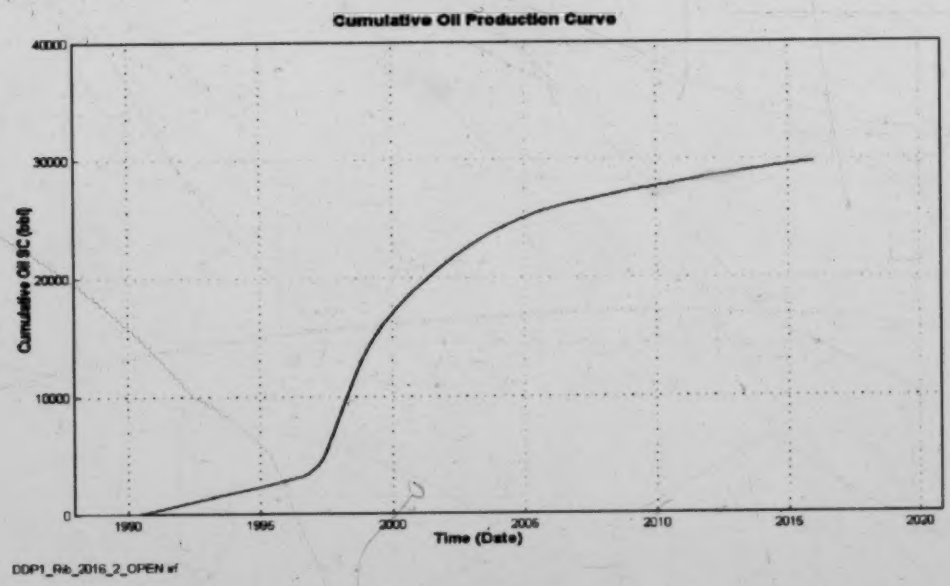

Figure 3.34: Cumulative oil production curve with totally perforated wells (Setting 4)

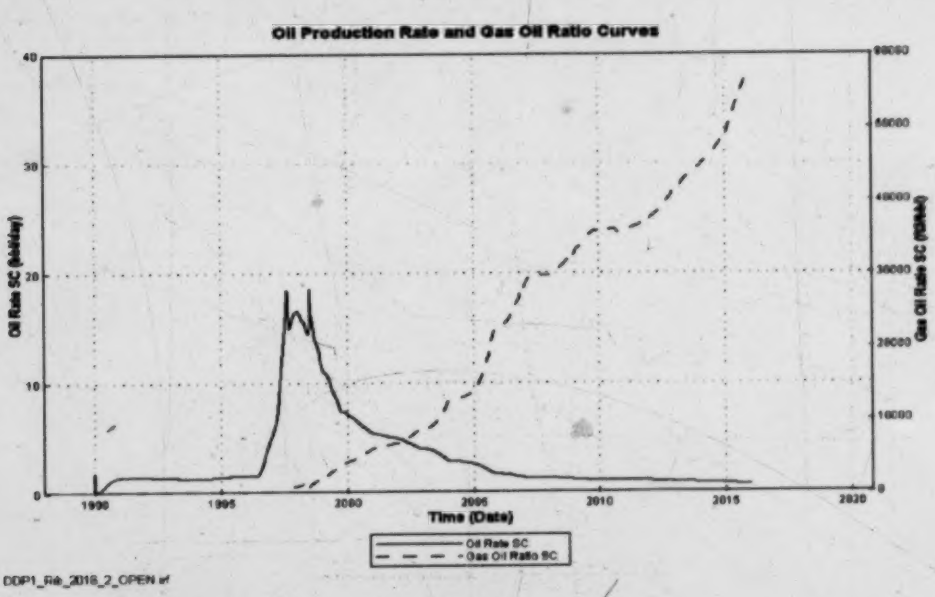

Figure 3.35: Oil production rate and gas oil ratio curves with totally perforated wells (Setting 4)

Figure 3.36: Oil distribution after ten years of DDP with reservoir dip of 8°

Figure 3.37: Oil distribution after ten years of DDP with reservoir dip of 30°

Figure 3.38: Oil distribution with reservoir dip of 30° and higher injection rate

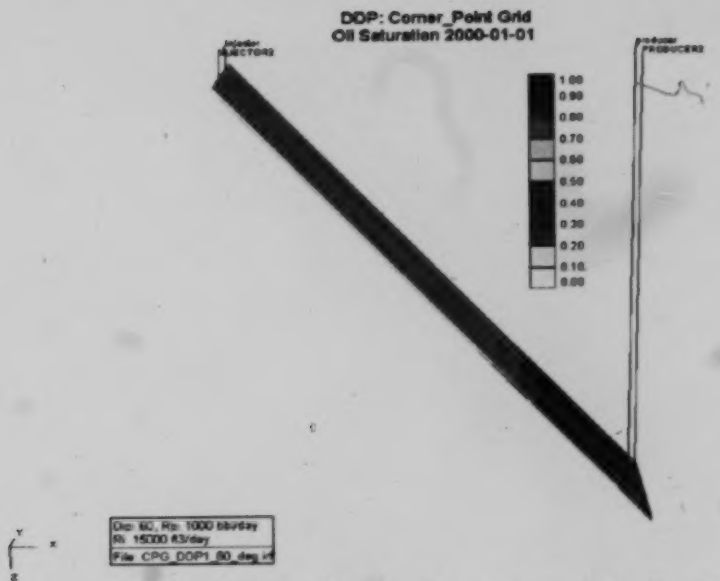

Figure 3.39: Oil distribution with reservoir dip of 60°

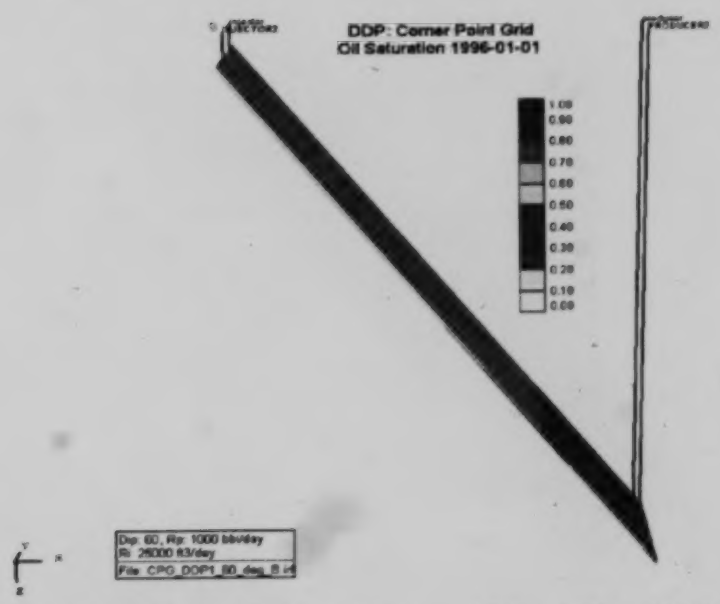

Figure 3.40: Oil distribution with reservoir dip of 60° and higher injection rate

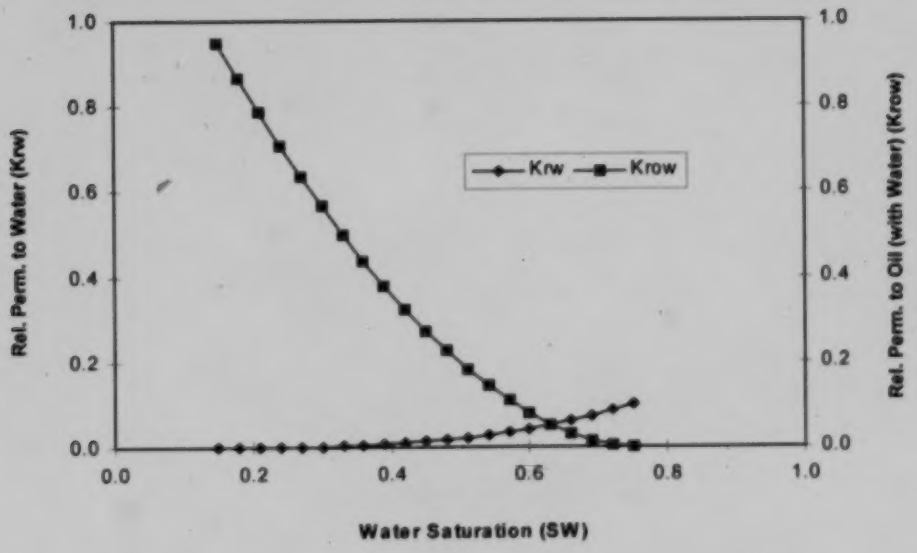

Figure 3.41: Oil & Water relative permeability curves (Setting 1)

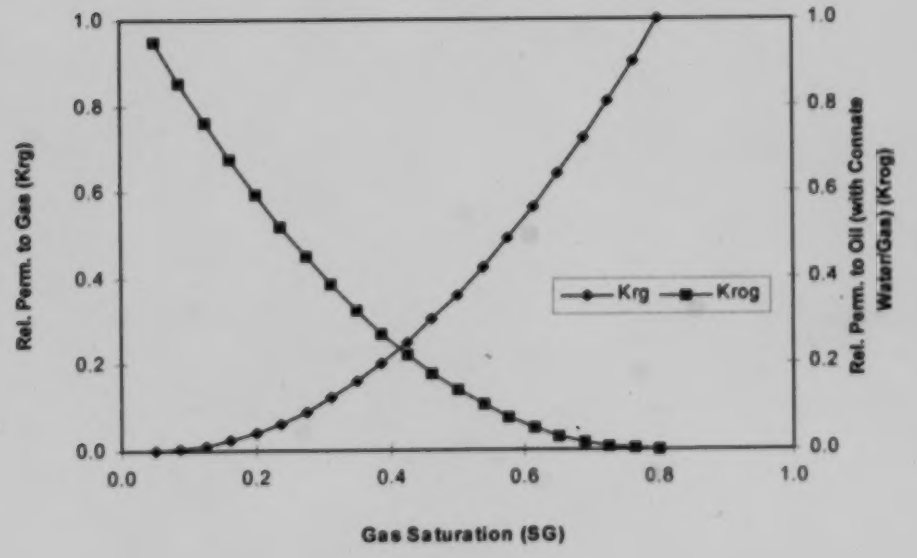

Figure 3.42: Gas & Oil relative permeability curves (Setting 1)

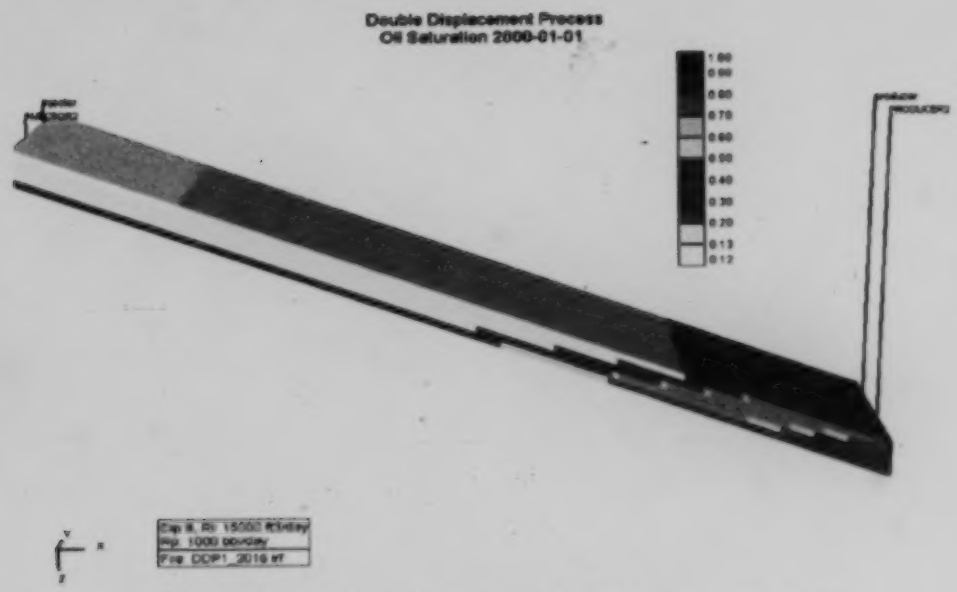

Figure 3.43: Oil distribution after ten years of DDP (Stone2)

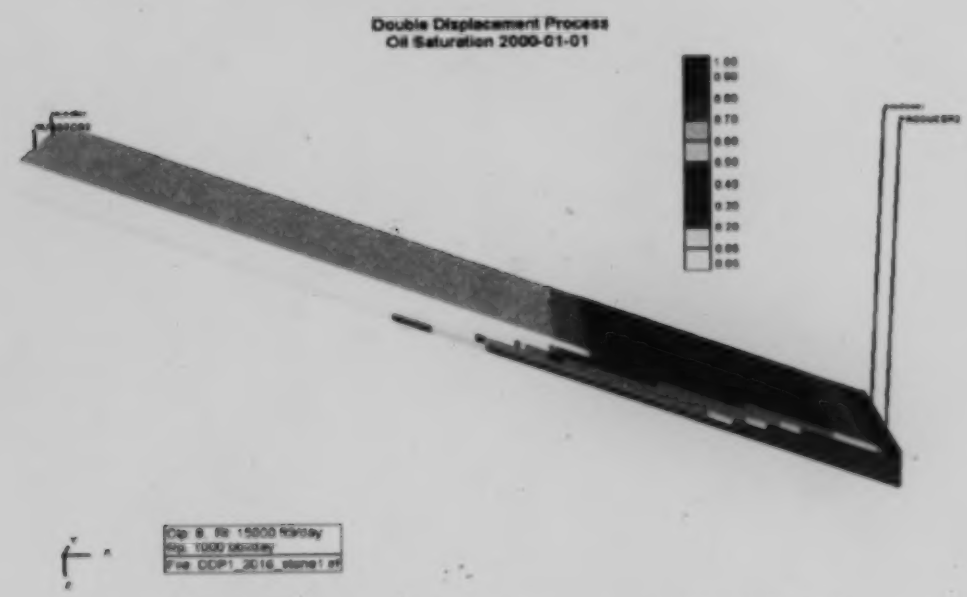

Figure 3.44: Oil distribution after ten years of DDP (Stone1)

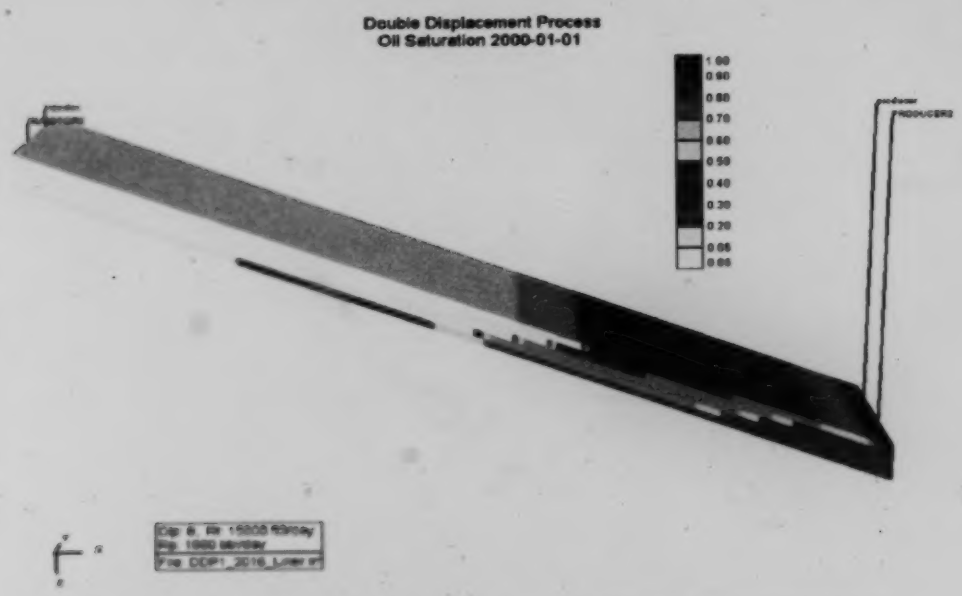

Figure 3.45: Oil distribution after ten years of DDP (Linear Isoperm)

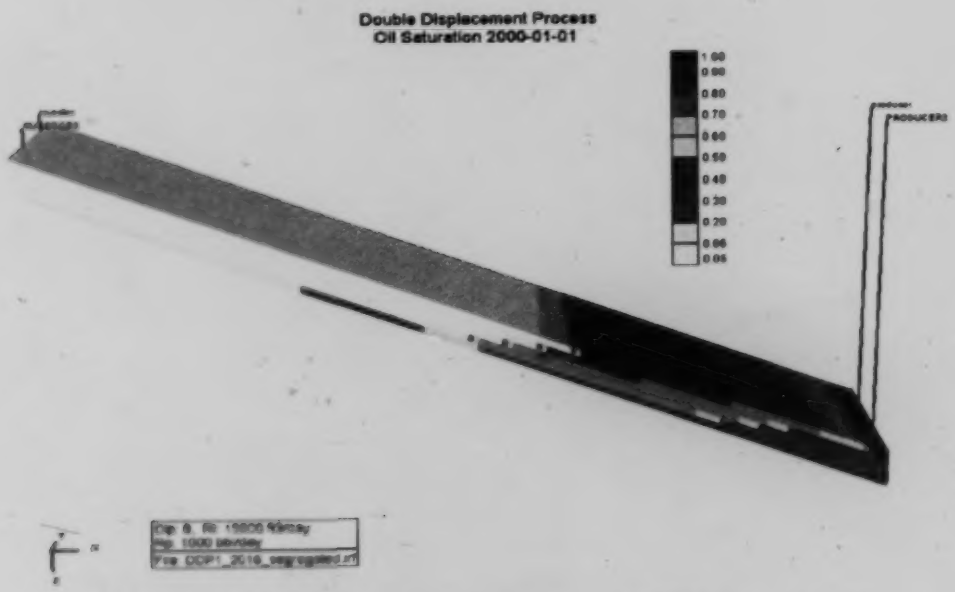

Figure 3.46: Oil distribution after ten years of DDP (Segregated)

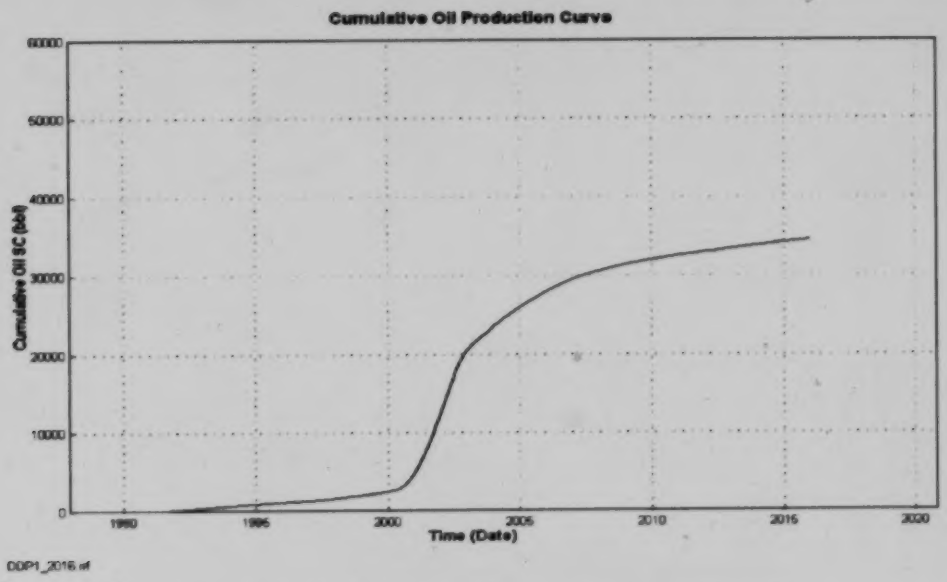

Figure 3.47: Cumulative oil production curve (Stone2)

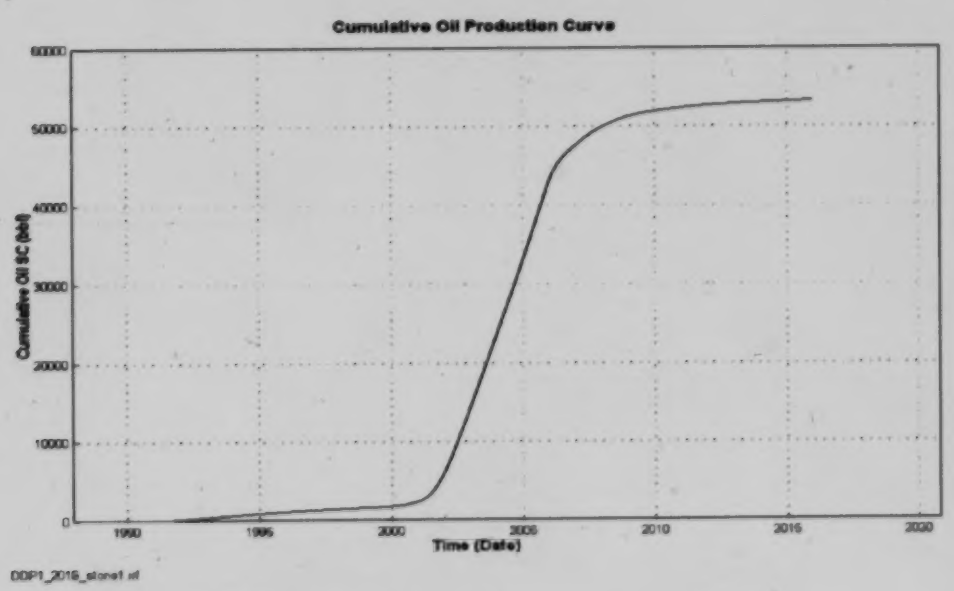

Figure 3.48: Cumulative oil production curve (Stone1)

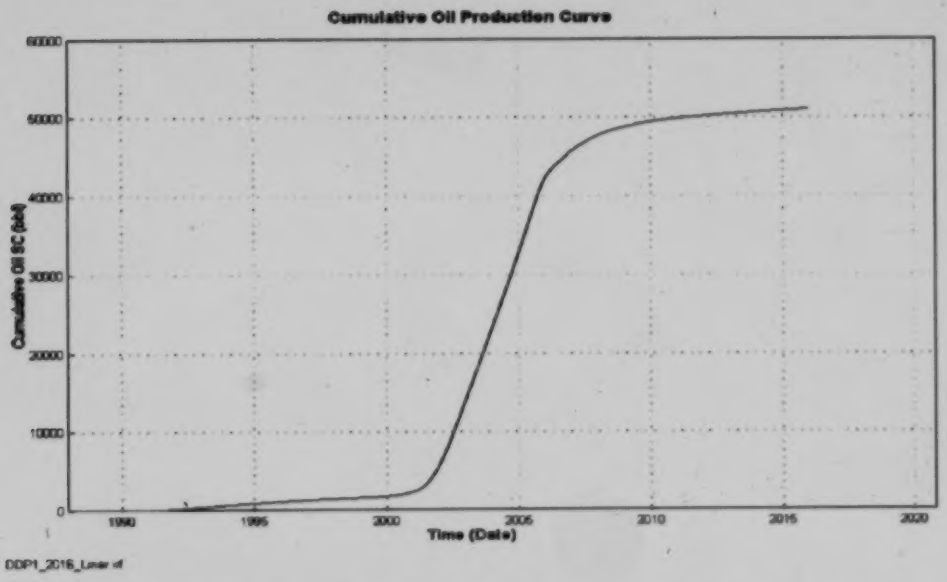

Figure 3.49: Cumulative oil production curve (Linear Isoperm)

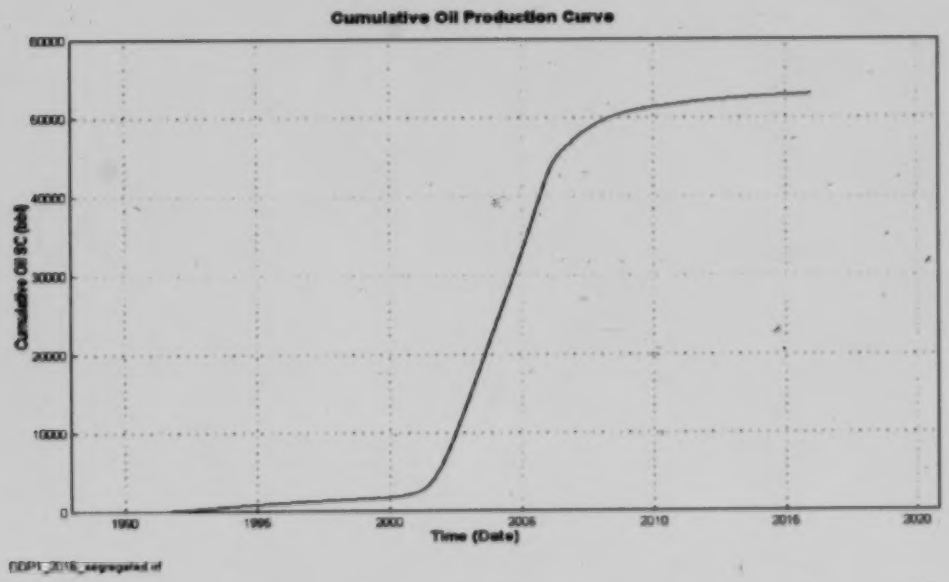

Figure 3.50: Cumulative oil production curve (Segregated)

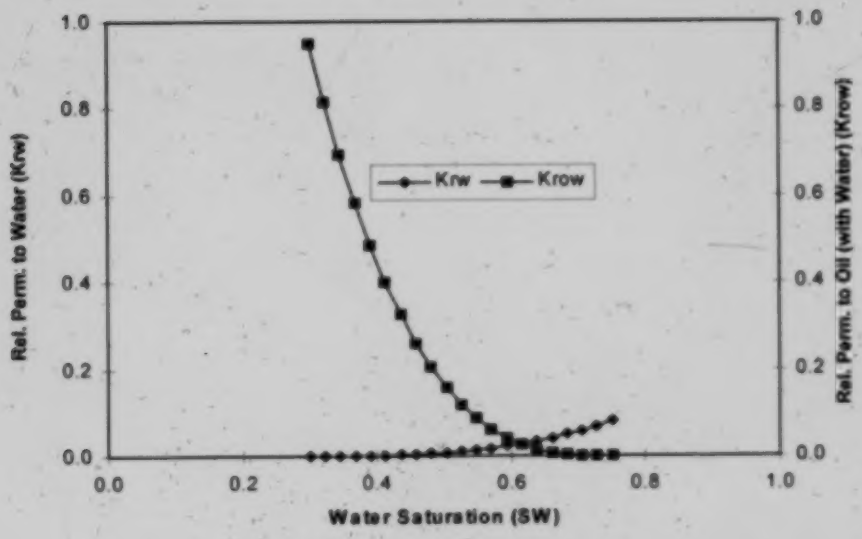

Figure 3.51: Oil & Water relative permeability curves (Setting 2)

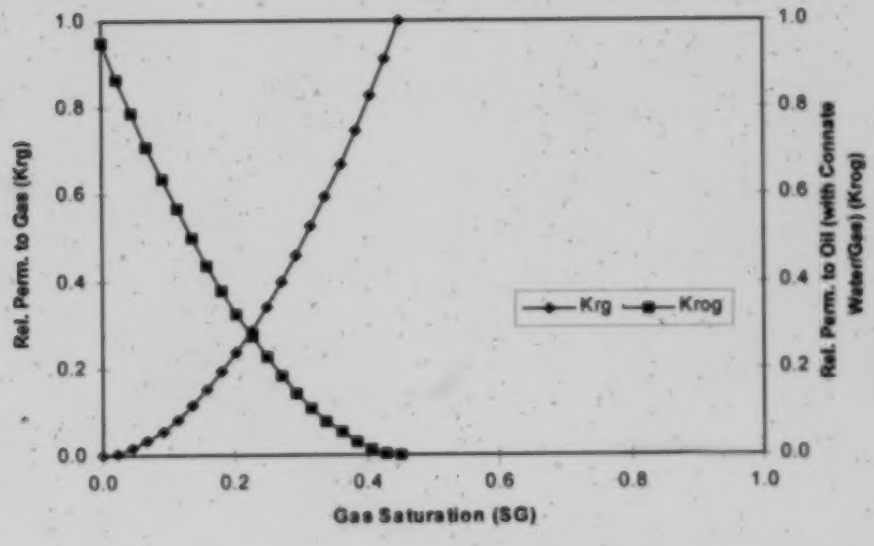

Figure 3.52: Gas & Oil relative permeability curves (Setting 2)

Figure 3.53: 2D oil distribution after ten years of DDP (Setting 1)

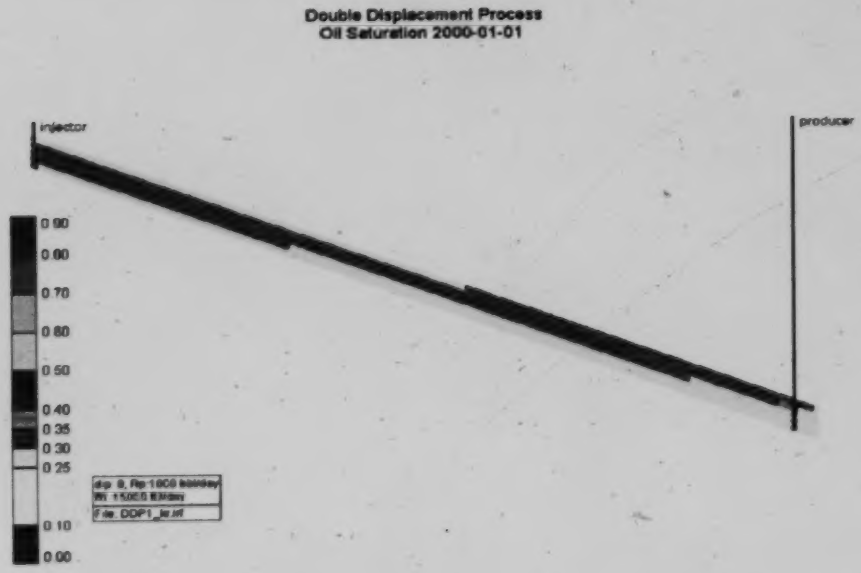

Figure 3.54: 2D oil distribution after ten years of DDP (Setting 2)

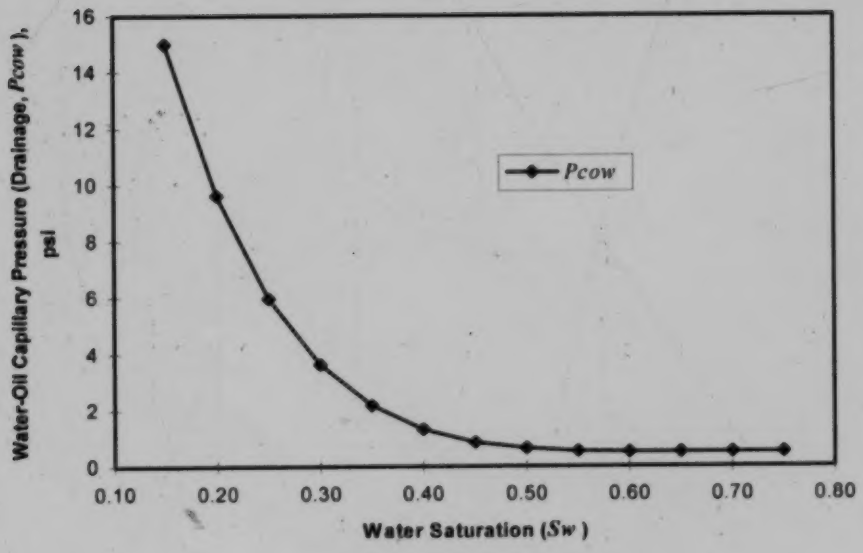

Figure 3.55: Water-Oil capillary pressure curve

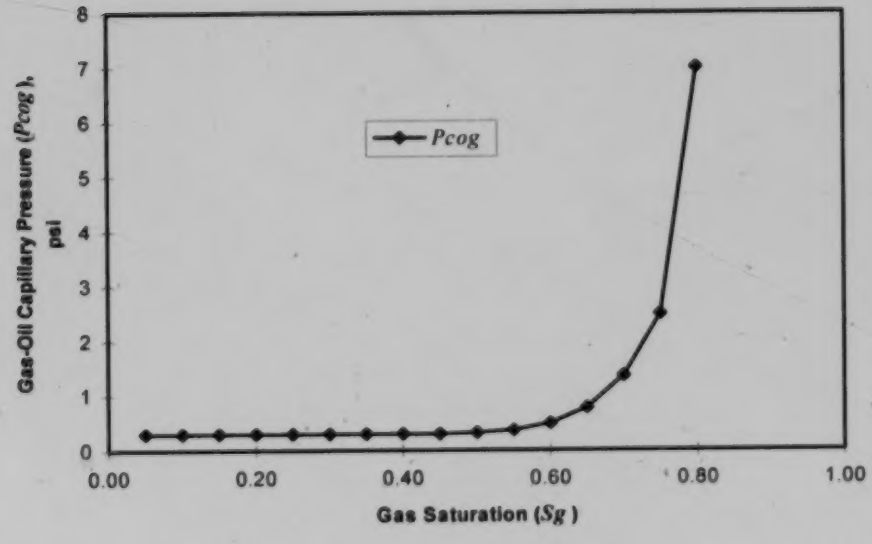

Figure 3.56: Gas-Oil capillary pressure curve

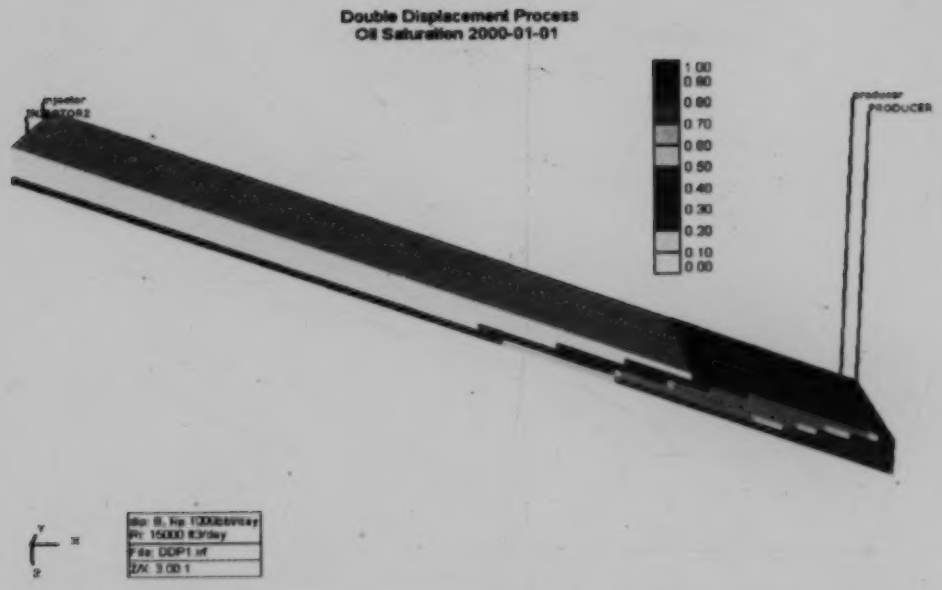

Figure 3.57. Oil distribution after ten years of DDP (without capillary pressure)

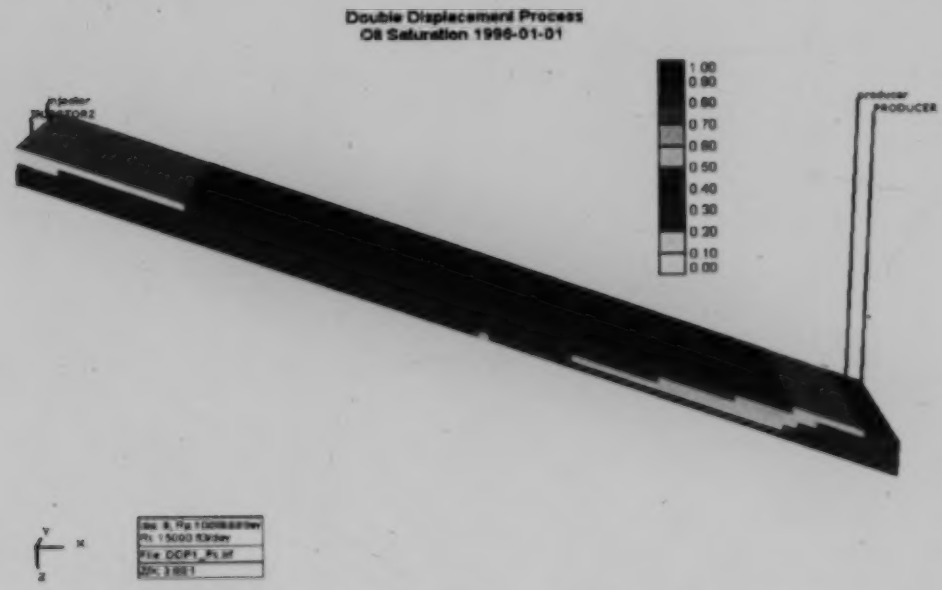

Figure 3.58: Oil distribution after eight years of DDP (with capillary pressure)

Figure 3.59: 2D oil distribution after ten years of DDP (without capillary pressure)

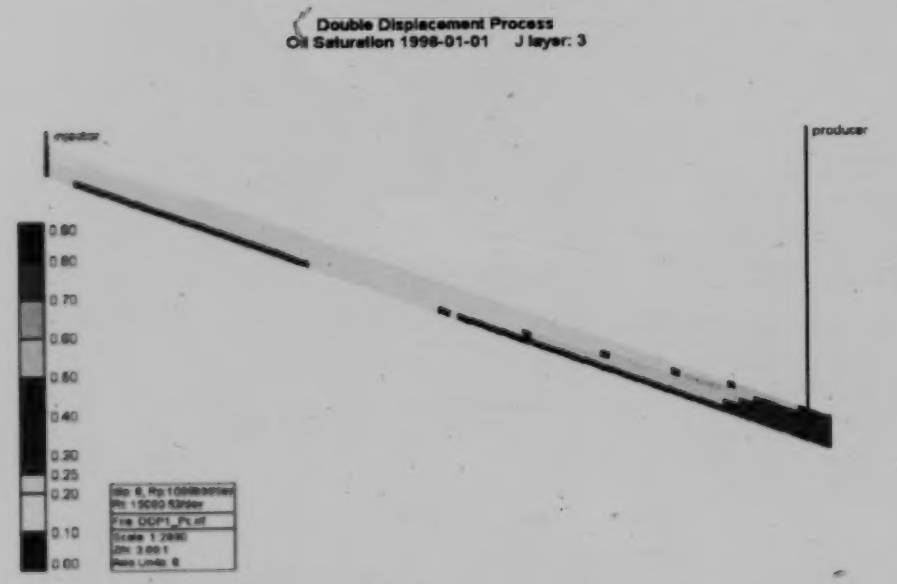

Figure 3.60: 2D oil distribution after eight years of DDP (with capillary pressure)

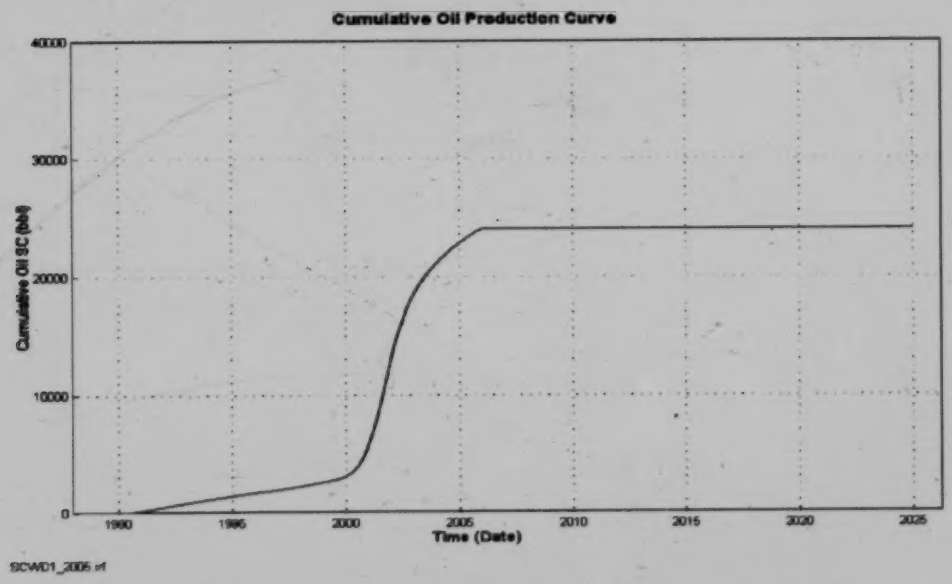

Figure 3.61: Cumulative oil production curve (SCWD with Sgc of 0.05)

Figure 3.62: 2D oil distribution before the SCWD process

Figure 3.63: 2D oil distribution after the SCWD process

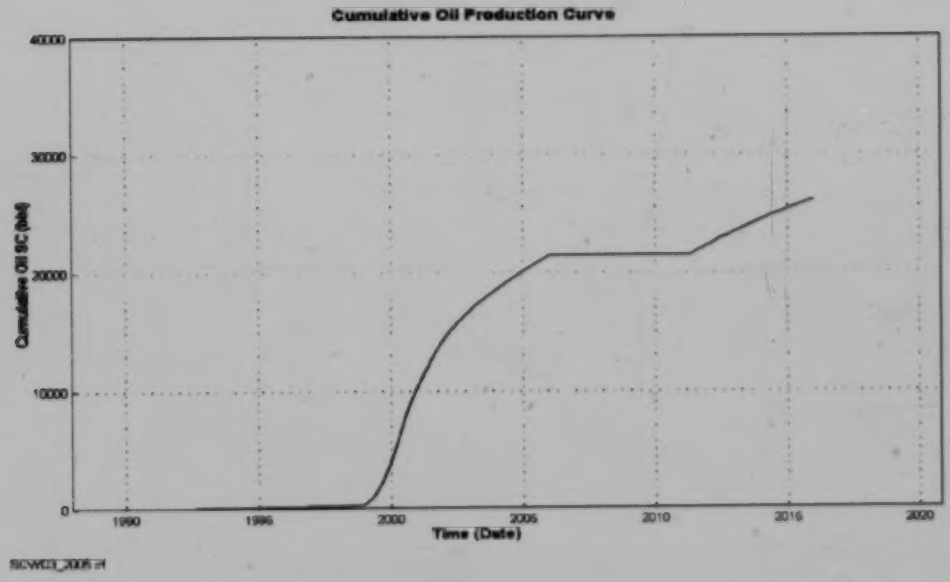

Figure 3.64: Cumulative oil production curve (SCWD with Sgc of 0.15)

Figure 3.65: 2D oil distribution before the SCWD process

Figure 3.66: 2D oil distribution after the SCWD process

CHAPTER 4

TRANSPARENT CELL EXPERIMENTS

Since Dumoré and Schols (1974) found out that very low residual oil saturations to gas can be achieved in the presence of connate water at high capillary pressures, numerous laboratory studies on tertiary gas injection have been published. Besides the macroscopic scale investigations conducted in sandstone cores, several efforts have been undertaken to investigate the microscopic mechanisms of the gravity assisted tertiary gas injection process (Kantzas et. al., 1988b; Oren et. al., 1992 and 1994; Soll et al., 1993; Lepski, 1995; Keller et al. 1997). Most of these studies used glass network models for pore-level visualization. The network model is a two-dimensional etched glass micromodel, and it has been used extensively in studying fluid displacement processes in a simple or idealized porous medium. The advantages of the network model are that the characteristics of simple porous media can be controlled carefully and that multiphase flow can be observed easily. However, due to simplification of the model, some important features are lost. For instance, it is impossible to simulate the irregular spatial distribution of natural pore space, and complex multiphase flow in a 3-dimensional reservoir rock system is much different than that in a 2-dimensional network system. Therefore, in some respects, the network models used in previous studies are not representative of reservoir rocks.

To achieve a better understanding of the pore-level mechanisms of the DDP and the SCWD process, a transparent, 3-dimensional, sand-pack model was constructed. This model is called a *transparent cell*. The up-dip tertiary gas injection and the second water flood were conducted in the cell to observe how fluids flow and, especially, to observe how the mobilization of the residual oil in a single pore takes place after gas invasion or after second water invasion. In addition, the water/gas, oil/gas and oil/water interfacial tensions were measured to determine the spreading coefficient of the oil over the water.

4.1. Model Construction

The construction procedure for the cell was similar to the procedure used by Lepski (1995). However, the cell was improved so that experiments under pressures up to 50 psi could be conducted. Moreover, the cell was built in such a way that the experiments could be conducted more easily and safely.

A picture of the cell is shown in Figure 4.1. The walls of the cell were two tempered glass plates, which were 8 inches in length, 3 inches in width and 0.5 inches in thickness. On one glass plate, there were two holes of 1/8 inch diameter drilled 0.5 inches away from both ends. A thin rubber gasket 0.032 inches in thickness, with a cut window 6.3 inches in height and 2.2 inches in width, was placed between two parallel glass plates to create a space for a sand pack. The space could be adjusted by compressing the rubber gasket. Two metal frames with the same size cut windows were made to compress the two glass plates, and a holder was made to hold the cell in the vertical position. Two more rubber gaskets were placed between the glass plates and frames to protect the glass. In the frame on the right side, two stainless steel fittings were fixed at locations directly above the two holes in the glass. An o-ring was installed on the bottom of each fitting to effect a seal, around a hole, between the fitting and the glass plate, thus preventing gas from leaking from the hole to the outside. These fittings were connected with transparent plastic lines to enable injection and production.

The porous medium was constructed of Cryolite (Na_3AlF_6) sand. The reason for choosing Cryolite was its strong water wetness and the fact that it turns transparent when contacted with water. Cryolite rocks were purchased from Ward's Natural Science Establishments Inc.. After crushing the rock and sieving the sand grains, 45-50 mesh clean cryolite sand grains were selected to inject into the cell. When the sand grains were being injected, a vacuum was applied at the outlet of the cell to withdraw the air from the cell in order to pack the sand grains tightly. Glass wool was put in the outlet fitting to prevent the grains from being drawn into the vacuum pump. When the

sand grains filled the space between the glass plates, a slight amount of vibration was applied until no more sand grains could be drawn into the cell.

The tightly packed sand grains were then consolidated by injecting a fresh chemical mixture, which consisted of 60 % tetraethyl orthosilicate, 32 % ethanol, and 8 % 0.1N HCl, into the cell. Air was then injected slowly into the cell to remove the excess mixture and dry out the cell. The dry mixture solidified as non-reactive silica and cemented the sand grains in place to form the desired porous medium with a small degree of heterogeneity.

The transparent cell was designed initially to be 24 inches long; however, due to the failure of the consolidation process in such a long cell, the current length of 8 inches was selected. Two transparent cells have been constructed. The DDP was conducted in the first cell. When it was going to be used for the SCWD process, after cleaning the cell, a glass plate was broken. Therefore, the second cell was constructed to perform the SCWD process.

4.2. Experimental Setup

The experimental setup is presented in Figure 4.2. The transparent cell was placed in a vertical position. Slim transparent plastic lines were connected to the fittings to enable injection and production. A GENIE programmable syringe pump was used to inject the fluid. For pore-level observation, a microscope with a magnification of 100 to 600 times was used. A TV and a VCR were connected to the microscope through a Sony 3CCD video camera to observe and to record all the images of fluid distribution at various stages of these processes. In addition, a Canon 8 mm video camcorder was used to record, in whole model view, the images.

4.3. Experimental Procedure

4.3.1. Preparation for Tertiary Gas Injection

For simulating the DDP and the SCWD process, the cell needed to be saturated initially with water. In order to displace the gas in the pores completely by water, the cell was flushed initially with several pore volumes of carbon dioxide to remove the air from the cell. Then the syringe pump was used to inject distilled water at a constant rate, at the bottom of the cell, to displace the carbon dioxide in the cell. A fast flow rate was used to ensure that the pressure in the cell was higher than atmospheric pressure. Therefore, no air came out of the injected water and the CO_2 was dissolved easily by the water. After 10 cm^3 of distilled water was injected, the cell was saturated completely with water. The volumes of water produced, and in the fittings and tubing, were measured to calculate the pore volume of the cell. A pore volume of about 3 cm^3 was obtained for both cells. Then, transducers were connected to the inlet and outlet fittings to measure the pressures at different flow rates. The absolute permeability of the cell, in both the upward and the downward direction, was calculated using Darcy's law.

The cell was oilflooded after these measurements. The oil used was a mixture of half bonnie glen crude oil (38.8°API and 11.1 cp at 40°C) and half decane. The mixture had a viscosity of 2.56 cp at 20°C. The oil was injected at the top of the cell at a constant flow rate until no more water was produced. The production line from the bottom of the cell was held above the cell so that the pressure in the cell was always higher than atmospheric pressure, thus preventing any gas from coming out of the water and oil. The volumes of oil produced, and in the fittings and tubing, were measured to calculate the irreducible water saturation. Again, transducers were connected to the inlet and outlet fittings to measure the pressures at different oil flow rates; this enabled the end-point effective permeability to oil to be calculated. After the permeability measurement was performed, the fluids in the cell were left for one day to equilibrate.

Water injection was then started to simulate waterflooding. Distilled water was injected into the bottom of the cell at a constant rate until no more oil was produced. At the end of the waterflood, the residual oil saturation and the end-point effective permeability to water at this oil saturation were obtained using the same procedure used before. Then the cell was shut down for one day so that the fluids inside the cell could find their natural, stable distribution. At this point, the cell was ready for up-dip tertiary gas injection.

4.3.2. Gravity Assisted Tertiary Gas Injection

Gravity assisted tertiary gas injection involves injecting gas at the top of reservoirs to displace, with the assistance of gravity, the residual oil as well as water in the reservoir. This requires the gas injection rate to be low enough to allow gravity drainage to take place. In this experimental study, pure nitrogen was injected into the cell through a 10 cm^3 gas-tight syringe at the slowest possible rate of 56 μl/hr. Therefore, the injection of 10 cm^3 of gas took about 8 days to complete, and gas breakthrough occurred in the first three days. Pure nitrogen was selected as the injected gas because the gravity assisted tertiary gas injection process is an immiscible process. The whole procedure was observed through the microscope and was recorded on videotapes in the EP mode through a VCR. Although the microscope could provide magnifications ranging from 100 to 600 times, the range of 100 to 200 times was used frequently because the clearness and the scope of the images of fluid flow in a single pore were best at this magnification. Each videotape had 6 hours of recording time in the EP mode. Therefore, the tapes were changed every 6 - 8 hours in the first three days of the experiment. After three days, only selected time periods were recorded.

Because in the DDP, the residual oil to water can be recovered by immiscible gas displacement and oil film flow, several things were expected to be observed in the laboratory experiment for this study: a) gas moving into a pore to displace the water and oil, resulting in the formation of an oil film between the water and the gas; b) oil bank formation at the gas-oil front and the mode the gas displaces the residual oil in

the watered zone; and c) connection of oil films to the oil bank enabling observation of how the oil films connect to the oil bank and how the oil flows through the oil films due to gravity drainage. To enable these observations, the most important thing was finding a good spot in the cell where the oil, gas and water flows could be seen clearly. At the beginning of the gas injection, a spot at the upper part of the cell was chosen, where a residual oil blob was centered in a pore channel, and the recording was started. It continued until the gas front passed the spot and the oil film was formed between the water and gas interfaces. If oil films weren't observed, the camera was moved downward to another spot and the filming was continued. This step was repeated until a clear picture of oil film formation was observed. Then, another spot was chosen in the front of the oil bank to see how the oil bubbles reconnected and flowed to the oil bank. After gas breakthrough, oil film flow was the main objective of the observation.

4.3.3. Second Contact Water Displacement Process

The SCWD process involves implementing a second waterflood after the main oil production of the DDP. As mentioned in the last section, gas breakthrough took place during the first three days of the DDP in the cell for an injection rate of 56 μl/hr. Gas breakthrough usually happened at a time close to the end of the main oil production period. Therefore, water was injected upward into the cell at a slow rate of 1 cm^3/hr after three days of the DDP. The injection of 10 cm^3 water took 10 hours. The whole procedure was observed through the microscope and recorded on videotapes in the EP mode through a VCR. Selection of observation spots in the cell was similar to the selection method used in gravity assisted tertiary gas injection. However, the spots were selected by starting at the bottom of the cell and then by working upwards towards the top of the cell.

4.4. Experimental Results and Discussion

The main purpose of the cell was to observe the pore-level mechanisms of the DDP and SCWD process. As indicated in the procedure, some properties of both cells and production amounts of the DDP and SCWD process were measured.

4.4.1. Properties of Transparent Cells and Production Amounts of the Processes

The measured properties of the two transparent cells are listed in Table 4.1. The bulk volume of both cells is 6.65 cm^3. The pore volume of the first cell is 3.0 - 3.1 cm^3, and that of the second cell is 3.0 cm^3. These values give rise to a porosity of 45.1% - 46.6% for the first cell and 45.1% for the second cell. These porosities are higher than the maximum value of porosity expected for normal reservoir rocks. The reason for the high porosity is probably the short separation distance between the two glass plates. This short distance was only 2.5 to 3 times the diameter of a sand grain. The cell was designed in this way to enable observation of the fluids flowing in the cell, which will be described in the next section. However, designing the cell in this way resulted in the creation of some large pore spaces between the grains and the flat glass plates. These pore spaces had a significant effect on the pore volume, and, moreover, they tended to increase unduly the permeability. However, because, at such a short distance between the two glass plates, wall effects are expected to be significant, the permeability of the cells might be decreased significantly. The absolute permeability of the first cell was about 17 darcies, while that for the second cell was about 12 darcies.

At the end of the oil flood, the oil saturation of the first cell was 80%, while the irreducible water saturation was 20%. At this saturation, the end-point effective permeability to oil was 4.22 darcies. For the second cell, the oil saturation at the end of the oil flood was 90%, while the irreducible water saturation was 10%.

At the end of the waterflood, the residual oil saturation was measured to be 40% for the first cell. At this saturation, the end-point effective permeability to water was calculated to be 6.06 darcies. For the second cell, the residual oil saturation after the waterflood was measured to be 43.3%.

These end-point effective permeabilities do not indicate that the porous medium is strongly water wet. This is because these data were not accurate. Several limitations of the cell resulted in inaccurate measurements. First, the pore volume of the cell was small and the total volume inside the fittings and tubing was larger than the pore volume; therefore, the fluids flowing in the fittings and tubing had a big impact on these measurements. Second, these data were measured using simple methods. For such a small cell, any error in reading fluid volumes and pressures caused a large percentage error in the results. Third, it was assumed that the cell was a strongly water-wet system, but the metal fittings and the plastic tubing were oil-wet, resulting in some oil being trapped in the fittings and tubing. This likely resulted in error being introduced into the measurements. However, the purpose of measuring these data was to get a rough idea of the properties of the cell, and to see how much oil could be produced after the DDP and SCWD process. For the first cell, at the end of the DDP, the oil produced was about 1 cm^3, which was 83.3% of the oil in place after the water flood. Most of the oil was produced in the main production period. Subsequently, only a very tiny amount of oil was produced during 4 - 5 days of gas injection. The final oil saturation was 6.7%. For the second cell, after three days of the DDP, the oil produced was about 1 cm^3 too, but it was 80.8% of the oil in place. The SCWD process was very short, only 10 hours. But, unfortunately, the SCWD process didn't produce any oil. This was because there was a bypassed area at the top of the cell. Most of the oil was blocked there. Otherwise, a small amount of oil would have been produced. The final oil saturation was 10%.

Overall, the experiment successfully indicated that a larger amount of oil could be recovered by the DDP. Moreover, it can be argued, as shown later, that it is possible to recover some oil by the SCWD process.

4.4.2. Observation of the Double Displacement Process

Under the microscope, the water, oil, gas and sand grains appeared to have different shapes and colors. The dry sand grains appeared to be black globules, which are shown in Figure 4.3 at 230x magnification. The cryolite sand was strongly water wet. When water reached the sand, the black sand grains immediately became bright and transparent. Figures 4.4 and 4.5 are pictures of different sites where the porous medium was saturated with water, oil, and gas. The interface between the water and the sand grains couldn't be observed. The existence of the water was indicated by the sand grains appearing to be bright or black. The oil was partially transparent and its color was brown. The light yellow indicates the co-existence of some water and a small amount of oil. The gas was non-transparent and its color was black. The interface between the water and the oil and between the oil and the gas can be seen easily.

As mentioned before, the distance between the two glass plates was only 2.5 to 3 times the sand grain size. Therefore, only two or three grains could fit between the glass plates in the direction perpendicular to the glass plates. Three or four pore spaces formed: one or two spaces between the sand grains, and the other two between the sand grains and the glass plates. Through the microscope the fluids flowing in the pore space between the glass plates and the sand grains could be seen directly and clearly. The fluids flowing in the pore space between the sand grains could be observed also if the sand grains were transparent. Although the transparent sand grains were not as easy to see through as the glass, the color change could be perceived easily, thereby enabling filming of the flowing fluids. This color change looked like a background color change so that it could be distinguished easily from the color change in the space located between the glass and the sand grains. This is shown clearly in Figure 4.6, which was taken at the same spot as Figure 4.5, but at a later time.

After the waterflood, the residual oil was distributed sparsely as isolated oil globules. There was very little bypassed oil due to the relatively low degree of heterogeneity of the porous medium within the cell.

When gas injection was started in the cell, it was observed that the gas front was not as flat as that of the oil flood and the waterflood. The gas front in the cell undulated significantly (Figure 4.7). Gas had a tendency to go faster in the middle of the cell first, then the front extended to both sides of the cell. However, it was observed that undulations of the front were always at the same level until they reached the outlet. Analysis (Richardson and Blackwell, 1970) of the results suggested that it was still a gravity stable displacement. The fingering occurred mainly because of the very low viscosity of the gas and the small size of the cell. If the displacement had taken place at the large scale of a field, the fingering would not have been so obvious and the gas front would have looked flat at the macroscopic scale. Around the gas front, there were lots of brown spots. Under the microscope, the oil in these spots was in continuous form. As the gas front moved downward, the brown spots were joined by more residual oil and the spots became linked together. Therefore, an oil bank was formed. When the oil bank moved out of the outlet, most of the residual oil was produced.

At the pore level, the gas entered a selected spot. Such entry was not always from the top. The gas could enter the spot from the bottom, the right or left side, or from the middle layer in a horizontal direction. Eventually, it would occupy all of the pores in the spot. When gas was entering pores that contained water and oil, it darted quickly into these pores and occupied most of the pore space. Then, the gas stayed still for quite a while before it darted forward again. As the gas entered a pore, some oil was displaced out of the pore. It was observed that some of the oil flowed out immediately before the invasion of gas. Some oil was left, so an oil layer or oil film was observed at the edge of the gas, or between the water and the gas (Figure 4.8). The residual oil and these oil films and oil layers were all linked together. Thus, the continuity of the oil was formed and this continuity provided a way for the oil to flow downward under

its own weight. As time went on, gas entered all of the pores, and, furthermore, gas occupied all of the available space in these pores. Based on this observation, I think that the oil flowing through the oil films is driven not only by its own weight, but also by the increasing volume of the gas. When gas enters a pore, the pressure of the gas must be higher than the threshold capillary pressure of the pore. This pressure is much higher than the oil or water pressure in the pore so that the gas moves quickly when it enters a pore. As the gas pressure builds up again before entering other pores, this pressure will also force more gas into a preoccupied pore and push the oil and water out of the pore. But once gas breakthrough occurs, the effect of the increased gas volume will be very small. Therefore, gas at a spot in the upper part of the cell appeared to occupy all of the pore space after several days of gas injection. However, at a spot in the lower part of the cell, oil still can be seen clearly in the oil films or layers even at the end of gas injection. A detailed pore-level observation of the DDP is shown in a series of pictures in Appendix C.

4.4.3. Observation of the SCWD Process

Prior to the SCWD process, the oil bank was produced, and the gas had broken through. At the pore level, most of the oil remaining existed as continuous oil films or layers in the lower part of the cell. The oil drained, by its own weight, slowly through these oil films and layers. In the upper part of the cell, oil and water volumes were much smaller, the oil and water existed as thin films, and the gas occupied all of the available pore space. When the second water injection was started, the water moved slowly upward from the bottom of the cell with a nearly flat front. When the front reached the middle of the cell, some brown spots appeared around the waterfront. As the water moved into the upper part of the cell, the front became concave downward (Figure 4.9). In the DDP, the gas front had an essentially similar shape (concave downward). However, with respect to the water front, the velocity of the front was low near the middle and higher near the walls, while for the gas front, the velocity was high near the middle, and lower near the walls. As the water from both sides joined

near the outlet, a bypassed area was formed (Figure 4.10). Most of the brown spots were blocked at the edge of this area. Although the bypassed area became smaller with time, the mobile oil in these brown spots entered the pores in this area, with the result that no oil was produced in the SCWD process. The formation of the bypassed area can be explained using pore level observations. When water enters a pore containing gas, water and oil, it's much easier for the water to enter a pore containing lots of water and oil than it is for the water to enter a pore containing very little water and oil. In the middle of the upper part of the cell, gas has displaced almost all of the water and oil; consequently, when water entered a pore, it took a long time for it to enter. But on the sides of the cell, there was still some water and oil left in the pores; hence, the water could go quickly towards the outlet. Eventually, this formed a bypassed area. This occurred because of the small size of the cell. At the large scale of a field, the bypassed area probably would not occur and the mobile oil would be produced.

How does the water in the SCWD process displace the oil? Let's think about a strongly water-wet system. After the gas flood, gas as the non-wetting phase stays at the center of pores and occupies all of the available pore space. Water as the wetting phase exists as a thin film along the rock surface, while oil as the intermediate phase exists as a thin film between the gas and water phases. When water enters a pore, water flows into the water film along the surface of the pore and displaces oil films and some of the gas out of the pore. Later, the water may displace all of the oil and gas out of the pore or leave some gas in the center of the pore. Figures 4.11 - 4.13 were selected to show the SCWD process. They were taken from the same spot but at different times. In Figure 4.13, there was some gas and a little oil trapped in the water swept area after the second water invasion. Compared with the residual oil to water shown in Figures 4.4 and 4.5, the residual oil after the SCWD process is much less. The trapped gas could be observed easily because there was sufficient gas left in the cell. Most of the oil remaining exists as a very thin oil film surrounding the gas globules. Only a few oil globules, trapped in the center of pores, were found. Therefore, the trapped gas is an important reason why there was such a low residual oil saturation after the second waterflood. It's not hard to imagine that more oil

globules would be trapped if no gas was trapped. This observation confirms the thought, obtained from the SCWD process reservoir simulation, that the trapped gas reduces the residual oil saturation in the second water flood. A detailed pore-level observation of the SCWD process is shown in a series of pictures in Appendix D.

4.5. Interfacial Tension Measurements

The interfacial tensions (IFT) were measured to calculate the spreading coefficient of the oil in the fluid system used in the transparent cell experiments. As mentioned before, the IFT plays an important role in controlling the fluid distributions in the pore space. If an oil in a fluid system has a positive spreading coefficient, when the gas enters a pore containing the oil and the water, the oil will spread as an oil film between the gas and the water phases. Because oil films were indeed observed in the experiment, a positive spreading coefficient is expected.

The Pendent Drop technique was used to measure the water/gas, oil/gas and oil/water interfacial tensions of the fluid system. Oil was an oil mixture, water was distilled water and gas was Nitrogen (Table 4.2).

Measurements were conducted on a Pendent Drop Apparatus at room temperature and pressure. Processed drops were filmed using the Canon 8 mm video camcorder with a set of close-up lenses (Hakuba 46 mm +4 and +1), which gave images a magnification up to 16x. Images of these drops were later transferred to a computer using the frame capture software SNAPPY Video Snapshot Version 3.0. Then, the drop dimensions were measured using measuring software SigmaScan Pro 5.0. For each pair of fluids, 16 IFT values were calculated based on 16 independently processed drops. The calculations of these IFT values are shown in Appendix E. After averaging them, the water/gas IFT was 72.3 mN/m, the oil/gas IFT was 24.7 mN/m and the oil/water IFT was 20.8 mN/m. Then, the spreading coefficient of oil over water in this fluid system was calculated to be 26.7 mN/m. Therefore, the spreading coefficient has a positive value corresponding to the oil films observed in the DDP.

Table 4.1: Properties of the transparent cell

Properties	Cell 1	Cell 2
Length	6.29 in	6.29 in
Width	2.15 in	2.15 in
Thickness	0.03 in	0.03 in
Sand Grains Size	45 -50 mesh (0.0110-0.0127 in)	50-55 mesh (0.0097-0.0110 in)
Porosity, ϕ	45.1 % - 46.6 %	45.1 %
Absolute Permeability, k	17.22 D / 16.72 D	11.85 D / 12.10 D
Irreducible Water Saturation, S_{wir}	20 %	10 %
End-Point Oil Relative Permeability, k_{row}	0.25	-
Residual Oil Saturation, S_{orw}	40 %	43.3 %
End-Point Water Relative Permeability, k_{rwo}	0.35	-
Finial Oil Saturation, S_o	6.7 %	10 %

Table 4.2: Data of IFT measurements

Fluid System	oil	50% bonnie glen crude oil + 50% decane	0.7682 g/cm^3
	water	distilled water	1.0226 g/cm^3
	gas	nitrogen	0.00125 g/cm^3
Interfacial Tension	gas/oil	24.7 mN/m	
	oil /water	20.8 mN/m	
	gas/water	72.3 mN/m	
Spreading Coefficient		+ 26.7	

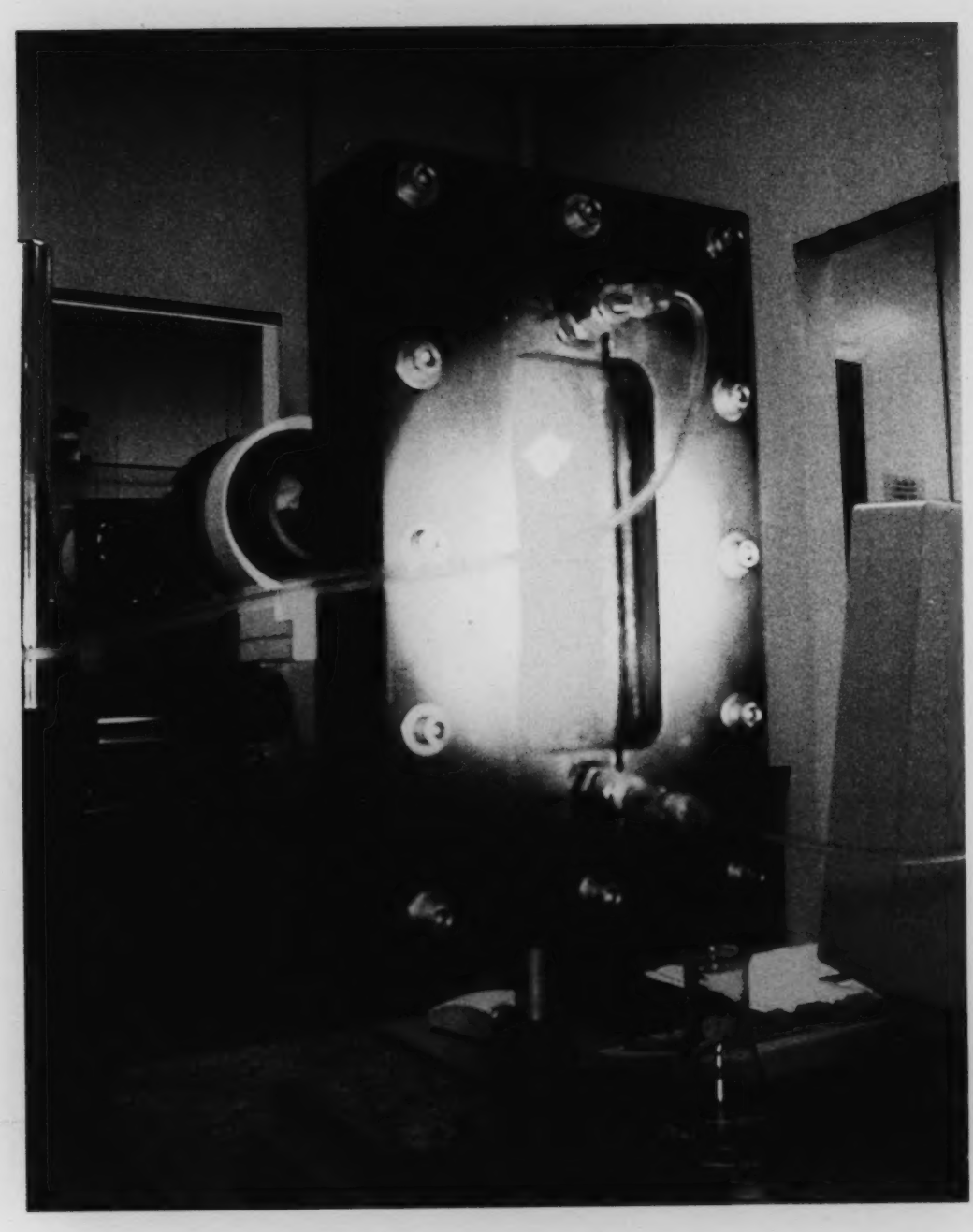

Figure 4.1: Transparent cell

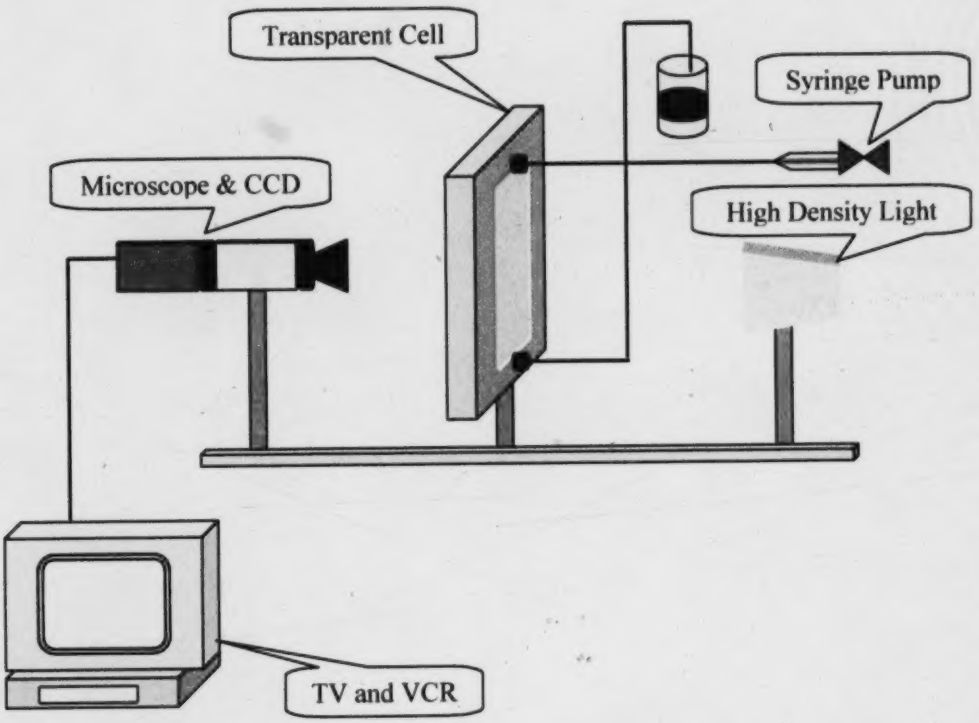

Figure 4.2: Experimental setup

Figure 4.3: Dry sand

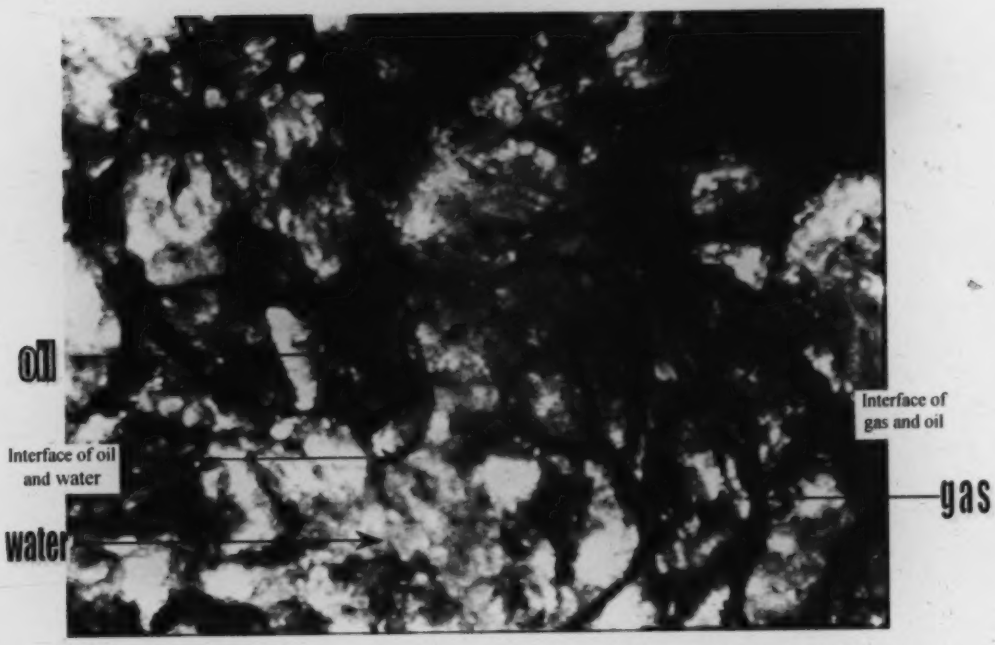

Figure 4.4: Oil, water, and gas in a spot at the top of the cell

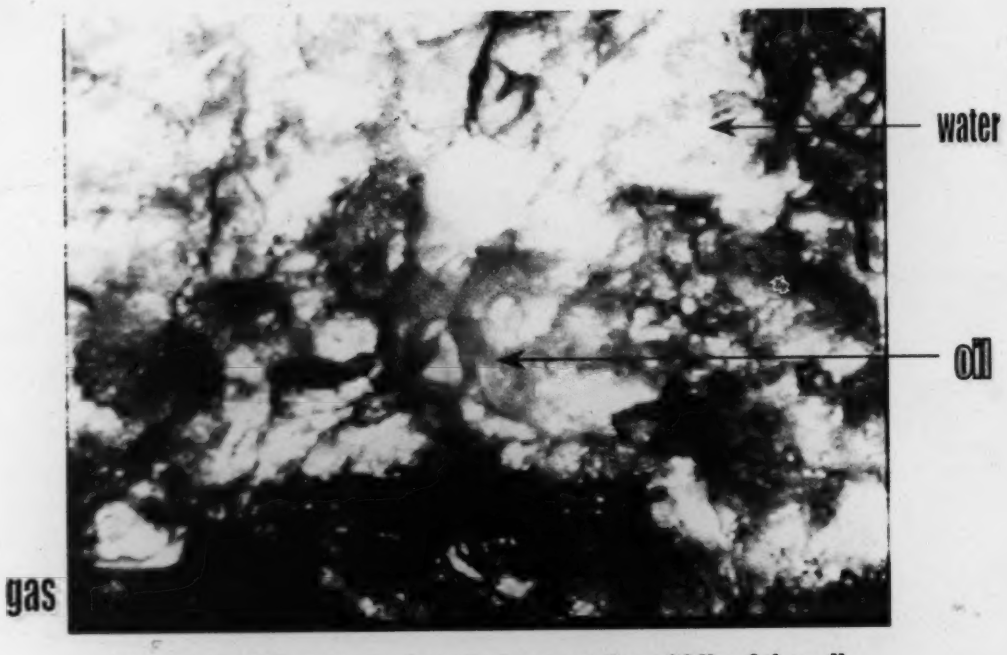

Figure 4.5: Oil, water and gas in a spot at the middle of the cell

Figure 4.6: Gas enters the front layer and the middle layer

Figure 4.7: Gas front in the DDP

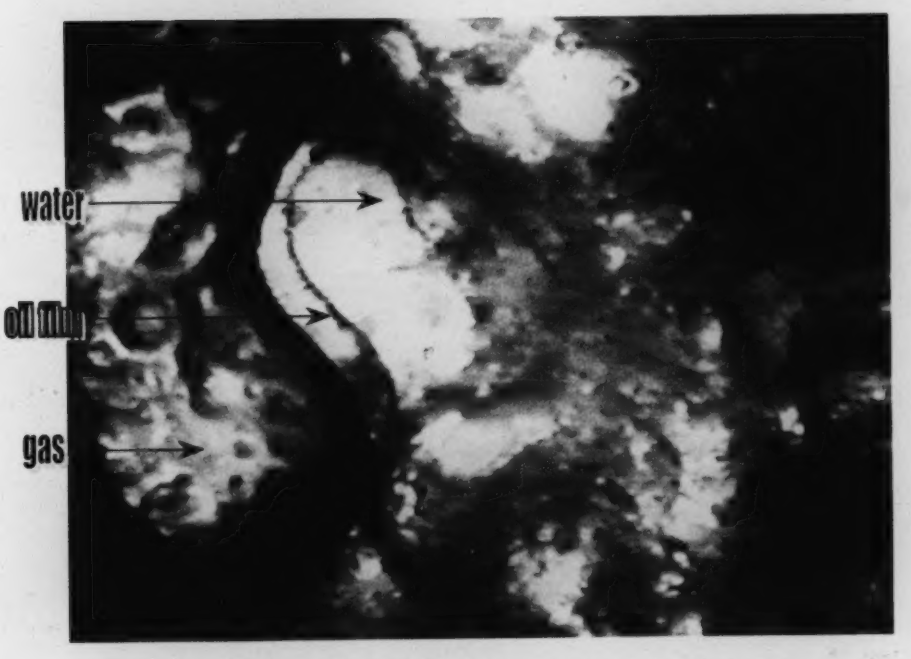

Figure 4.8: Oil film between gas and water

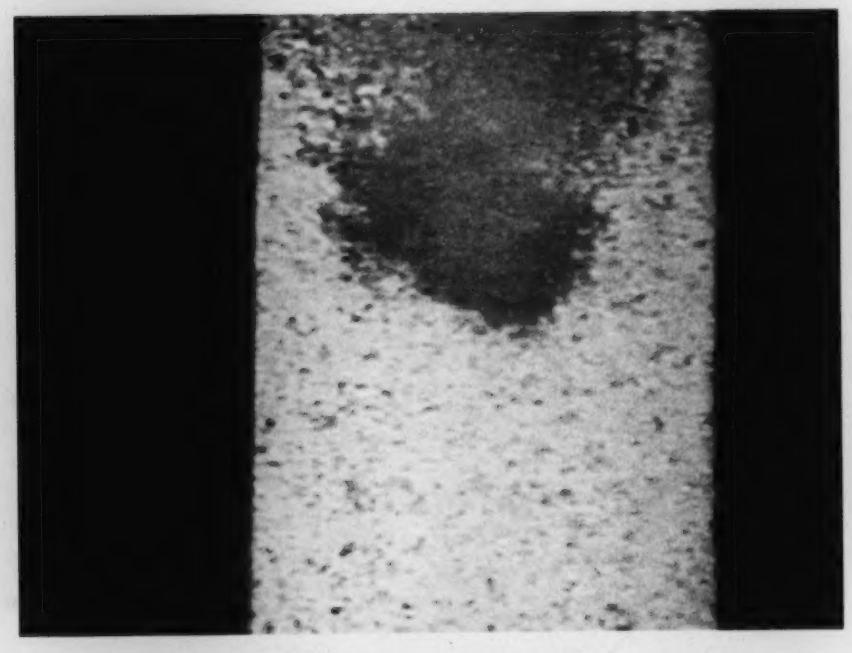

Figure 4.9: Water front in the SCWD process

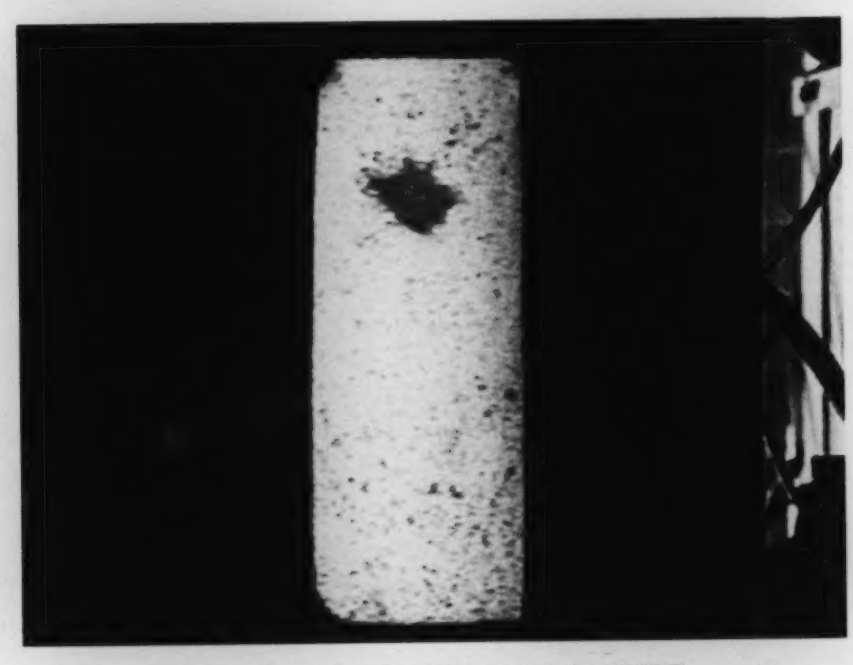

Figure 4.10: Bypassed area at the end of the SCWD process

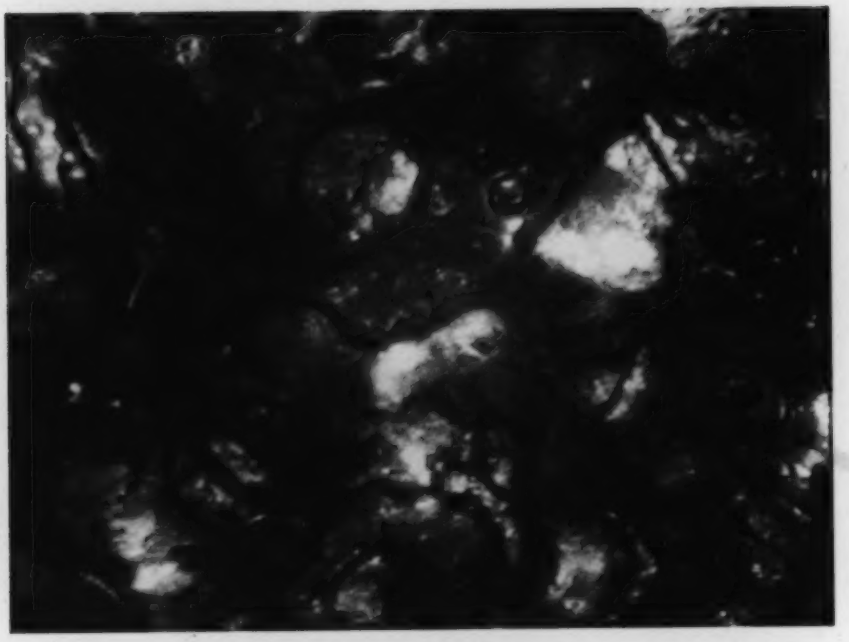

Figure 4.11: Before the SCWD process

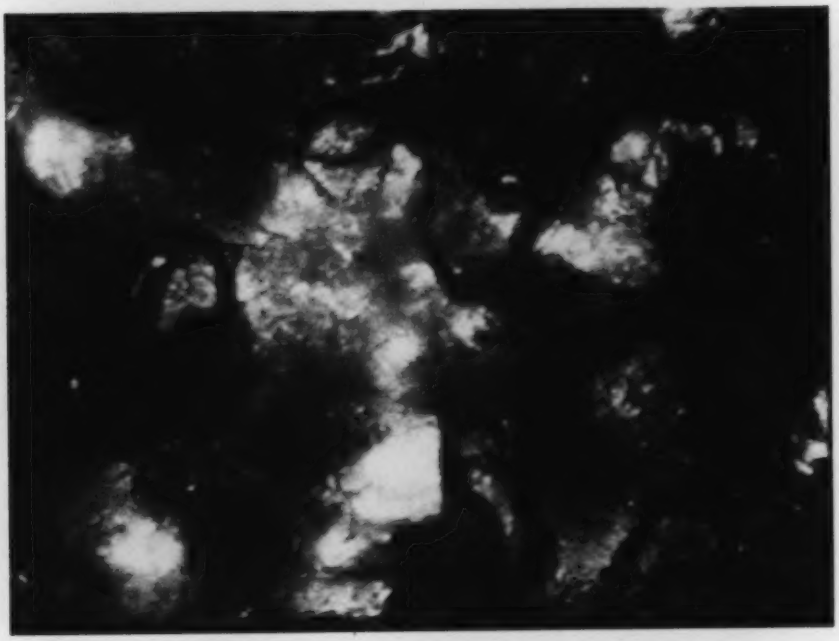

Figure 4.12: Water enters from the left

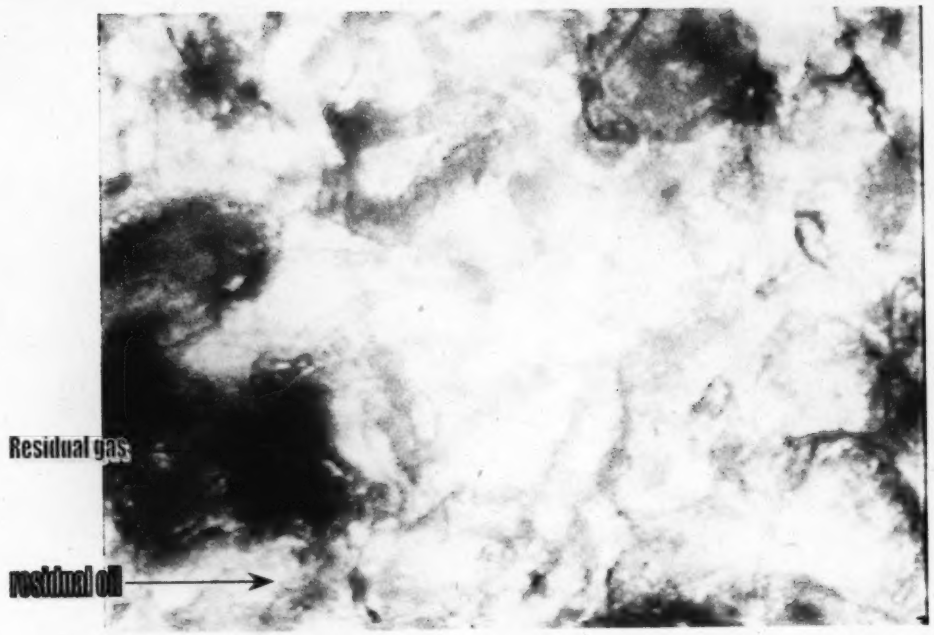

Figure 4.13: After the SCWD process

CHAPTER 5

CONCLUSIONS AND RECOMMENDATIONS

5.1. Summary and Conclusions

In this study, the Double Displacement Process and the Second Contact Water Displacement process were investigated using the CMG IMEX numerical simulator and a transparent porous media micromodel. A reservoir simulation at reservoir scale of the DDP was performed to investigate the macroscopic level mechanisms of the process. The effects of some of the parameters on the performance of the process were studied for the purpose of developing a set of screening criteria for selecting candidate reservoirs for the process. Moreover, the SCWD process was simulated to investigate the feasibility of the SCWD process. In the laboratory, the DDP and the SCWD process were simulated physically in the micromodel -- transparent cell. The pore level observations of the processes in the cell were used to investigate the microscopic level mechanisms of the processes. Based on the results of the study, the following conclusions can be drawn.

1. When applying the gravity assisted tertiary gas injection process in a reservoir, the injection and production rates play a very important role in controlling the formation of the oil bank, the shape of the oil-gas front and the oil drainage rate.

2. For the production wells, perforating only the lower part of the well increases the oil recovery.

3. Highly dipping reservoirs are favorable candidates for the gravity assisted tertiary gas injection process.

4. Accurate three-phase oil relative permeabilities in the low oil saturation region, and three-phase capillary pressures are necessary when using reservoir simulation to predict accurately the oil recovery achieved when using the tertiary gas injection process.

5. The oil film or layer plays a very important role in achieving high recovery efficiencies in tertiary gas injection. Oil flowing through the oil films and layers is driven not only by its own weight, but also by the increasing volume of the gas.

6. The interfacial tension measurements indicated that the formation of the oil film corresponded to an oil in a fluid system which has a positive spreading coefficient.

7. In the SCWD process, gas occupies the center of a pore, water enters a pore along the surface of the pore and displaces the oil films and some gas out of the pore first; later water may displace all of the oil and gas out of the pore.

8. The SCWD process is much shorter when compared to the period of low oil production of the DDP. Trapped gas reduces the possibility of the residual oil being trapped in the center of pores. Therefore, for situations where the source of gas is not sufficient, and where the formation has a high irreducible gas saturation, the SCWD process is a good choice.

5.2. Recommendations

Several studies are suggested to extend the present study:

1. Construct a larger transparent cell, which is longer and wider than the one used in this study, to reduce the fingering and to increase the pore volume of the cell.

2. Use water-wet fittings and tubing for the cell and more accurate equipment to do the measurements.

3. Use an oil with a negative spreading coefficient to do the DDP and SCWD process to see if the oil film or layer appears.

4. Develop a set of screening criteria for selecting candidate reservoirs for the DDP and the SCWD process.

REFERENCES

Alemán, M. A. and Slattery, J. C.: "Estimation of Three-Phase Relative Permeabilities", *Transport in Porous Media* **3**, 111-131, 1988.

Aziz, K. and Settari, T.: "Petroleum Reservoir Simulation", Applied Science Publishers, London, 1979.

Baker, L. E.: "Three-Phase Relative Permeability Correlations", SPE 17369 paper presented at the SPE/DOE Symposium on Enhanced Oil Recovery, Tulsa, OK, April 17–20, 1988.

Bensaid, F.: "Effects of Dip Angle, Absolute Permeability and Relative Permeability on the Double Displacement Process", M.Sc. Thesis, Louisiana State University, Baton Rouge, LA, 1995.

Blunt, M. J.: "An Empirical Model for Three-Phase Relative Permeability", SPE 56474 paper presented at the proceedings of the SPE Annual Conference, Houston, TX, October 3-6, 1999.

Blunt, M. J., Fenwick, D. H. and Zhou, D.: "What Determines Residual Oil Saturation in Three-phase Flow?", SPE/DOE 27816 paper presented at the SPE/DOE ninth Symposium, Tulsa, OK, April 17-20, 1994.

Bourgoyne, T. T.: "Tertiary Recovery of Oil by Up-dip Gas Injection", Ph.D. Dissertation, Louisiana State University, Baton Rouge, LA, 1996.

Cardwell, W. T. and Parsons, R. L.: "Gravity Drainage Theory", *Trans.*, AIME **179**, 199-215, 1949.

Carlson, L. O.: "Performance of Hawkins Field Unit Under Gas Drive Pressure Maintenance Operations and Development of an Enhanced Oil Recovery Project", SPE/DOE 17324 paper presented at the SPE/DOE Symposium on Enhanced Oil Recovery, Tulsa, OK, April 17-20, 1988.

Catalan, L. J. J., Dullien, F. A. L. and Chatzis, I.: "The Effects of Wettability and Heterogeneities on the Recovery of Waterflood Residual Oil with Low Pressure

Inert Gas Injection Assisted by Gravity Drainage", *SPE Advance Technology Series* **2**(2), 140-149, 1994.

Computer Modelling Group Ltd.: "User's Guide IMEX: Advanced Oil/Gas Reservoir Simulator Version 2000".

Chalier, G., Giry, V., Madaoui, K., Sakthikumar, S. and Maquignon, Ph.: "Three Phase Oil Relative Permeability Determination as a Key Point in the Evaluation of a Tertiary Gas Gravity Drainage Project", SPE 30761 paper presented at the proceedings of the SPE Annual Conference, Dallas, October 22-25, 1995.

Chatzis, I., Kantzas, A. and Dullien, F. A. L.: "On the Investigation of Gravity-Assisted Inert Gas Injection Using Micromodels, Long Berea Sandstone Cores, and Computer-Assisted Tomography", SPE 18284 paper presented at the 63rd SPE Annual Technical Conference and Exhibition, Houston, TX, October 2-5, 1988.

Corey, A. T., Rathjens, C. H., Henderson, J. H. and Wyllie, M. R. J.: "Three-Phase Relative Permeability", *Trans.*, AIME **207**, 349-351, 1956.

Dehghani, K., Bansal, A., Ogbe, D. O. and Ostermann, R. D.: "The Effect of the Presence of a Third Phase on Capillary Pressure by Centrifuge Method and CT Scanning", SPE 18793 paper presented at the 1989 SPE California Regional Meeting, Bakersfield, April 5-7, 1989.

Delshad, M. and Pope, G. A.: "Comparison of the Three-phase Oil Relative Permeability Models", *Transport in Porous Media* **4**, 59-83, 1989.

DiCarlo, D. A., Sahni, A. and Blunt, M. J.: "The Effect of Wettability on Three-Phase Relative Permeability", SPE 49317 paper presented at the proceedings of the SPE Annual Conference, New Orleans, LA, September 27-30, 1998.

Dietz, D. N.: "A Theoretical Approach to the Problem of Encroaching and By-Passing Edge Water", *Proc. Kon. Neder. Adad. Wetenshaflen,* Series B-56, 83-92, 1953.

Dong, M., Dullien, F. A. L. and Chatzis, I.: "Imbibition of Oil in Film Form over Water Present in Edges of Capillaries with an Angular Cross Section", *Journal of Colloid and Interface Science* **172**, 21-36, 1995.

Dumoré, J. M. and Schols R. S.: "Drainage Capillary-Pressure Functions and the Influence Of Connate Water", *Society of Petroleum Engineers Journal* **14** (5), 437-444, 1974.

Dykstra, H.: "The Prediction of Oil Recovery by Gravity Drainage", *Journal of Petroleum Technology* **30**, 818-830, 1978.

Fassihi, M. R. and Gillham, T. H.: "The Use of Air Injection to Improve the Double Displacement Process", SPE 26374 paper presented at the 68th Annual SPE Technical Conference and Exhibition, Houston, TX, October 3-6, 1993.

Fassihi, M. R., Yannimaras, D. V., Westfall, E. E. and Gillham, T. H.: "Economics of Light Oil Air Injection Projects", SPE/DOE 35393 paper presented at the 1996 SPE/DOE Symposium on Enhanced Oil Recovery, Tulsa, OK, April 21-24, 1996.

Fayers, F. J. and Matthews, J. D.: "Evaluation of Normalized Stone's Methods of Estimating Three-Phase Relative Permeabilities", *Society of Petroleum Engineers Journal* **24** (2), 224-232, 1984.

Fenwick, D. H. and Blunt M. J.: "Use of Network Modeling to Predict Saturation Paths, Relative Permeabilities and Oil Recovery for Three Phase Flow in Porous Media", SPE 38881 paper presented at the SPE Annual Technical Conference and Exhibition, San Antonio, TX, October 5-8, 1997.

Flock, D. L., Lee, T. H. and Gibeau, J. P.: "The Effect of Temperatures on the Interfacial Tension of Heavy Crude Oils Using the Pendent Drop Apparatus", paper presented at the 35th Annual Technical Meeting of the Petroleum Society of CIM, Calgary, AB, June 10-13, 1984.

Gillham T. H., Cerveny, B. W., Fornea, M. A. and Bassiouni, Z.: "Low Cost IOR: An Update on the W. Hackberry Air Injection Project", SPE 39642 paper presented at the SPE/DOE Symposium on Enhanced Oil Recovery, Tulsa, OK, April 18-22, 1998.

Gillham T. H., Cerveny, B. W., Turek, E. A. and Yannimaras, D. V.: "Keys to Increasing Production via Air Injection in Gulf Coast Light Oil Reservoirs", SPE 38848 paper presented at the 1997 Annual Technical Conference and Exhibition, San Antonio, TX, October 5-8, 1997.

Gunawan, S. and Caié, D.: "Handil Field: Three Years of Lean Gas Injection into Waterflooded Reservoirs", SPE 57289 paper presented at the 1999 SPE Asia Pacific Improved Oil Recovery Conference, Kuala Lumpur, Malaysia, October 25-26, 1999.

Hagoort, J.: "Oil Recovery by Gravity Drainage", *Society of Petroleum Engineers Journal* **20** (3), 139-150, 1980.

Hicks, P. J., Jr. and Grader, A. S.: "Simulation of Three-phase Displacement Experiments", *Transport in Porous Media* **24**, 221-245, 1996.

Hui, M. and Blunt, M. J.: "Pore-Scale Modeling of Three-Phase Flow and the Effects of Wettability", SPE 59309 paper presented at the 2000 SPE/DOE meeting, Tulsa, OK, April 3-5, 2000.

Jerauld, G. R.: "Prudhoe Bay Gas/Oil Relative Permeability", *SPE Reservoir Engineering* **12**, 66-73, 1997.

Johnston, J. R.: "Weeks Island Gravity Stable CO_2 Pilot", SPE/DOE 17351 paper presented at the SPE/DOE Symposium on Enhanced Oil Recovery, Tulsa, OK, April 17-20, 1988.

Kalaydjian, F.: "Performance and Analysis of Three-Phase Capillary Pressure Curves for Drainage and Imbibition in Porous Media", SPE 24878 paper presented at 67th Annual Technical Conference and Exhibition, Washington, DC, October 4-7, 1992.

Kalaydjian, F., Moulu, J. C., Vizika, O. and Munkerud, P. K.: "Three-Phase Flow in Water-Wet Porous Media: Gas/Oil Relative Permeabilities for Various Spreading Conditions", SPE 26671 paper presented at the 68th Annual Technical Conference and Exhibition, Houston, TX, October 3-6, 1993.

Kantzas, A., Chatzis, I. and Dullien, F. A. L.: "Enhanced Oil Recovery by Inert Gas Injection", SPE 17379 paper presented at the 1988 SPE/DOE Symposium on Enhanced Oil Recovery, Tulsa, OK, April 17–20, 1988.

Kantzas A., Chatzis I. and Dullien F. A. L.: "Mechanisms of Capillary Displacement of Residual Oil by Gravity-Assisted Inert Gas Injection", SPE 17506 paper presented at the SPE Rocky Mountain Regional Meeting, Casper, WY, May 11-13, 1988.

Kantzas A., Marentette D. F., Erno B. P. and Chatzis I.: "Recovery of Heavy Oil Using Horizontal Wells and Gravity Drainage with Pressure Maintenance", Paper No. 14, presented at the CIM/CANMET 4th Petroleum Conference, Regina, Sask., October 7-9, 1991.

Kantzas A., Nikakhtar B., Wit P., Pow M., and JHA K. M.: "Design of a Gravity Assisted Immiscible Gas Injection Program for Application in a Vuggy Fractured Reef", *Journal of Canadian Petroleum Technology* **32** (10), 15-23, 1993.

Keller, A. A., Blunt, M. J. and Roberts, P. V.: "Micromodel Observation of the Role of Oil Layers In Three-Phase Flow", *Transport in Porous Media* **26**, 277-297, 1997.

Langenberg, M. A., Henry, D. M. and Chlebana, M. R.: "Performance and Expansion Plans for the Double Displacement Process in the Hawkins Field Unit", SPE 28603 paper presented at the 69th Annual Technical Conference and Exhibition, New Orleans, LA, September 25-28, 1994.

Lepski, B.: "Physical Modeling of the Oil Displacement by Gas in Waterflooded Zones", M.Sc. Thesis, Louisiana State University, Baton Rouge, LA, 1995.

Lepski, B., Bassiouni, Z. and Wolcott, J.: "Second-Contact Water Displacement Oil Recovery Process", SPE 35360 paper presented at the 1996 SPE/DOE Symposium on Enhanced Oil Recovery, Tulsa, OK, April 21-24, 1996.

Lepski, B., Bassiouni, Z. and Wolcott, J.: "Screening Of Oil Reservoirs For Gravity Assisted Gas Injection", SPE 39659 paper presented at the 1998 SPE/DOE Symposium on Enhanced Oil Recovery, Tulsa, OK, April 19-22, 1998.

Lewis, J. O.: "Gravity Drainage in Oil Fields", *Trans.*, AIME **155**, 133-154, 1944.

Mani, V. and Mohanty, K. K.: "Effect of the Spreading Coefficient on Three-Phase Flow in Porous Media", *Journal of Colloid and Interface Science* **187**, 45-56, 1997.

Naylor P. and Frorup, M.: "Gravity-Stable Nitrogen Displacement of Oil", SPE 19641 paper presented at the 1989 SPE Annual Technical Conference and Exhibition, San Antonio, TX, October 8-11, 1989.

Oak, M. J.: "Three-Phase Relative Permeabilities of Water-Wet Berea", SPE/DOE 20183 paper presented at the SPE/DOE Symposium on Enhanced Oil Recovery, Tulsa, OK, April 22-25, 1990.

Oak, M. J., Baker, L. E. and Thomas, D.C.: "Three-Phase Relative Permeability of Berea Sandstone", *Journal of Petroleum Technology* **42**, 1054-1061, 1990.

Oren, P. E., Billiotte, J., Paris, E. M. and Pinczewski, W. V.: "Pore-Scale Network Modelling of Waterflood Residual Oil Recovery by Immiscible Gas Flooding", SPE/DOE 27814 paper presented at the SPE/DOE 9th Symposium on Improved Oil Recovery, Tulsa, OK, April 17-20, 1994.

Oren, P. E., Billiotte, J. and Pinczewski, W. V.: "Mobilization of Waterflood Residual Oil by Gas Injection for Water-Wet Conditions", *SPE Formation Evaluation* **7** (1), 70-78, 1992.

Oren, P. E. and Pinczewski, W. V.: "Effect of Wettability and Spreading on Recovery of Waterflood Residual Oil by Immiscible Gasflooding", *SPE Formation Evaluation* **9** (2), 149-156, 1994.

Oren, P. E. and Pinczewski, W. V.: "Fluid Distribution and Pore Scale Displacement Mechanisms in Drainage Dominated Three Phase Flow", *Transport Porous Media* **20**, 105-133, 1995.

Pereira, G. G., Pinczewski, W. V., Chan, D. Y., Paterson, L. and Oren, P. E.: "Pore-Scale Network Model for Drainage-Dominated Three-phase Flow in Porous Media", *Transport in Porous Media* **24**, 167-201, 1996

Rao, D. N.: "Gas Injection EOR-A New Meaning in the New Millennium", *Journal of Canadian Petroleum Technology* **40** (2), 11-19, 2001.

Richardson, J. G. and Blackwell, R. J.: "Use of Simple Mathematical Models for Predicting Reservoir Behavior", SPE 2928 paper presented at 45th Annual Fall Meeting of the SPE of AIME, Houston, TX, October 4-7, 1970.

Robinson, R. L. and Slattery, J. C.: "Estimation of Three-Phase Relative Permeabilities", *Transport in Porous Media* **16**, 263-287, 1994.

Sahni, A., Burger, J. and Blunt, M.: "Measurement of Three Phase Relative Permeability during Gravity Drainage using CT", SPE 39655 paper presented at

the SPE/DOE Symposium on Enhanced Oil Recovery, Tulsa, OK, April 19-22, 1998.

Soll, W. E., Celia, M. A. and Wilson, J. L.: "Micromodel Studies of Three-Fluid Porous Media Systems: Pore-Scale Process Relating to Capillary Pressure-Saturation Relationships", *Water Resources Research* **29** (9), 2963-2974, 1993.

Stahl, R. F., Martin, W. A. and Huntington, R. L.: "Gravitational Drainage of Liquids from Unconsolidated Wilcox Sand", *Trans*., AIME **146**, 138-146, 1943.

Stone, H. L.: "Probability Model for Estimating Three-Phase Relative Permeabilities", *Journal of Petroleum Technology* **22**, 214-218, 1970.

Stone, H. L.: "Estimation of Three-Phase Relative Permeability and Residual Oil Data", *Journal of Canadian Petroleum Technology* **12** (4), 53-61, 1973.

Terwilliger, P. L., Wilsey, L. E., Hall, H. N., Bridges, P. M. and Morse, R. A.: "An Experimental and Theoretical Investigation of Gravity Drainage Performance", *Trans*., AIME **192**, 285-296, 1951.

Vizika, O. and Lombard, J. M.: "Wettability and Spreading: Two Key Parameters in Oil Recovery with Three-phase Gravity Drainage", *SPE Reservoir Engineering* **11** (1), 54-60, 1996.

APPENDIX A: BASIC DDP SIMULATION DATA SET

```
RESULTS SIMULATOR IMEX
RESULTS SECTION INOUT
*INUNIT *FIELD
*OUTUNIT *FIELD

*INTERRUPT *RESTART-STOP
*RANGECHECK *ON
*XDR *ON
*WPRN *WELL  *TIME
*WPRN *SECTOR  *TIME
*WPRN *GRID  *TIME
*WPRN *ITER  *NONE
*OUTPRN *WELL *BRIEF
*OUTPRN *TABLES *ALL
*WSRF *WELL  1
*WSRF *SECTOR  *TIME
*WSRF *GRID  *TIME
*OUTSRF *RES *ALL
*OUTSRF *WELL *LAYER  *NONE
*OUTDIARY *BRIEF *PRESAQ *HEADER  20

RESULTS XOFFSET 0.
RESULTS YOFFSET 0.
RESULTS ROTATION 0

GRID CART 180 10 5
KDIR DOWN
DIP -8 0
DI CON 10.
DJ CON 10.
DK CON 6.
DEPTH 1 1 1 4500.

**$ RESULTS PROP NULL  Units: Dimensionless
**$ RESULTS PROP Minimum Value: 1  Maximum Value: 1
**$ 0 = NULL block, 1 = Active block
NULL CON 1.
**$ RESULTS PROP PINCHOUTARRAY  Units: Dimensionless
**$ RESULTS PROP Minimum Value: 1  Maximum Value: 1
**$ 0 = PINCHED block, 1 = Active block
PINCHOUTARRAY CON 1.
RESULTS SECTION GRID
RESULTS PINCHOUT-VAL      0.0002 'ft'
RESULTS SECTION NETPAY
RESULTS SECTION NETGROSS
RESULTS SECTION POR

**$ RESULTS PROP POR  Units: Dimensionless
**$ RESULTS PROP Minimum Value: 0.25  Maximum Value: 0.25
POR CON 0.25
```

```
RESULTS SECTION PERMS
**$ RESULTS PROP PERMI  Units: md
**$ RESULTS PROP Minimum Value: 1500  Maximum Value: 1500
PERMI CON 1500.
**$ RESULTS PROP PERMJ  Units: md
**$ RESULTS PROP Minimum Value: 1500  Maximum Value: 1500
PERMJ CON 1500.
**$ RESULTS PROP PERMK  Units: md
**$ RESULTS PROP Minimum Value: 800  Maximum Value: 800
PERMK CON 800.
RESULTS SECTION TRANS
RESULTS SECTION FRACS
RESULTS SECTION GRIDNONARRAYS
CPOR  MATRIX  3.E-06
PRPOR MATRIX  14.69232
RESULTS SECTION VOLMOD
RESULTS SECTION SECTORLEASE
RESULTS SECTION ROCKCOMPACTION
RESULTS SECTION GRIDOTHER
RESULTS SECTION MODEL
MODEL *BLACKOIL
*TRES   200.
**$ OilGas Table 'Table A'
*PVT *EG 1
** P       Rs      Bo      EG      VisO    VisG
   14.7    0.04    1.0664  4.43879 2.8064  0.01819
   213.72  0.37    1.0664  64.4802 2.7995  0.018191
   412.74  0.78    1.0664  124.3884 2.7911  0.018191
   611.76  1.22    1.0665  184.118 2.782   0.018192
   810.78  1.69    1.0665  243.6254 2.7723  0.018193
   1009.8  2.19    1.0665  302.868 2.7623  0.018194
   1208.82 2.7     1.0665  361.805 2.7519  0.018195
   1407.84 3.24    1.0666  420.399 2.7412  0.018197
   1606.86 3.78    1.0666  478.613 2.7304  0.018198
   1805.88 4.35    1.0666  536.415 2.7194  0.018199
   2004.9  4.92    1.0666  593.772 2.7082  0.018201
   2203.92 5.51    1.0667  650.658 2.6969  0.018202
   2402.94 6.11    1.0667  707.045 2.6855  0.018204
   2601.96 6.71    1.0667  762.911 2.674   0.018205
   2800.98 7.33    1.0667  818.237 2.6625  0.018207
   3000.   7.96    1.0668  873.002 2.6509  0.018208
   4200.   11.9    1.0669  1190.647 2.5806  0.018219
   5400.   16.08   1.0671  1485.828 2.5105  0.01823
   6600.   20.46   1.0673  1758.796 2.4417  0.018243
   7800.   25.01   1.0675  2010.927 2.3747  0.018256
   9000.   29.7    1.0677  2244.064 2.3098  0.01827
**$ OilGas Table 'Table A'
**$ OilGas Table 'Table A'
*DENSITY *OIL 53.976
*DENSITY *GAS 0.0007
*CVO    0
*BWI    1.026204
*CW     3.02608E-06
*CO     7.869E-06
*REFPW  4000.
```

```
*VWI    0.312797
*CVW    0
*DENSITY *WATER 60.8066
RESULTS SECTION MODELARRAYS
RESULTS SECTION ROCKFLUID

*ROCKFLUID
*RPT 1
*KROIL *STONE2 *SWSG
*SWT
0.150000000 0.000000000 0.950000000 0.000000000 0.000000000
0.180000000 0.000013000 0.866216000 0.000000000 0.000000000
0.210000000 0.000100000 0.785887000 0.000000000 0.000000000
0.240000000 0.000338000 0.709051000 0.000000000 0.000000000
0.270000000 0.000800000 0.635749000 0.000000000 0.000000000
0.300000000 0.001563000 0.566023000 0.000000000 0.000000000
0.330000000 0.002700000 0.499920000 0.000000000 0.000000000
0.360000000 0.004288000 0.437490000 0.000000000 0.000000000
0.390000000 0.006400000 0.378788000 0.000000000 0.000000000
0.420000000 0.009113000 0.323874000 0.000000000 0.000000000
0.450000000 0.012500000 0.272816000 0.000000000 0.000000000
0.480000000 0.016638000 0.225687000 0.000000000 0.000000000
0.510000000 0.021600000 0.182571000 0.000000000 0.000000000
0.540000000 0.027463000 0.143564000 0.000000000 0.000000000
0.570000000 0.034300000 0.108778000 0.000000000 0.000000000
0.600000000 0.042188000 0.078346000 0.000000000 0.000000000
0.630000000 0.051200000 0.052430000 0.000000000 0.000000000
0.660000000 0.061413000 0.031238000 0.000000000 0.000000000
0.690000000 0.072900000 0.015056000 0.000000000 0.000000000
0.720000000 0.085738000 0.004324000 0.000000000 0.000000000
0.750000000 0.100000000 0.000000000 0.000000000 0.000000000

*SLT
0.200000000 1.000000000 0.000000000 0.000000000
0.237500000 0.902500000 0.001760194 0.000000000
0.275000000 0.810000000 0.007546118 0.000000000
0.312500000 0.722500000 0.017681343 0.000000000
0.350000000 0.640000000 0.032350917 0.000000000
0.387500000 0.562500000 0.051688940 0.000000000
0.425000000 0.490000000 0.075801577 0.000000000
0.462500000 0.422500000 0.104777130 0.000000000
0.500000000 0.360000000 0.138691418 0.000000000
0.537500000 0.302500000 0.177611010 0.000000000
0.575000000 0.250000000 0.221595335 0.000000000
0.612500000 0.202500000 0.270698128 0.000000000
0.650000000 0.160000000 0.324968474 0.000000000
0.687500000 0.122500000 0.384451584 0.000000000
0.725000000 0.090000000 0.449189390 0.000000000
0.762500000 0.062500000 0.519221011 0.000000000
0.800000000 0.040000000 0.594583123 0.000000000
0.837500000 0.022500000 0.675310262 0.000000000
0.875000000 0.010000000 0.761435069 0.000000000
0.912500000 0.002500000 0.852988501 0.000000000
0.950000000 0.000000000 0.950000000 0.000000000
```

```
RESULTS SECTION ROCKARRAYS
RESULTS SECTION INIT
*INITIAL
*USER_INPUT
**$ Data for PVT Region 1
**$ ---------------------------------------
RESULTS SECTION INITARRAYS
**$ RESULTS PROP SW  Units: Dimensionless
**$ RESULTS PROP Minimum Value: 0.7  Maximum Value: 0.7
SW CON 0.7
**$ RESULTS PROP PRES  Units: psi
**$ RESULTS PROP Minimum Value: 3000  Maximum Value: 3000
PRES CON 3000.
**$ RESULTS PROP PB  Units: psi
**$ RESULTS PROP Minimum Value: 3000  Maximum Value: 3000
PB CON 3000.
**$ RESULTS PROP SO  Units: Dimensionless
**$ RESULTS PROP Minimum Value: 0.3  Maximum Value: 0.3
SO CON 0.3
RESULTS SECTION NUMERICAL
*NUMERICAL
*DTMAX 365.
*DTMIN 0.001
*NORM *PRESS 235.113
*NORM *SATUR 0.01
*NORM *PBUB 435.113
*MAXCHANGE *SATUR 0.1

RESULTS SECTION NUMARRAYS
RESULTS SECTION GBKEYWORDS
RUN

DATE 1988 01 01.

WELL  1 'injector'
INJECTOR MOBWEIGHT 'injector'
INCOMP GAS
OPERATE MAX STG  1.5E+04 CONT
OPERATE MAX BHP  3100. CONT
GEOMETRY K 0.25 0.37 1. 0.
PERF GEO  'injector'
        1  3  1 1. FLOW-FROM 'SURFACE'
        1  3  2 1. FLOW-FROM 1
        1  3  3 1. FLOW-FROM 2
        1  3  4 1. FLOW-FROM 3
        1  3  5 1. FLOW-FROM 4
GUIDEI STG 'injector'       1.E+05

WELL  2 'INJECTOR2'
INJECTOR MOBWEIGHT 'INJECTOR2'
INCOMP GAS
OPERATE MAX STG  1.5E+04 CONT
OPERATE MAX BHP  3100. CONT
GEOMETRY K 0.25 0.37 1. 0.
PERF GEO  'INJECTOR2'
```

```
        1  7  1 1. FLOW-FROM 'SURFACE'
        1  7  2 1. FLOW-FROM 1
        1  7  3 1. FLOW-FROM 2
        1  7  4 1. FLOW-FROM 3
        1  7  5 1. FLOW-FROM 4
GUIDEI STG 'INJECTOR2'          1.E+05

WELL  3 'producer'
PRODUCER 'producer'
OPERATE MIN BHP  3000. CONT
OPERATE MAX BHF  1000. STOP
GEOMETRY K 0.25 0.37 1. 0.
PERF GEO   'producer'
        175  3  1 1. FLOW-TO 'SURFACE'
        175  3  2 1. FLOW-TO 1
        175  3  3 1. FLOW-TO 2
        175  3  4 1. FLOW-TO 3
        175  3  5 1. FLOW-TO 4

WELL  4 'PRODUCER2'
PRODUCER 'PRODUCER2'
OPERATE MIN BHP  3000. CONT
OPERATE MAX BHF  1000. STOP
GEOMETRY K 0.25 0.37 1. 0.
PERF GEO   'PRODUCER2'
        175  7  1 1. FLOW-TO 'SURFACE'
        175  7  2 1. FLOW-TO 1
        175  7  3 1. FLOW-TO 2
        175  7  4 1. FLOW-TO 3
        175  7  5 1. FLOW-TO 4

SHUTIN 'injector'
SHUTIN 'INJECTOR2'
SHUTIN 'producer'
SHUTIN 'PRODUCER2'

DATE 1990 01 01.

OPEN 'injector'
OPEN 'producer'
OPEN 'INJECTOR2'
OPEN 'PRODUCER2'

DATE 1991 01 01.

OPEN 'injector'
OPEN 'producer'
OPEN 'INJECTOR2'
OPEN 'PRODUCER2'

DATE 1992 01 01.

OPEN 'injector'
OPEN 'producer'
OPEN 'INJECTOR2'
```

```
OPEN 'PRODUCER2'

DATE 1993 01 01.

OPEN 'injector'
OPEN 'producer'
OPEN 'INJECTOR2'
OPEN 'PRODUCER2'

DATE 1994 01 01.

OPEN 'injector'
OPEN 'producer'
OPEN 'INJECTOR2'
OPEN 'PRODUCER2'

DATE 1995 01 01.

OPEN 'injector'
OPEN 'producer'
OPEN 'INJECTOR2'
OPEN 'PRODUCER2'

DATE 1996 01 01.

OPEN 'injector'
OPEN 'producer'
OPEN 'INJECTOR2'
OPEN 'PRODUCER2'

DATE 1997 01 01.

OPEN 'injector'
OPEN 'producer'
OPEN 'INJECTOR2'
OPEN 'PRODUCER2'

DATE 1998 01 01.

OPEN 'injector'
OPEN 'producer'
OPEN 'INJECTOR2'
OPEN 'PRODUCER2'

DATE 1999 01 01.

OPEN 'injector'
OPEN 'producer'
OPEN 'INJECTOR2'
OPEN 'PRODUCER2'

DATE 2000 01 01.
STOP
RESULTS SECTION WELLDATA
RESULTS SECTION PERFS
```

APPENDIX B: BASIC SCWD SIMULATION DATA SET

```
RESULTS SIMULATOR IMEX
RESULTS SECTION INOUT
*INUNIT *FIELD
*OUTUNIT *FIELD
*INTERRUPT *RESTART-STOP
*RANGECHECK *ON
*XDR *ON
*WPRN *WELL  *TIME
*WPRN *SECTOR  *TIME
*WPRN *GRID  *TIME
*WPRN *ITER  *NONE
*OUTPRN *WELL *BRIEF
*OUTPRN *TABLES *ALL
*WSRF *WELL  1
*WSRF *SECTOR  *TIME
*WSRF *GRID  *TIME
*OUTSRF *RES *ALL
*OUTSRF *WELL *LAYER  *NONE
*OUTDIARY *BRIEF *PRESAQ *HEADER  20
RESULTS XOFFSET 0.
RESULTS YOFFSET 0.
RESULTS ROTATION 0

GRID CART 180 10 5
KDIR DOWN
DIP -8 0
DI CON 10.
DJ CON 10.
DK CON 6.
DEPTH 1 1 1 4500.
**$ RESULTS PROP NULL  Units: Dimensionless
**$ RESULTS PROP Minimum Value: 1  Maximum Value: 1
**$ 0 = NULL block, 1 = Active block
NULL CON 1.
**$ RESULTS PROP PINCHOUTARRAY  Units: Dimensionless
**$ RESULTS PROP Minimum Value: 1  Maximum Value: 1
**$ 0 = PINCHED block, 1 = Active block
PINCHOUTARRAY CON 1.
RESULTS SECTION GRID
RESULTS PINCHOUT-VAL      0.0002 'ft'
RESULTS SECTION NETPAY
RESULTS SECTION NETGROSS
RESULTS SECTION POR
**$ RESULTS PROP POR  Units: Dimensionless
**$ RESULTS PROP Minimum Value: 0.25  Maximum Value: 0.25
POR CON 0.25
RESULTS SECTION PERMS
**$ RESULTS PROP PERMI  Units: md
**$ RESULTS PROP Minimum Value: 1500  Maximum Value: 1500
PERMI CON 1500.
```

```
**$ RESULTS PROP PERMJ  Units: md
**$ RESULTS PROP Minimum Value: 1500  Maximum Value: 1500
PERMJ CON 1500.
**$ RESULTS PROP PERMK  Units: md
**$ RESULTS PROP Minimum Value: 800  Maximum Value: 800
PERMK CON 800.
RESULTS SECTION TRANS
RESULTS SECTION FRACS
RESULTS SECTION GRIDNONARRAYS
CPOR  MATRIX  3.E-06
PRPOR MATRIX  14.69232
RESULTS SECTION VOLMOD
RESULTS SECTION SECTORLEASE
RESULTS SECTION ROCKCOMPACTION
RESULTS SECTION GRIDOTHER
RESULTS SECTION MODEL
MODEL *BLACKOIL
*TRES   200.
**$ OilGas Table 'Table A'
*PVT *EG 1
**  P       Rs      Bo      EG      VisO    VisG
   14.7     0.04    1.0664  4.43879 2.8064  0.01819
   213.72   0.37    1.0664  64.4802 2.7995  0.018191
   412.74   0.78    1.0664  124.3884 2.7911  0.018191
   611.76   1.22    1.0665  184.118 2.782   0.018192
   810.78   1.69    1.0665  243.6254 2.7723  0.018193
   1009.8   2.19    1.0665  302.868 2.7623  0.018194
   1208.82  2.7     1.0665  361.805 2.7519  0.018195
   1407.84  3.24    1.0666  420.399 2.7412  0.018197
   1606.86  3.78    1.0666  478.613 2.7304  0.018198
   1805.88  4.35    1.0666  536.415 2.7194  0.018199
   2004.9   4.92    1.0666  593.772 2.7082  0.018201
   2203.92  5.51    1.0667  650.658 2.6969  0.018202
   2402.94  6.11    1.0667  707.045 2.6855  0.018204
   2601.96  6.71    1.0667  762.911 2.674   0.018205
   2800.98  7.33    1.0667  818.237 2.6625  0.018207
   3000.    7.96    1.0668  873.002 2.6509  0.018208
   4200.    11.9    1.0669  1190.647 2.5806  0.018219
   5400.    16.08   1.0671  1485.828 2.5105  0.01823
   6600.    20.46   1.0673  1758.796 2.4417  0.018243
   7800.    25.01   1.0675  2010.927 2.3747  0.018256
   9000.    29.7    1.0677  2244.064 2.3098  0.01827
**$ OilGas Table 'Table A'
**$ OilGas Table 'Table A'
*DENSITY *OIL 53.976
*DENSITY *GAS 0.0007
*CVO    0
*BWI    1.026204
*CW     3.02608E-06
*CO     7.869E-06
*REFPW  4000.
*VWI    0.312797
*CVW    0
*DENSITY *WATER 60.8066
RESULTS SECTION MODELARRAYS
```

RESULTS SECTION ROCKFLUID

*ROCKFLUID
*RPT 1
*KROIL *STONE2 *SWSG
*SWT
0.150000000 0.000000000 0.950000000 0.000000000 0.000000000
0.180000000 0.000013000 0.866216000 0.000000000 0.000000000
0.210000000 0.000100000 0.785887000 0.000000000 0.000000000
0.240000000 0.000338000 0.709051000 0.000000000 0.000000000
0.270000000 0.000800000 0.635749000 0.000000000 0.000000000
0.300000000 0.001563000 0.566023000 0.000000000 0.000000000
0.330000000 0.002700000 0.499920000 0.000000000 0.000000000
0.360000000 0.004288000 0.437490000 0.000000000 0.000000000
0.390000000 0.006400000 0.378788000 0.000000000 0.000000000
0.420000000 0.009113000 0.323874000 0.000000000 0.000000000
0.450000000 0.012500000 0.272816000 0.000000000 0.000000000
0.480000000 0.016638000 0.225687000 0.000000000 0.000000000
0.510000000 0.021600000 0.182571000 0.000000000 0.000000000
0.540000000 0.027463000 0.143564000 0.000000000 0.000000000
0.570000000 0.034300000 0.108778000 0.000000000 0.000000000
0.600000000 0.042188000 0.078346000 0.000000000 0.000000000
0.630000000 0.051200000 0.052430000 0.000000000 0.000000000
0.660000000 0.061413000 0.031238000 0.000000000 0.000000000
0.690000000 0.072900000 0.015056000 0.000000000 0.000000000
0.720000000 0.085738000 0.004324000 0.000000000 0.000000000
0.750000000 0.100000000 0.000000000 0.000000000 0.000000000

*SLT
0.200000000 1.000000000 0.000000000 0.000000000
0.237500000 0.902500000 0.001760194 0.000000000
0.275000000 0.810000000 0.007546118 0.000000000
0.312500000 0.722500000 0.017681343 0.000000000
0.350000000 0.640000000 0.032350917 0.000000000
0.387500000 0.562500000 0.051688940 0.000000000
0.425000000 0.490000000 0.075801577 0.000000000
0.462500000 0.422500000 0.104777130 0.000000000
0.500000000 0.360000000 0.138691418 0.000000000
0.537500000 0.302500000 0.177611010 0.000000000
0.575000000 0.250000000 0.221595335 0.000000000
0.612500000 0.202500000 0.270698128 0.000000000
0.650000000 0.160000000 0.324968474 0.000000000
0.687500000 0.122500000 0.384451584 0.000000000
0.725000000 0.090000000 0.449189390 0.000000000
0.762500000 0.062500000 0.519221011 0.000000000
0.800000000 0.040000000 0.594583123 0.000000000
0.837500000 0.022500000 0.675310262 0.000000000
0.875000000 0.010000000 0.761435069 0.000000000
0.912500000 0.002500000 0.852988501 0.000000000
0.950000000 0.000000000 0.950000000 0.000000000

RESULTS SECTION ROCKARRAYS
RESULTS SECTION INIT
*INITIAL
*USER_INPUT

```
**$ Data for PVT Region 1
**$ ----------------------------------
RESULTS SECTION INITARRAYS
**$ RESULTS PROP SW  Units: Dimensionless
**$ RESULTS PROP Minimum Value: 0.7  Maximum Value: 0.7
SW CON 0.7
**$ RESULTS PROP PRES  Units: psi
**$ RESULTS PROP Minimum Value: 3000  Maximum Value: 3000
PRES CON 3000.
**$ RESULTS PROP PB  Units: psi
**$ RESULTS PROP Minimum Value: 3000  Maximum Value: 3000
PB CON 3000.
**$ RESULTS PROP SO  Units: Dimensionless
**$ RESULTS PROP Minimum Value: 0.3  Maximum Value: 0.3
SO CON 0.3
RESULTS SECTION NUMERICAL
*NUMERICAL
*DTMAX 365.
*DTMIN 0.001
*NORM *PRESS 235.113
*NORM *SATUR 0.01
*NORM *PBUB 435.113
*MAXCHANGE *SATUR 0.1
RESULTS SECTION NUMARRAYS
RESULTS SECTION GBKEYWORDS
RUN

DATE 1988 01 01.

WELL  1 'injector'
INJECTOR MOBWEIGHT 'injector'
INCOMP GAS
OPERATE MAX STG  1.5E+04 CONT
OPERATE MAX BHP  3100. CONT
GEOMETRY K 0.25 0.37 1. 0.
PERF GEO   'injector'
        1  3  1 1. FLOW-FROM 'SURFACE'
        1  3  2 1. FLOW-FROM  1
        1  3  3 1. FLOW-FROM  2
        1  3  4 1. FLOW-FROM  3
        1  3  5 1. FLOW-FROM  4
GUIDEI STG 'injector'       1.E+05

WELL  2 'INJECTOR2'
INJECTOR MOBWEIGHT 'INJECTOR2'
INCOMP GAS
OPERATE MAX STG  1.5E+04 CONT
OPERATE MAX BHP  3100. CONT
GEOMETRY K 0.25 0.37 1. 0.
PERF GEO   'INJECTOR2'
        1  7  1 1. FLOW-FROM 'SURFACE'
        1  7  2 1. FLOW-FROM  1
        1  7  3 1. FLOW-FROM  2
        1  7  4 1. FLOW-FROM  3
        1  7  5 1. FLOW-FROM  4
```

```
GUIDEI STG 'INJECTOR2'        1.E+05

WELL  3 'producer'
PRODUCER 'producer'
OPERATE MIN BHP  3000. CONT
OPERATE MAX BHF  1000. STOP
GEOMETRY K 0.25 0.37 1. 0.
PERF GEO   'producer'
        180  3  1 1. OPEN FLOW-TO 'SURFACE'
        180  3  2 1. OPEN FLOW-TO  1
        180  3  3 1. OPEN FLOW-TO  2
        180  3  4 1. OPEN FLOW-TO  3
        180  3  5 1. OPEN FLOW-TO  4

WELL  4 'PRODUCER2'
PRODUCER 'PRODUCER2'
OPERATE MIN BHP  3000. CONT
OPERATE MAX BHF  1000. STOP
GEOMETRY K 0.25 0.37 1. 0.
PERF GEO   'PRODUCER2'
        180  7  1 1. OPEN FLOW-TO 'SURFACE'
        180  7  2 1. OPEN FLOW-TO  1
        180  7  3 1. OPEN FLOW-TO  2
        180  7  4 1. OPEN FLOW-TO  3
        180  7  5 1. OPEN FLOW-TO  4

SHUTIN 'injector'
SHUTIN 'INJECTOR2'
SHUTIN 'producer'
SHUTIN 'PRODUCER2'

DATE 1990 01 01.

OPEN 'injector'
OPEN 'producer'
OPEN 'INJECTOR2'
OPEN 'PRODUCER2'

DATE 1991 01 01.

OPEN 'injector'
OPEN 'producer'
OPEN 'INJECTOR2'
OPEN 'PRODUCER2'

DATE 1992 01 01.

OPEN 'injector'
OPEN 'producer'
OPEN 'INJECTOR2'
OPEN 'PRODUCER2'

DATE 1993 01 01.

OPEN 'injector'
```

```
OPEN 'producer'
OPEN 'INJECTOR2'
OPEN 'PRODUCER2'

DATE 1994 01 01.

OPEN 'injector'
OPEN 'producer'
OPEN 'INJECTOR2'
OPEN 'PRODUCER2'

DATE 1995 01 01.

OPEN 'injector'
OPEN 'producer'
OPEN 'INJECTOR2'
OPEN 'PRODUCER2'

DATE 1996 01 01.

OPEN 'injector'
OPEN 'producer'
OPEN 'INJECTOR2'
OPEN 'PRODUCER2'

DATE 1997 01 01.

OPEN 'injector'
OPEN 'producer'
OPEN 'INJECTOR2'
OPEN 'PRODUCER2'

DATE 1998 01 01.

OPEN 'injector'
OPEN 'producer'
OPEN 'INJECTOR2'
OPEN 'PRODUCER2'

DATE 1999 01 01.

OPEN 'injector'
OPEN 'producer'
OPEN 'INJECTOR2'
OPEN 'PRODUCER2'

DATE 2000 01 01.

OPEN 'PRODUCER2'
OPEN 'injector'
OPEN 'producer'
OPEN 'INJECTOR2'

DATE 2001 01 01.
```

```
OPEN 'injector'
OPEN 'producer'
OPEN 'INJECTOR2'
OPEN 'PRODUCER2'

DATE 2002 01 01.

OPEN 'PRODUCER2'
OPEN 'INJECTOR2'
OPEN 'injector'
OPEN 'producer'

DATE 2003 01 01.

OPEN 'injector'
OPEN 'producer'
OPEN 'INJECTOR2'
OPEN 'PRODUCER2'

DATE 2004 01 01.

OPEN 'injector'
OPEN 'producer'
OPEN 'INJECTOR2'
OPEN 'PRODUCER2'

DATE 2005 01 01.

OPEN 'injector'
OPEN 'producer'
OPEN 'INJECTOR2'
OPEN 'PRODUCER2'

DATE 2006 01 01.

WELL  5 'S-PRODUCER1'
PRODUCER 'S-PRODUCER1'
OPERATE MIN BHP  2950. CONT
OPERATE MAX BHF  800. CONT
GEOMETRY K 0.25 0.37 1. 0.
PERF GEO   'S-PRODUCER1'
        1  3  1 1. FLOW-TO 'SURFACE'
        1  3  2 1. FLOW-TO  1
        1  3  3 1. FLOW-TO  2
        1  3  4 1. FLOW-TO  3
        1  3  5 1. FLOW-TO  4

WELL  6 'S-PRODUCER2'
PRODUCER 'S-PRODUCER2'
OPERATE MIN BHP  2950. CONT
OPERATE MAX BHF  800. CONT
GEOMETRY K 0.25 0.37 1. 0.
PERF GEO   'S-PRODUCER2'
        1  7  1 1. FLOW-TO 'SURFACE'
        1  7  2 1. FLOW-TO  1
```

```
        1  7  3 1. FLOW-TO  2
        1  7  4 1. FLOW-TO  3
        1  7  5 1. FLOW-TO  4

WELL  7 'S-INJECTOR1'
INJECTOR MOBWEIGHT 'S-INJECTOR1'
INCOMP WATER
OPERATE MAX BHP  3100. CONT
OPERATE MAX BHW  800. CONT
GEOMETRY K 0.25 0.37 1. 0.
PERF GEO   'S-INJECTOR1'
        180  3  1 1. FLOW-FROM 'SURFACE'
        180  3  2 1. FLOW-FROM  1
        180  3  3 1. FLOW-FROM  2
        180  3  4 1. FLOW-FROM  3
        180  3  5 1. FLOW-FROM  4

WELL  8 'S-INJECTOR2'
INJECTOR MOBWEIGHT 'S-INJECTOR2'
INCOMP WATER
OPERATE MAX BHP  3100. CONT
OPERATE MAX BHW  800. CONT
GEOMETRY K 0.25 0.37 1. 0.
PERF GEO   'S-INJECTOR2'
        180  7  1 1. FLOW-FROM 'SURFACE'
        180  7  2 1. FLOW-FROM  1
        180  7  3 1. FLOW-FROM  2
        180  7  4 1. FLOW-FROM  3
        180  7  5 1. FLOW-FROM  4

OPEN 'S-PRODUCER1'
OPEN 'S-PRODUCER2'
OPEN 'S-INJECTOR1'
OPEN 'S-INJECTOR2'
SHUTIN 'injector'
SHUTIN 'INJECTOR2'
SHUTIN 'producer'
SHUTIN 'PRODUCER2'

DATE 2007 01 01.

OPEN 'S-PRODUCER1'
OPEN 'S-PRODUCER2'
OPEN 'S-INJECTOR1'
OPEN 'S-INJECTOR2'
SHUTIN 'injector'
SHUTIN 'INJECTOR2'
SHUTIN 'producer'
SHUTIN 'PRODUCER2'

DATE 2008 01 01.

OPEN 'S-PRODUCER1'
OPEN 'S-PRODUCER2'
OPEN 'S-INJECTOR1'
```

```
OPEN 'S-INJECTOR2'
SHUTIN 'injector'
SHUTIN 'INJECTOR2'
SHUTIN 'producer'
SHUTIN 'PRODUCER2'

DATE 2009 01 01.

OPEN 'S-PRODUCER1'
OPEN 'S-PRODUCER2'
OPEN 'S-INJECTOR1'
OPEN 'S-INJECTOR2'
SHUTIN 'injector'
SHUTIN 'INJECTOR2'
SHUTIN 'producer'
SHUTIN 'PRODUCER2'

DATE 2010 01 01.

OPEN 'S-PRODUCER1'
OPEN 'S-PRODUCER2'
OPEN 'S-INJECTOR1'
OPEN 'S-INJECTOR2'
SHUTIN 'injector'
SHUTIN 'INJECTOR2'
SHUTIN 'producer'
SHUTIN 'PRODUCER2'

DATE 2011 01 01.

OPEN 'S-PRODUCER1'
OPEN 'S-PRODUCER2'
OPEN 'S-INJECTOR1'
OPEN 'S-INJECTOR2'
SHUTIN 'injector'
SHUTIN 'INJECTOR2'
SHUTIN 'producer'
SHUTIN 'PRODUCER2'

DATE 2012 01 01.

OPEN 'S-PRODUCER1'
OPEN 'S-PRODUCER2'
OPEN 'S-INJECTOR1'
OPEN 'S-INJECTOR2'
SHUTIN 'injector'
SHUTIN 'INJECTOR2'
SHUTIN 'producer'
SHUTIN 'PRODUCER2'

DATE 2013 01 01.

OPEN 'S-PRODUCER1'
OPEN 'S-PRODUCER2'
OPEN 'S-INJECTOR1'
```

```
OPEN 'S-INJECTOR2'
SHUTIN 'injector'
SHUTIN 'INJECTOR2'
SHUTIN 'producer'
SHUTIN 'PRODUCER2'

DATE 2014 01 01.

OPEN 'S-PRODUCER1'
OPEN 'S-PRODUCER2'
OPEN 'S-INJECTOR1'
OPEN 'S-INJECTOR2'
SHUTIN 'injector'
SHUTIN 'INJECTOR2'
SHUTIN 'producer'
SHUTIN 'PRODUCER2'

DATE 2015 01 01.

OPEN 'S-PRODUCER1'
OPEN 'S-PRODUCER2'
OPEN 'S-INJECTOR1'
OPEN 'S-INJECTOR2'
SHUTIN 'injector'
SHUTIN 'INJECTOR2'
SHUTIN 'producer'
SHUTIN 'PRODUCER2'

DATE 2016 01 01.
STOP
RESULTS SECTION WELLDATA
RESULTS SECTION PERFS
```

APPENDIX C: DDP OBSERVATION

The following pictures were taken from one spot located at the middle of the cell but at different stages of the DDP.

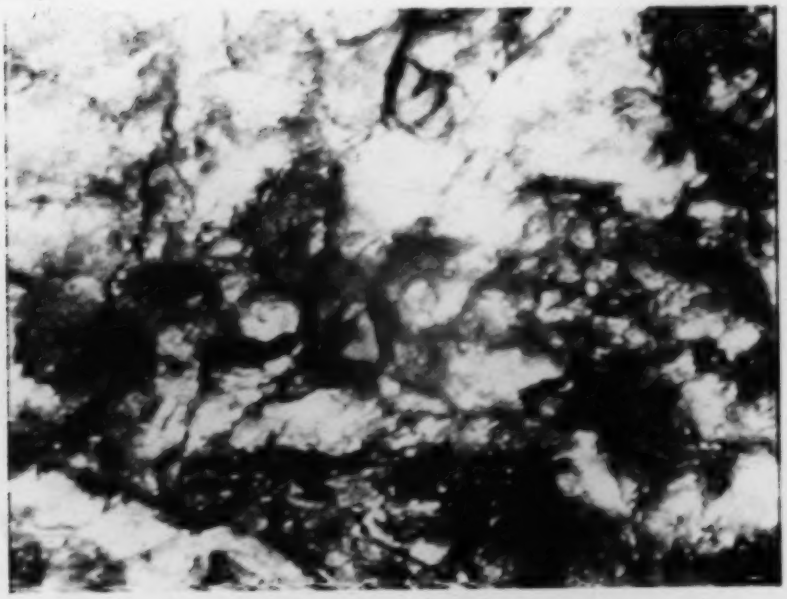

Figure C.1: Before the DDP, water (white) and oil (brown)

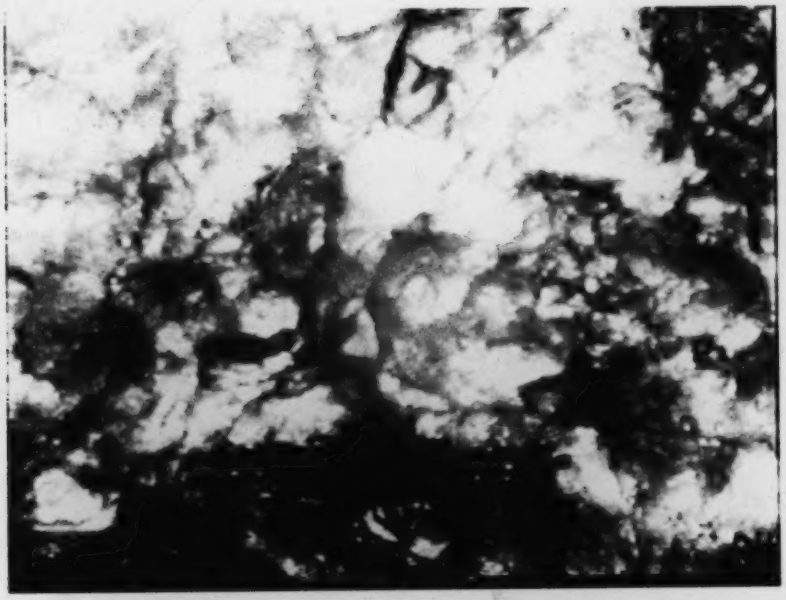

Figure C.2: Gas entered from the left at the bottom

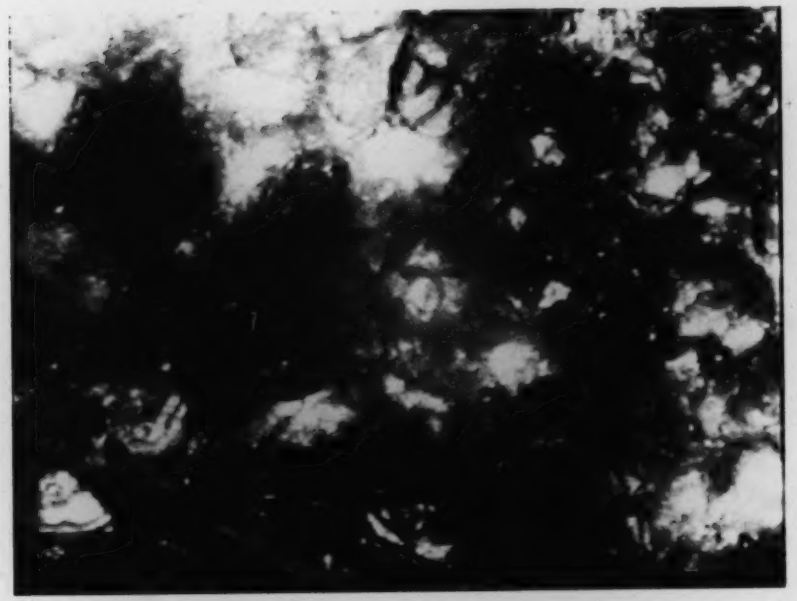

Figure C.3: Gas entered the middle layer

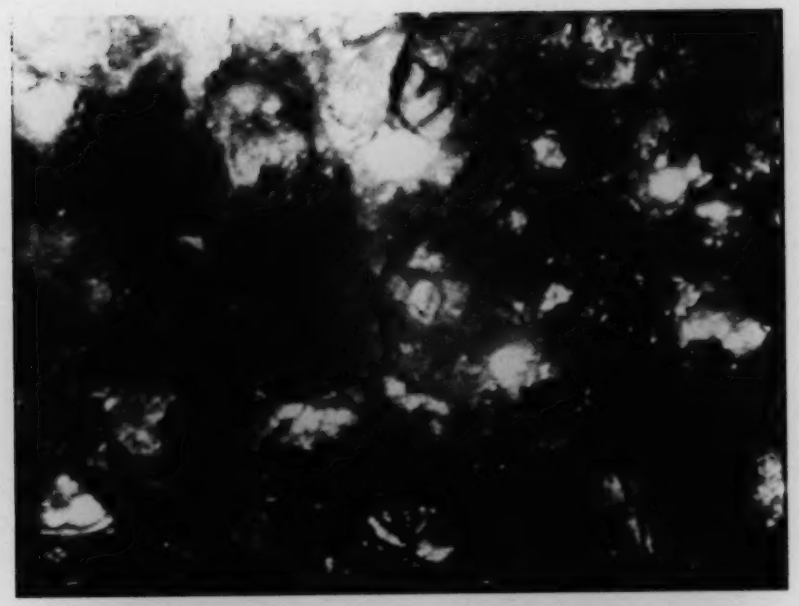

Figure C.4: Oil moved into the front layer first (the left upper part)

Figure C.5: Gas moved into the front layer (center)

Figure C.6: Gas entered from the left upper corner

Figure C.7: Gas entered from the left lower corner

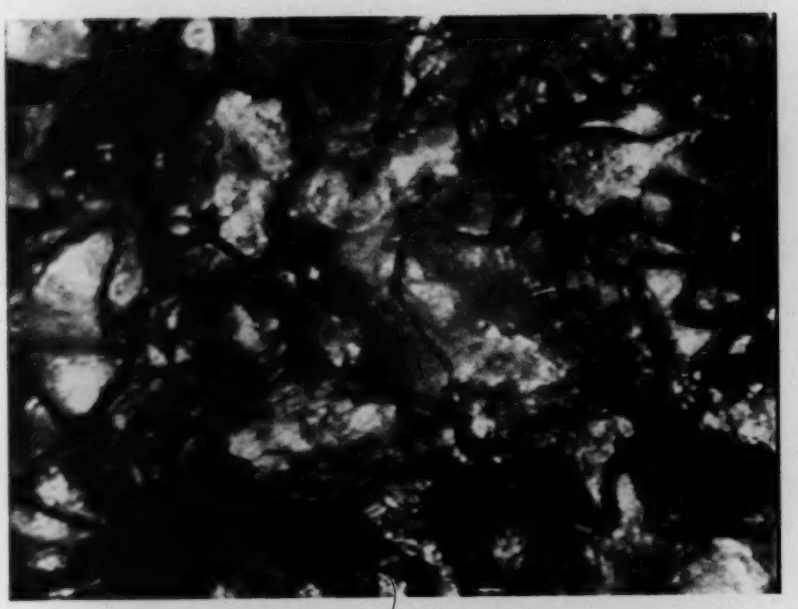

Figure C.8: Gas occupied available space; oil films and oil layers formed

Figure C.9: Less oil left in the form of oil films and layers

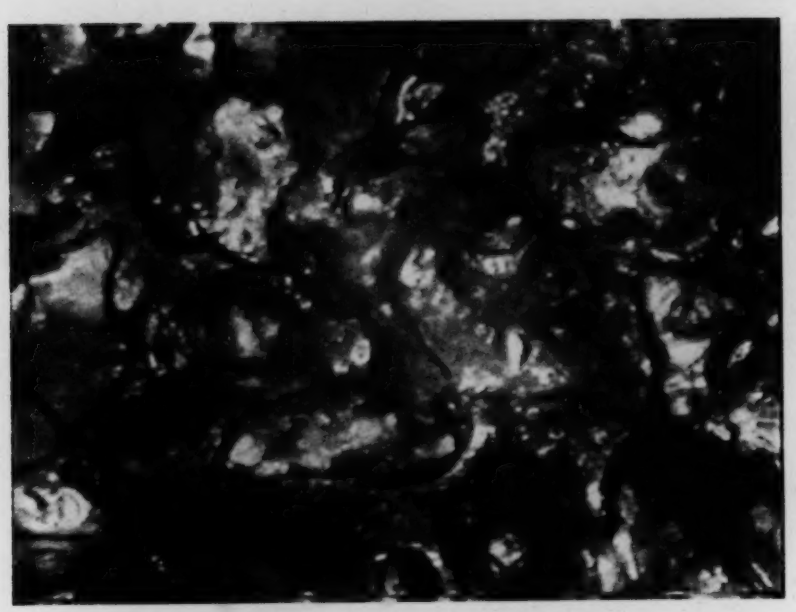

Figure C.10: At a later stage of the DDP

APPENDIX D: SCWD OBSERVATION

The following pictures were taken from one spot located at the middle of the cell but at different stages of the SCWD process.

Figure D.1: Before the SCWD process, oil in oil films

Figure D.2: Water entered from the left

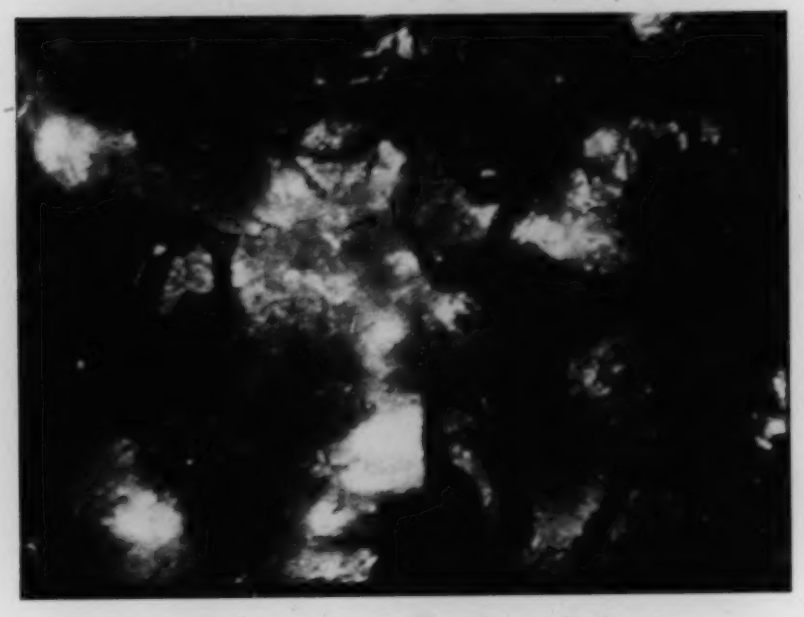

Figure D.3: Some gas and oil were displaced

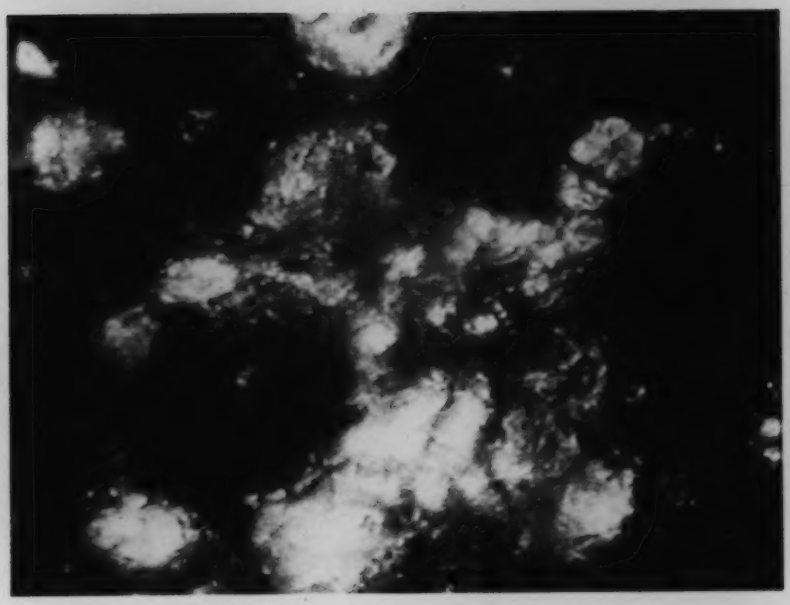

Figure D.4: Some gas was trapped

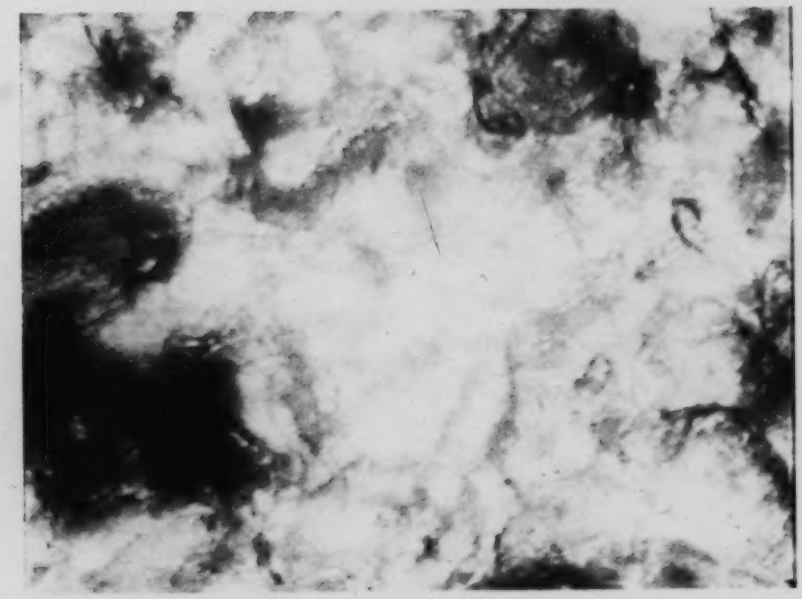

Figure D.5: After the SCWD process

APPENDIX E: CALCULATIONS OF IFT

The IFT was calculated based on the equation:

$$\sigma = \Delta\rho\, g\, (1/H)\, (De)^2$$

where σ is the interfacial tension in mN/m; $\Delta\rho$ is the density difference in g/cm^3; g is the gravitational constant at the point of measurement, 980.2 cm/sec^2 was used; $1/H$ is the shape factor which is based on the value of S; $1/H$ was read from the table by C. E. Stauffer, J. Phys. Chem. 69, 1933; De is the maximum diameter of the unmagnified drop in cm; it can be calculated by:

$$De = D_t\, (d_e/d_i)$$

where D_t is the outside diameter of the tip. For the oil and gas IFT, D_t was 0.15875 cm. For the other two IFT values, a smaller tip was used, and D_t was 0.0889 cm.

A detailed description of the Pendent Drop Apparatus, and the techniques required to use it can be found in Flock et al.'s paper (1984).

Table E.1: Oil and water interfacial tension

No.	d_e	d_s	d_t	$S = d_s/d_e$	$1/H$	d_e/d_t	D_e	IFT: σ
1	182	120	55	0.6593	0.94176	3.3091	0.2942	20.3232
2	182	113	54	0.6209	1.10036	3.3704	0.2996	24.6335
3	175	111	54	0.6343	1.04225	3.2407	0.2881	21.5723
4	179	111	54	0.6201	1.10501	3.3148	0.2947	23.9288
5	226	147	70	0.6504	0.97435	3.2286	0.2870	20.0157
6	226	143	69	0.6327	1.04657	3.2754	0.2912	22.1270
7	237	157	70	0.6624	0.92861	3.3857	0.3010	20.9783
8	210	135	70	0.6429	1.00446	3.0000	0.2667	17.8160
9	228	151	70	0.6623	0.92872	3.2571	0.2896	19.4175
10	237	159	69	0.6709	0.8983	3.4348	0.3054	20.8860
11	239	157	70	0.6569	0.9493	3.4143	0.3035	21.8091
12	228	146	69	0.6404	1.01495	3.3043	0.2938	21.8399
13	230	150	71	0.6522	0.96851	3.2394	0.2880	20.0299
14	241	160	71	0.6639	0.92327	3.3944	0.3018	20.9644
15	226	149	71	0.6593	0.94176	3.1831	0.2830	18.8051
16	221	145	71	0.6561	0.9531	3.1127	0.2767	18.1988

Average: 20.8341

Table E.2: Gas and water interfacial tension

No.	d_e	d_s	d_t	$S = d_s/d_e$	$1/H$	d_e/d_t	D_e	IFT: σ
1	170	112	53	0.6588	0.94176	3.2075	0.2852	76.6618
2	171	113	52	0.6608	0.93431	3.2885	0.2923	79.9410
3	166	115	53	0.6928	0.82525	3.1321	0.2784	64.0535
4	167	118	51	0.7066	0.78593	3.2745	0.2911	66.6760
5	170	115	53	0.6765	0.87746	3.2075	0.2852	71.4276
6	168	108	53	0.6429	1.00446	3.1698	0.2818	79.8532
7	171	118	53	0.6901	0.83471	3.2264	0.2868	68.7494
8	171	115	52	0.6725	0.89122	3.2885	0.2923	76.2541
9	167	109	54	0.6527	0.96463	3.0926	0.2749	72.9960
10	159	104	54	0.6541	0.96077	2.9444	0.2618	65.9051
11	167	111	55	0.6647	0.91964	3.0364	0.2699	67.0839
12	171	114	52	0.6667	0.91242	3.2885	0.2923	78.0680
13	166	114	52	0.6867	0.84431	3.1923	0.2838	68.0776
14	164	109	52	0.6646	0.91964	3.1538	0.2804	72.3755
15	168	115	53	0.6845	0.8508	3.1698	0.2818	67.6374
16	171	111	53	0.6491	0.98029	3.2264	0.2868	80.7398

Average: 72.2813

Table E.3: Oil and gas interfacial tension

No.	d_e	d_s	d_t	$S = d_s/d_e$	$1/H$	d_e/d_t	D_e	IFT: σ
1	143	118	91	0.8252	0.52133	1.5714	0.2495	24.3900
2	144	115	93	0.7986	0.56738	1.5484	0.2458	25.7717
3	143	115	93	0.8042	0.55811	1.5376	0.2441	24.9997
4	143	116	90	0.8112	0.54547	1.5889	0.2522	26.0896
5	142	116	92	0.8169	0.53494	1.5435	0.2450	24.1443
6	142	115	92	0.8099	0.56364	1.5435	0.2450	25.4397
7	142	117	92	0.8239	0.523	1.5435	0.2450	23.6054
8	142	116	92	0.8169	0.53494	1.5435	0.2450	24.1443
9	142	118	92	0.8310	0.51306	1.5435	0.2450	23.1568
10	142	116	92	0.8169	0.53494	1.5435	0.2450	24.1443
11	143	116	91	0.8112	0.54547	1.5714	0.2495	25.5193
12	144	115	90	0.7986	0.56738	1.6000	0.2540	27.5184
13	143	117	91	0.8182	0.53322	1.5714	0.2495	24.9462
14	141	119	91	0.8440	0.4908	1.5495	0.2460	22.3239
15	144	116	91	0.8056	0.55446	1.5824	0.2512	26.3040
16	141	118	91	0.8369	0.50176	1.5495	0.2460	22.8224

Average: 24.7075